TRIBHUVAN UNIVERSITY

INSTITUTE OF ENGINEERING

PULCHOWK CAMPUS

THESIS NO.: M-413-MSREE-2024-2026

Numerical Comparison of Ventilation Approaches for Thermal Comfort and Air Distribution in a Classroom

by

Binod KC

A THESIS

SUBMITTED TO THE DEPARTMENT OF MECHANICAL AND AEROSPACE ENGINEERING IN PARTIAL FULLFILLMENT OF THE REQUIREMENTS FOR THE DEGREE OF MASTER OF SCIENCE IN RENEWABLE ENERGY ENGINEERING

DEPARTMENT OF MECHANICAL AND AEROSPACE ENGINEERING

LALITPUR, NEPAL

APRIL 2026

COPYRIGHT

TRIBHUVAN UNIVERSITY

INSTITUTE OF ENGINEERING

PULCHOWK CAMPUS

DEPARTMENT OF MECHANICAL AND AEROSPACE ENGINEERING

The undersigned certify that read, and recommended to the Institute of Engineering for acceptance, a thesis entitled **"Numerical Comparison of Ventilation Approaches for Thermal Comfort and Air Distribution in a Classroom"** submitted by Binod KC (080MSREE007), in partial fulfillment of the requirements for the degree of Master of Science in Renewable Energy Engineering.

Supervisor: Dr. Hari Bahadur Darlami

Associate Professor

Department of Mechanical and Aerospace Engineering

External Examiner: Dr. Bibek Baral

Professor

Department of Mechanical Engineering, Kathmandu University

Committee Chairman, Sudip Bhattrai, Ph.D.

Head of Department

Department of Mechanical and Aerospace Engineering

Tribhuvan University
Institute of Engineering
Department of Mechanical and Aerospace Engineering
Pulchowk Campus

Date: 30 April, 2026

ABSTRACT

This paper numerically compares the ventilation performance and thermal comfort features of four classroom air distribution strategies: displacement ventilation (DV), stratum ventilation (SV), ceiling diffuser ventilation (CD) and wall grill ventilation (WG). The analysis was carried out on a high-occupancy classroom (48 students and a single teacher) measuring 11 m x 7 m x 3.6 m. All the cases were simulated under the same operating conditions, which included 6 air changes per hour, the same temperature of the supply air, and equal rate of internal heat, moisture, and carbon dioxide generation so that the difference in performance could be explained primarily by the ventilation approach and velocities per approach. A computational fluid dynamics model was used based on the finite volume approach with the RNG $k-\varepsilon$ turbulence mode with an enhanced wall treatment. Carbon dioxide and water vapor distribution were modeled using the species transport equations, and a scalar transport equation was used to compute local mean age of air. The numerical procedure was validated against published experimental data for an indoor ventilation chamber.

The findings indicate that the air distribution strategy and supply velocity had a strong impact on the ventilation performance. DV achieved the highest average CRE of about 131%, followed by SV 106%, CD 96%, and WG 82%. SV also showed good performance, especially at 0.8 m/s. CD and WG had mixing-dominated airflow. The analysis of thermal comfort indicated that DV had the lowest draft risk at seated and breathing heights, whereas WG at 2.84 m/s produced the highest draft risk, reaching about 24.5% at 1.1 m. The air distribution index validated overall ranking, where the average values of DV, SV, CD, and WG were 2.20, 1.97, 1.67, and 1.61, respectively. Where space or architectural constraints limit DV installation, SV can be considered an effective alternative. Of the mixed ventilation systems, CD showed higher performance than WG, and thus, it is the better of the two systems when a traditional mixing-based system is needed.

Keywords: Indoor Air Quality; Computational Fluid Dynamics; Heating Ventilation and Air Conditioning; Thermal Comfort

ACKNOWLEDGEMENTS

To begin with, I want to express my deepest gratitude to my supervisor, Associate Professor Dr. Hari Bahadur Darlami, who provided me with a strong support and guidance in the course of the research. His experience, constructive feedback, and insightful suggestions have significantly contributed to complete this work.

I am also thankful to the members of my thesis committee, for their insightful comments and suggestions, which greatly improved the quality of this work. I would like to express my gratitude to the faculty and staff of the Department of Mechanical and Aerospace Engineering, Pulchowk Campus, who have been supportive of my academic research and provision of the resources needed to conduct this research.

I would also like to thank my classmates of the MSREE 2080 batch in creating an insightful environment throughout the Masters study. With your presence, this study trip has been made interesting and informative. Finally, I want to express my utmost gratitude to my family as it has been able to support me through thick and thin. My academic life has been based on their understanding and sacrifices.

TABLE OF CONTENTS

LIST OF TABLES

LIST OF FIGURES

LIST OF ABBREVIATIONS

ACE	Air Change Effectiveness
ACH	Air Changes per Hour
ADI	Air Distribution Index
AoA	Age of Air
Ar	Archimedes Number
CD	Ceiling Diffuser
CFD	Computational Fluid Dynamics
CO_2	Carbon Dioxide
CRE	Contaminant Removal Effectiveness
DR	Draft Risk
DV	Displacement Ventilation
FVM	Finite Volume Method
HVAC	Heating, Ventilation and Air Conditioning
IAQ	Indoor Air Quality
SIMPLE	Semi-Implicit Method for Pressure Linked Equations
SV	Stratum Ventilation
WG	Wall Grill

CHAPTER ONE: INTRODUCTION

1.1 Background

Classrooms are among the most critical indoor environments because educational buildings typically have occupant densities that are three to four times higher than those of residential or many commercial buildings, which increases the likelihood of heat buildup, contaminant accumulation, and ventilation inadequacy Students also spend about 6 to 8 hours per weekday in classrooms, so the indoor thermal and air-distribution conditions of these spaces influence a substantial portion of their daily exposure and comfort experience (Jia et al., 2021). Indoor air quality in educational facilities has been repeatedly recognized as a determinant of student health, attendance, and learning performance, which means that classroom ventilation is not only a building-services issue but also an educational quality issue (Branco et al., 2024).

Research has further shown that classroom air quality is associated with children's school performance, the need for better ventilation and environmental control in teaching spaces (Wargocki et al., 2020). Studies focused on K–12 classrooms have likewise identified indoor air quality factors as important contributors to academic performance outcomes, which strengthens the argument for ventilation-focused classroom design research (Kabirikopaei et al., 2021). The urgency of this issue is evident in field investigations from different climates, where many classrooms fail to maintain acceptable thermal comfort and indoor air quality simultaneously (Miao et al., 2023). A Mediterranean field study covering 32 naturally ventilated classrooms, around 600 students, and more than 460 hours of monitoring reported recurring indoor air quality and thermal comfort deficiencies, especially when windows and doors remained closed during winter (Miao et al., 2023).

A recent seasonal assessment of school classrooms found that hourly average carbon dioxide concentrations frequently exceeded 1000 ppm, with winter class-hour values ranging from 760 to 1118 ppm, indicating that many students were exposed to under-ventilated conditions during occupancy periods (Charres et al., 2025). An international study of 75 primary school classrooms reported winter median ventilation rates of only 0.47 h^{-1} in Slovakia and 0.57 h^{-1} in the United Arab Emirates, compared with 3.2 h^{-1} in Sweden, demonstrating large cross-country differences in classroom ventilation

performance (Eldanaf et al., 2025). A year-long study of university classrooms in Xi'an also reported that nearly 30% of surveyed classrooms consistently exceeded 1500 ppm carbon dioxide, showing that insufficient ventilation remains common in educational buildings with sustained occupancy (X. Wang et al., 2021).

The challenge becomes even more serious in high-occupancy classrooms because an higher number of students in a smaller space simultaneously releases sensible heat, moisture, exhaled carbon dioxide, and respiratory aerosols within a limited volume of air (H. Li et al., 2025). Under these conditions ventilation effectiveness depends not only on how much air is supplied but also on how that air is distributed through the occupied zone and around the breathing level of seated students (Pollozhani et al., 2024). Recent study from mixed mode classrooms in a hot humid climate showed that only 13 percentage to 16 percentage of the monitored time met optimal indoor environmental quality conditions, showing how difficult it is to achieve acceptable comfort and air quality in real school operation (Hwang et al., 2025). Further studies in Mediterranean schools have similarly shown that natural ventilation alone may be unable to satisfy both indoor air quality and thermal comfort targets under extreme weather conditions, whereas mechanical and forced ventilation provides more reliable compliance as compared to natural ventilation (Maiques et al., 2025).

Even in Nepalese classrooms, where summer natural ventilation can produce very high air change rates, field survey and simulation results indicate that high airflow alone does not automatically ensure controlled and effective classroom air distribution due to various factors (Shrestha et al., 2022). These concerns for health and comfort make the selection of an appropriate air distribution strategy very important in high occupancy classrooms, where small differences in jet behavior, stratification, recirculation, and exhaust capture can directly influence student comfort and contaminant removal (Pollozhani et al., 2024).

Displacement ventilation is particularly relevant because it relies on buoyancy and thermal plumes generated by occupants and internal loads to lift warm and contaminated air upward, thereby creating a stratified indoor environment that can benefit the occupied zone when designed properly (Tognon & Zarrella, 2024). Stratum ventilation is also promising for dense classrooms because it attempts to deliver fresh air more directly across the breathing zone rather than fully mixing the entire room

volume before removal (H. Li et al., 2025). Ceiling mounted systems such as ceiling diffusers are widely applied because they are practical and conventional, but their performance depends strongly on diffuser throw, mixing pattern, and interaction with thermal loads inside the room (Saad et al., 2023). Wall grill systems are likewise common in practice, yet their jets can interact strongly with occupants and room geometry, which may lead to higher local velocities and less favorable air distribution conditions in the occupied zone causing higher risk of draft in the occupancy zone (Zhao et al., 2021).

Experimental classroom evidence already shows that air-distribution choice can substantially alter local thermal conditions and draft risk even when the same space is used for teaching (Zhao et al., 2021). In a simulated classroom, displacement ventilation and ceiling-diffuser supply maintained occupied-zone air speeds below 0.23 m/s with draft rates below 20%, whereas the wall grill arrangement produced local velocities around 0.4 m/s, indicating a higher potential for draft discomfort (Zhao et al., 2021). The same study reported that displacement ventilation was less sensitive to changing internal loads, which is an important advantage for classrooms where occupancy and metabolic gains vary across the day (Zhao et al., 2021).

A full-scale school test-bed study also demonstrated that airflow configuration changes pollutant-removal performance, with a floor-return arrangement reducing the time required to improve PM 2.5 from unhealthy to good conditions by 35% relative to an upper-return arrangement (Son & Jang, 2022). Monitoring in Swedish primary schools further confirmed that different ventilation strategies, including constant-air-volume and variable-air-volume systems, are associated with measurable differences in classroom indoor air quality (Cabovská et al., 2022).

Although research on school ventilation has expanded in recent years, many studies still assess only one or two systems, one climate context, or one performance indicator such as carbon dioxide concentration, leaving a need for more integrated comparisons that include thermal comfort and air distribution together(Branco et al., 2024).

Recent dense-classroom experiments comparing multiple ventilation strategies showed that the choice of ventilation mode can significantly change contaminant-removal effectiveness, thermal comfort, energy utilization, and infection risk, even under the same classroom use context (H. Li et al., 2025).

Therefore, a numerical comparison of displacement ventilation, stratified ventilation, a ceiling diffuser system, and a wall grill system is highly justified for a high-occupancy classroom because these four approaches represent distinctly different airflow philosophies with potentially different implications for comfort and occupied-zone air delivery (Pollozhani et al., 2024). Such a study is particularly valuable when performed through computational fluid dynamics, because CFD can resolve temperature fields, velocity distribution, thermal stratification, and local air-distribution behavior in ways that room-average measurements cannot fully capture (Tognon & Zarrella, 2024).

1.2 Statement of problem

High-occupancy classrooms are prone to inadequate thermal comfort and poor air distribution because large numbers of occupants generate significant sensible heat, moisture, and carbon dioxide within a limited indoor volume. Schools are particularly vulnerable indoor environments because they combine high occupancy, prolonged exposure time, and frequently inadequate ventilation conditions, making ventilation performance a critical issue in classroom design (Pollozhani et al., 2024). Even though a number of ventilation strategies are practiced, their performance could vary significantly based on the introduction, distribution, and removal of supply air into the occupied zone. In the classroom, inadequate air distribution can result in non-uniform distribution of heat and indoor contaminants, draft discomfort, stagnant areas, and ineffective heat and indoor contaminant removal. Experimental evidence has shown that different classroom air distribution methods can produce markedly different occupied-zone velocities and draft conditions, with wall grill supply in particular generating high local velocities of around 0.4 m/s, while displacement ventilation was found to be less sensitive to changes in load conditions (Zhao et al., 2021).

Previous studies have shown that displacement, stratified, ceiling-based, and wall-mounted air distribution systems each have distinct airflow characteristics. Recent dense-classroom research has also demonstrated that ventilation strategy can significantly affect contaminant removal effectiveness, draught rate, infection risk, and energy utilization, confirming that the choice of system has consequences beyond simple air supply volume alone (H. Li et al., 2025). However, a clear numerical comparison of these four ventilation approaches under the same high-occupancy classroom conditions remains limited. In particular, there is insufficient evidence on

how these systems differ in terms of thermal comfort and air distribution within the occupied zone when applied to a densely occupied classroom. This gap is especially important for displacement-based systems, because their performance is closely linked to buoyancy effects, thermal plumes, and indoor stratification, which makes system behavior highly dependent on room conditions and air distribution design (Tognon & Zarrella, 2024).

Therefore, the problem addressed in this study is the lack of a comparative understanding of how displacement ventilation, stratified ventilation, 4-way ceiling diffusion, and wall grill ventilation perform in a high-occupancy classroom with respect to thermal comfort and air distribution. This creates uncertainty in selecting the most suitable ventilation strategy for maintaining a comfortable and well-ventilated classroom environment.

1.3 Objectives

1.3.1 Main objective

To perform numerical analysis of airflow characteristics and thermal comfort of displacement ventilation, stratum ventilation, ceiling diffusers, and wall grills in a high-occupancy classroom

1.3.2 Specific objectives

The specific objectives of this study are:

- To analyze temperature and velocity distribution for each ventilation approach
- To analyze the role of inlet velocity on temperature gradient on occupancy zone
- To assess the ventilation effectiveness of each ventilation approaches
- To assess thermal comfort indices under different ventilation approach

1.4 Limitations of the study

Although a comprehensive study was undertaken to determine the study's outputs, there were certain limitations that arose during the research. These limitations include:

- The simulations are conducted under steady-state conditions and therefore do not capture transient effects such as fluctuating occupancy, door opening, or time-dependent HVAC operation

- Students are represented as heat and contaminant sources rather than detailed human geometries
- The study is limited to one classroom geometry; therefore, findings may not be directly generalizable to other room sizes or ventilation systems
- The CFD model is numerically verified but not validated against in-situ measurements for the specific classroom

CHAPTER TWO: LITERATURE REVIEW

The indoor environmental quality in classrooms has become one of the concerns of research due to a combination of the long exposure period, a high number of occupants, and a high sensitivity of users to the thermal discomfort and polluted indoor air. School buildings are especially susceptible since students spend long periods in the same room where metabolic heat, moisture, carbon dioxide and bioeffluents build up in a relatively small volume making ventilation design a key determinant of the health, comfort, and learning conditions (Pollozhani et al., 2024).

There is still significant geographical and building type variation in the ventilation performance of schools which is a significant concern given that the importance of IAQ in classrooms is an issue that has been gathering momentum over the last several years. (Eldanaf et al., 2025).

In a survey of 75 primary school classrooms across the countries of Sweden, Slovakia, and the United Arab Emirates, median winter ventilation rates were reported as 3.2 h^{-1} in Sweden, 0.47 h^{-1} in Slovakia, and 0.57 h^{-1} in the UAE, showing the wide spread in actual classroom ventilation performance under real operating conditions (Eldanaf et al., 2025). Field evidence has also shown that school hour pollutant concentrations frequently rise above outdoor levels, confirming that classroom ventilation system must be assessed not only by airflow rates but also by the ability of the system to dilute and remove internally generated contaminants effectively.

These environmental shortcomings are closely associated with school performance, as opposed to being viewed solely as a matter of mechanical design. Surveys of school ventilation strategies have noted that proper ventilation can reduce the risk of airborne infections by more than 50 percent besides providing thermal comfort and acceptable levels of pollutants, which gives the design of airflow in classrooms both a public-health and pedagogical role (Pollozhani et al., 2024). The perception studies of children in Swedish primary schools have also showed that, the lower the ventilation rate is, the worse the evaluation of the indoor environment by the children occupying the classroom (Vasquez et al., 2023).

The other prominent theme of the recent scholarship is that it is becoming increasingly difficult to meet the targets of thermal comfort and indoor air quality under climate

stress, extreme seasons, and energy constraints. Wholesale modeling of school buildings Mediterranean has demonstrated that natural ventilation may fail to meet concurrent indoor air quality and comfort goals in extreme weather, whilst mechanical systems reliably achieve their compliance goals over a broader climatic range (Maiques et al., 2025). The same study also noted that mechanical ventilation has the capability to achieve up to 95% compliance to favorable climatic conditions as well as record average HVAC energy savings of approximately 80 percent under some of the standardized conditions, which is critical in highlighting the importance of matching ventilation strategy to climatic conditions and performance target as opposed to relying on some generalized solution (Maiques et al., 2025). Evidence from naturally ventilated classrooms in Ireland also showed a lot of variation between schools and offices. This supports the idea that how well classrooms are ventilated depends on the situation and is hard to control without more careful air-distribution design (Collison et al., 2025). Consequently, contemporary literature inquires not merely about the ventilation of classrooms, but also whether the selected airflow distribution strategy can ensure adequate thermal comfort and effective air delivery within the occupied zone amidst dense and dynamic classroom environments (Pollozhani et al., 2024).

Computational fluid dynamics has become one of the most important tools for numerically study how to ventilate and provide thermal comfort in classrooms. CFD is very useful because it can accurately predict the distributions of air velocity, temperature, turbulence, and contaminant concentration in three-dimensional space for estimating thermal comfort and air distribution. Which can help to design better ventilation system or choose one system over another or to find the performance of currently used system. Room average measurements alone can't do this (Olivas & Yee, 2025). A recent study on systematic review of indoor airflow field reconstruction methods noted that CFD remains a trusted numerical/reference approach for detailed indoor airflow prediction even though it is computationally intensive, because it can represent localized thermal plumes, stratification, and contaminant transport with much greater fidelity than simplified multizone method Because of this, CFD is especially useful in classrooms, where the presence of many students, desks, supply devices, and heat sources creates flow structures that are not uniform in space and directly affect comfort and exposure at head level (Cetin et al., 2025). A CFD and Taguchi-based

optimization study of a 31 occupant classroom revealed that window position was the most significant factor affecting both CO_2 concentration and draught risk, illustrating how airflow configuration significantly impacts indoor conditions, even when the room type is unchanged. (Cetin et al., 2025). Similarly, CFD studies on classroom furniture and aperture optimization revealed that pollutant concentrations were especially sensitive within the 0 to 1.6 m height range, precisely where students breathe and feel comfortable. (Tikul et al., 2022).

CFD is also a big part of the shift from traditional whole-room mixing to more advanced ventilation ideas for occupied zones. A recent review of advanced ventilation strategies highlighted that traditional systems frequently consume considerable energy in conditioning unoccupied room volume, whereas contemporary strategies aim to directly target the occupied zone to enhance both livability and sustainability concurrently (Zhang & Lin, 2026). This transition has made numerical comparison especially important because the performance difference between ventilation modes often depends on subtle interactions among supply momentum, buoyancy, exhaust placement, and occupant location (Murga et al., 2024). Large CFD datasets are now being used even for surrogate modeling of classroom infection risk, and one such study based on 224 CFD cases found that the choice of ventilation strategy could alter transmission risk more strongly than increasing air change rate alone in some seating locations (Lee & Rim, 2024). That study further reported that displacement ventilation reduced infection risk by 49% to 77% relative to mixing ventilation under the modeled classroom scenarios, illustrating the practical significance of supply layout and air-distribution pattern (Lee & Rim, 2024).

Among the non-uniform ventilation approaches, displacement ventilation remains one of the most extensively studied and theoretically established. Displacement ventilation is a buoyancy-driven system that introduces low-velocity cool air near floor level, allowing internal thermal plumes from occupants and heat sources to transport warm and polluted air upward toward the exhaust (Tognon & Zarrella, 2024). Its central advantage is the creation of a relatively clean and thermally acceptable lower occupied zone beneath a warmer and more contaminated upper layer, which can improve breathing-zone conditions when pollutant sources are associated with human bodies and convective heat release (Tognon & Zarrella, 2024). The method depends on vertical

stratification rather than full mixing, its performance depends strongly on interface height, load distribution, occupant movement, and supply temperature, making it highly suitable for detailed CFD analysis (Mateus & Carrilho Da Graça, 2015). The requirement for stratification-aware modeling is well recognized in the literature, and validated multi-node approaches have been proposed precisely because fully mixed assumptions cannot represent the characteristic vertical gradients of displacement ventilation (Mateus & Carrilho Da Graça, 2015).

The practical potential of displacement ventilation has repeatedly been demonstrated in school and classroom studies. In Norwegian schools that were fitted with demand-controlled displacement ventilation, daytime air volume was cut by 65 percent to 75 percent, average airflow by approximately half, fan energy by 87 percent, and heating energy by 21 percent indicating that the energy-saving potential of the approach when properly controlled was strong (Wachenfeldt et al., 2007). The same study explained the basic pattern of displacement as a clean lower zone that is separated off of a mixed upper contaminated layer, which is very similar to the theoretical benefits commonly cited in support of classrooms and other high-occupancy areas (Wachenfeldt et al., 2007). A successful Applied Energy study of a classroom-oriented 9.77 m x 7.25 m x 3.00 m room with 30 students and one teacher also demonstrated that displacement ventilation could be successfully integrated with heat-recovery systems and still maintain acceptable thermal and air-quality performance in school buildings (Y. Wang et al., 2014). Closely related work on passive school buildings has demonstrated that displacement-oriented natural ventilation similarly is strongly influenced by thermal buoyancy, further supporting the need to evaluate it using models that account behaviorally for buoyant plume behavior, rather than just nominal supply rate (Y. Wang et al., 2014).

Nevertheless, the literature also clearly shows that displacement ventilation is not always better in all locations of sources and boundary conditions. Comparative work in tutorial rooms found that displacement ventilation could save 13 percent to 45 percent of cooling and ventilation energy compared to mixing ventilation, but it was also reported that the air quality benefit of displacement ventilation depends upon the fact that the pollutants are coupled to sources of warmth rather than sources of the pollutants themselves (Shan et al., 2016). The same study warned that displacement ventilation

may raise cold feet or excessive vertical temperature gradients unless it is carefully designed which can be directly applied to the classroom applications where students sit long periods (Shan et al., 2016). Recent reviews so characterize displacement ventilation as a high-potential but condition-sensitive approach the effectiveness of whose implementation is dependent on the correspondence between buoyancy, load distribution and diffuser design and actual occupancy pattern of the room (Tognon & Zarrella, 2024).

Among the responses to the inefficiency of conditioning the entire room volume when the occupants are confined to a small lower zone of the room is the emergence of stratum ventilation as a concept in the literature. Instead of putting air at the ceiling, as in conventional mixing, stratum ventilation adds conditioned air at the sidewall terminals, near the breathing zone, instead of at the ceiling (Lin et al., 2009). The primary reason why stratum ventilation has been considered as a promising strategy to both cool and prevent infection in classrooms, offices and other highly populated areas is this occupied-zone delivery concept (Zhang et al., 2019). Subsequent reviews and experiments describe the supply terminals of stratum ventilation as being located either at breathing-zone height or slightly higher than head level on the sidewall which is conceptually consistent with classroom layouts that locate the supply at breathing-zone height or slightly above head level on the sidewall (Al-Rikabi et al., 2024). Recent experimental studies of sidewall air-supply heating systems also observe that in such systems the height of the installation is less than the upper limit of the occupied space, taken as 1.8 m above the floor, since this will help to reduce the heat and momentum lost outside the occupied space (Cheng et al., 2023).

The early foundational study by Lin et al. has introduced stratum ventilation as a possible solution to high indoor temperatures since it attempts to provide acceptable conditions at the point where people actually reside and not across the entire volume of the room (Lin et al., 2009). Later studies discovered that the supply conditions and terminal arrangement have a powerful influence on the resultant performance of stratum ventilation. A reported experiment and numerical study of the types of air terminals reported that the location of exhaust and the rate of supply jet and return circuit interaction both contributed to the air-diffusion behavior of the terminal and showed that the stratum ventilation was not determined solely by the inlet height but rather by

an interaction between the supply jet and the return configuration (Yao & Lin, 2014). The study of asymmetrically loaded offices had found that stratum ventilation could be used to maintain thermal comfort to cooling loads up to 90 W/m² with very hot supply temperatures of 19 to 21 °C, but even very hot facade conditions could push PMV to the upper comfort limit (Huan et al., 2016). This demonstrates that a good stratum ventilation can be achieved under realistic internal loads but is sensitive to local heat sources and façade asymmetry: something that is relevant in classrooms with solar gains or distribution of the heat load asymmetry (Huan et al., 2016).

The literature also connects stratum ventilation to airborne infection control because its horizontal supply path can reduce the transport distance between fresh-air source and breathing zone. An investigation into anti-airborne infection performance found that stratum ventilation could provide meaningful advantages over conventional alternatives by improving the delivery of clean air where occupants inhale (Lin et al., 2012). Optimization studies have likewise treated PMV, PPD, and droplet nuclei concentration as simultaneous design objectives under stratum ventilation, which shows how strongly this approach is associated with integrated comfort-and-contaminant control rather than temperature alone (Liu et al., 2021). A recent numerical study of differentiated thermal subzones under stratum ventilation further reported achievable PMV differences up to 1.46 between subzones without strong draught or local discomfort, indicating that the system has unusual flexibility for targeted conditioning when the supply direction and velocity are deliberately controlled (Liu et al., 2022).

Classroom-specific evidence on stratum ventilation is particularly relevant to the present thesis because it shows strong dependence on supply parameters and room geometry. An experimental study in a field environmental chamber designed as a two-row classroom found that winter stratum ventilation could keep overall thermal sensation within ISO Category C while maintaining draught rate below 20% under supply velocities of 0.8 to 1.4 m/s and supply temperatures of 23 to 30 °C (Cheng et al., 2022). Another classroom study with pulsating stratum ventilation reported that more than 87% of occupants felt thermally comfortable, while draft dissatisfaction could be reduced from 34% to 8% and overall discomfort from 16% to 4% under optimized pulsation conditions (Tian et al., 2019). Research on supply mode has further shown that horizontal contaminant distribution under stratum ventilation depends on

source location and air-direction strategy, meaning that seating arrangement and source placement remain important design variables even when the supply is placed favorably near the breathing zone (Lu et al., 2023). Combined, these studies demonstrate that stratum ventilation is a configuration-dependent, but potentially appealing strategy that could be particularly beneficial for classroom use, where the vertical space of the occupied zone is limited and plan area is dense (Zhang et al., 2019).

Air distribution based on ceiling remains the most popular practical solution in most learning buildings and ceiling diffuser is one of its most widespread terminal forms. It is widely used due to its architectural convenience, mature commercial availability, and capacity to provide symmetrical supply jets which will promote broad room mixing in case of centrally mounted supply jets. Due to this popularity, the ceiling diffuser frequently forms the basis of mixing system used in studies of classroom and office CFD where non-uniform mixing systems are compared with the ceiling diffuser (Djunaedy & Cheong, 2002). Because of this prevalence, the ceiling diffuser is frequently used as the standard system to which other systems are compared in classroom and office CFD studies (Villafruela et al., 2013). The modeling of this problem is important in comparative studies because the velocity and temperature characteristics of the near-ceiling jets produced by ceiling diffusers influence the velocity and temperature uniformity in the occupied zone, and the near-ceiling velocity distribution of the supplied air affects the characteristics of the plume (Awwad et al., 2017).

In recent years, efforts have been made to enhance modeling and performance prediction of these terminals. In the case of the 68-point air-opening representation of four-way square diffusers, a case study showed that an average of 0.7 to 1.0 °C difference at the most (RMSE) was achieved, indicating that reasonably accurate diffuser simulation is possible if all the blade detail is not fully resolved (Y. Li et al., 2024). Optimization of louver face ceiling diffusers revealed that the angle of the diffuser blades had a significant effect on the attachment to the ceiling and the occupied-zone behavior, with 65° being more suitable to the attachment to the ceiling and 45° being more suitable to taller rooms (Awwad et al., 2017). These results are important to classroom CFD because, while the 4-way diffuser is a seemingly simple

configuration, the velocity and temperature fields can vary significantly depending on the terminal geometry and mounting assumptions (Y. Li et al., 2024).

Indoor environmental performance is another attribute generally related to ceiling-based systems, where mixing ventilation may achieve reasonably uniform temperature, but may also lead to high local velocities if the air descends from the ceiling into the occupied space too strongly. Comparative infection-control studies which incorporated a 4-way ceiling inlet showed that inlet type significantly influenced exposure outcomes, indicating that the type of terminal inlets in the ceiling (even in mixing ventilation) is relevant to exposure (Hatif et al., 2023). Additional studies of diffuse ceiling ventilation also have shown that ceiling supply strategies can provide acceptable thermal environments during both heating and cooling; the rate of contaminant removal and temperature effectiveness values are generally more positive in cooling than in heating (Peng et al., 2023).

In some other circumstances, ceiling systems may not act as a purely mixed system, as a field study carried out in a classroom with diffuse ceiling ventilation demonstrated a relatively mixed occupied zone with no draught during actual operation, but still exhibited some displacement-like effects (Kristensen et al., 2017). Ceiling diffusers continue to play an important role in the literature, not only because they are a standard benchmark, but also because they serve as a reminder that standard mixing systems can exhibit a significant difference in performance depending on the diffuser design and room boundary conditions (Awwad et al., 2017).

Another important type of wall grill systems is those that are installed in classrooms via sidewall supply grills or high sidewall outlets. Wall grilles typically create more powerful directional jet streams which can interact significantly with people's use, depending on throw and discharge angle and return position, compared to ceiling diffusers (Yau et al., 2024). This makes them useful and versatile, but also poses a risk of local draught and temperature imbalances if the jet is directed towards seated occupants prior to proper mixing (Yau et al., 2024). In classrooms, numerical studies of comfort conditions for high sidewall grills revealed that varying the discharge angle significantly affected the results, while the presence of obstructions in the ceiling space affected the thermal conditions due to alteration of the jet trajectories and mixing (Yau et al., 2024). Additional aerosol-transport studies over the last few years have also

indicated that having the right space supply layout is often more effective than simply raising ventilation rate, while also highlighting the need to focus on wall-jet organization instead of just quantity of ventilation airflow (Xu et al., 2025).

In classroom studies, Zhao et al. is particularly useful, as it directly compared a corridor-wall grille, displacement ventilation, a ceiling diffuser, and a perforated duct diffuser in a mock-up classroom both while heating and cooling. That study showed that the wall grill configuration produced velocities in the occupied zone of approximately 0.4 m/s, while the displacement ventilation and ceiling diffuser resulted in velocities less than 0.23 m/s with draft rates less than 20 percentage, which meant that there was much higher draft risk in the wall grill configuration (Zhao et al., 2021). That same study also demonstrated that the ceiling diffuser system and the displacement ventilation system were better classroom alternatives to the corridor-wall or ceiling grille under the conditions tested, because of their less-sensitive nature to the effects of internal loads and drafts in the occupied zone (Zhao et al., 2021). This is very relevant to high occupancy classrooms as the sidewall jets that might look okay at design level may put many desks and seated occupants in locally uncomfortable flow conditions (Zhao et al., 2021).

If the literature is studied comparatively, a few patterns emerge, that occupancy zone-based systems like displacement and stratum ventilation can improve conditions in the breathing zone by minimizing the amount of supply energy required to condition the unoccupied volume of the upper room. Second, the relative ranking of systems has been found to be highly sensitive to the performance measure used a strategy that works well for contaminant removal may not work well for draft risk or temperature uniformity (Zhang & Lin, 2026). Second, the relative ranking of systems has been found to be highly sensitive to the performance measure used a strategy that works well for contaminant removal may not work well for draft risk or temperature uniformity (Hatif et al., 2023). Third, as has been reported in classrooms, the arrangement of the classroom can have a significant effect on the transport and comfort of aerosols, particularly in high occupancy rooms where the location of the source and seated breathing height are of great importance, and ventilation layout is now reported to affect this more than air change rate alone (Lee & Rim, 2024). Fourth, the literature always confirms comparative evaluation using CFD since these differences are of spatial nature

and cannot be fully explained by using room averages or single point measurements (Olivas & Yee, 2025).

There is still a gap in the available literature, however, that the present thesis can help address, in spite of the significant progress made. Most of the studies only contrast two or three types of ventilation, examine a single performance parameter or test only offices or generic chambers instead of classrooms where students are more densely distributed (H. Li et al., 2025). A number of key papers address the issue of displacement ventilation in schools, but there are fewer that directly compare it with the conventional ceiling diffuser, stratum ventilation, and wall grill systems, under the same classroom geometry and boundary conditions (Y. Wang et al., 2014). Similarly, many of the papers in the stratum ventilation literature are either office, chamber or infection-control or parameter optimization studies, and not comparative studies with the same set of conventional alternatives which are widely utilized in educational buildings at the classroom scale (Liu et al., 2021). Although the use of ceiling diffuser and wall grill systems is common, they are frequently referred to as 'generic mixing systems', and the details of how the airflow structure of these systems affects thermal comfort and air distribution at student level in high occupancy classrooms are under discussed (Yau et al., 2024). Therefore, a numerical thesis that compares displacement ventilation, stratum ventilation with sidewall supply around occupied-zone height, a centrally distributed ceiling diffuser system, and a wall grill system within the same high-occupancy classroom is well aligned with the unresolved needs identified in the recent literature (Pollozhani et al., 2024). Such a comparison is especially valuable when thermal comfort and air distribution are evaluated together, because the literature shows that no single ventilation strategy can be assumed optimal without examining the coupled fields of temperature, velocity, and occupied-zone airflow behavior under realistic classroom loads (Murga et al., 2024).

CHAPTER THREE: METHODOLOGY

3.1 Research framework overview

In this study, a numerical approach based on the Computational Fluid Dynamics (CFD) is applied to compare the ventilation performance and thermal comfort characteristics of four different ventilation strategies in a highly occupied classroom. The research framework is developed to systematically study the effect of different air distribution methods on the indoor airflow pattern, temperature distribution, contaminant transport and occupant comfort for the same classroom operating conditions. The methodology is presented in a sequential way in order to guarantee clarity, consistency and reproducibility of the simulation results.

The general approach is based on the comparative evaluation of four ventilation strategies, i.e. displacement ventilation, stratum ventilation, ceiling diffuser ventilation and wall grill ventilation. The same classroom geometry, occupancy condition and cooling load scenario are applied for each ventilation system to clearly isolate the impact of ventilation design and the impact of inlet velocity. All cases are kept in the same physical space and same load conditions internally allowing the systems to be directly compared in terms of their ability to provide effective air distribution, contaminant removal and thermal comfort in a densely occupied educational environment at different ventilation strategies and their varying supply velocities.

The methodology of the study starts with the three-dimensional geometric modelling of the classroom which includes the room dimensions, the occupied zone, the location of the supply air inlet and the exhaust outlet. Students and teacher are modelled as internal sources for sensible heat, latent heat and carbon dioxide, which represents the realistic operating conditions in a classroom. Internal loads are determined based on occupancy in the classroom and they are constant for all cases of ventilation, which are applied according to the ASHRAE standard for different metabolic rates for seated occupants and teacher which has a slightly higher metabolic activity. This ensures that the only major difference between the simulated scenarios is the ventilation strategy and the inlet velocities.

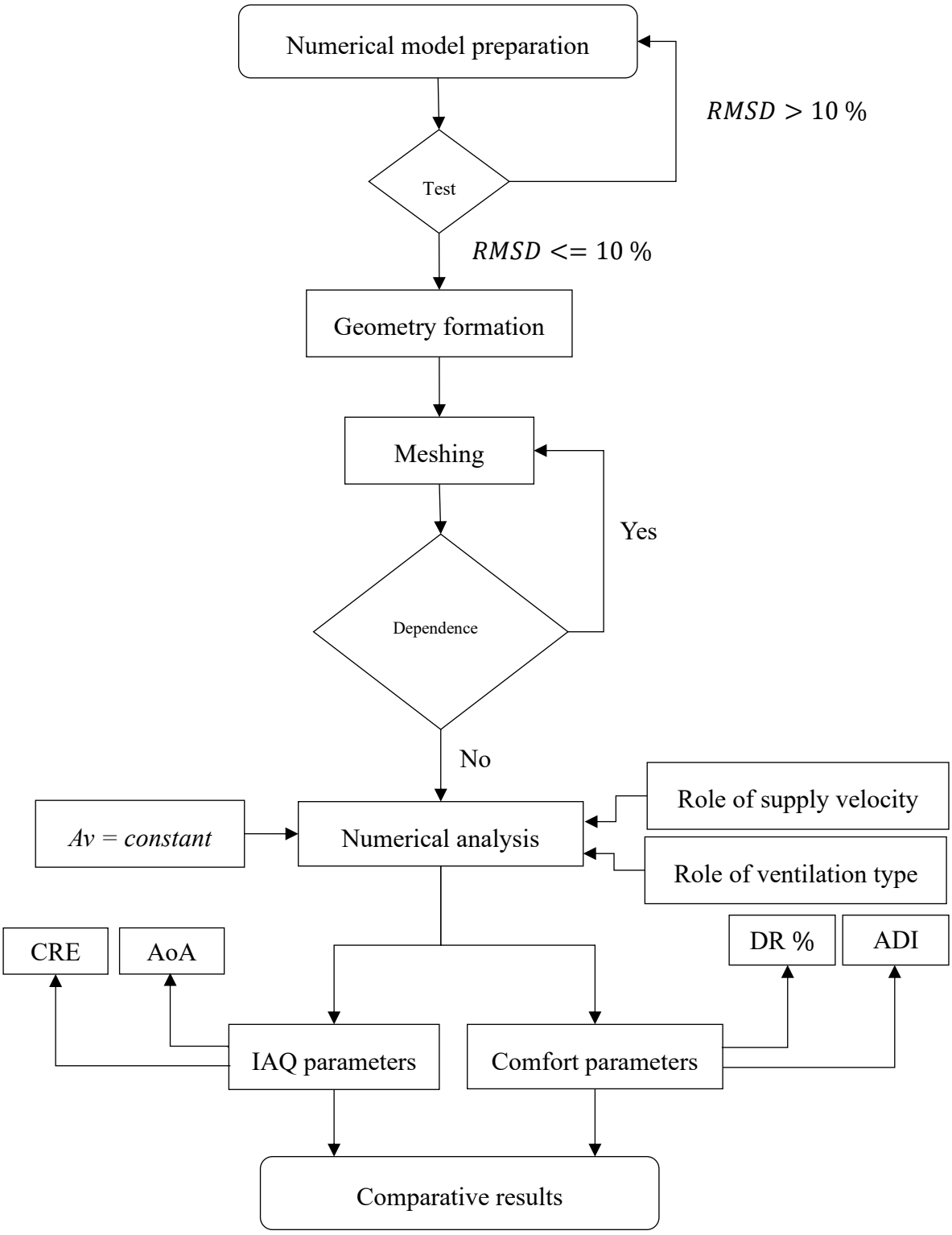

Figure 3.1: Methodological flowchart

After the geometric and physical model is set up, CFD simulations are carried out for each ventilation approaches. The numerical model solves the steady-state governing equations of conservation of mass, momentum and energy then later the numerical

simulation is further solved using pseudo-transient solver for solution stability. A validated turbulence model for indoor air distribution is used to model the turbulent indoor airflow behavior. Also, scalar transport equations are used to simulate carbon dioxide concentration, water vapor distribution and local mean age of air.

The performance of each ventilation strategy and their different velocities cases are evaluated in terms of a set of indicators related to airflow, thermal comfort and ventilation effectiveness. These are airflow pattern, air velocity distribution, temperature field, carbon dioxide concentration in the breathing plane, local mean age of air in the breathing plane, draft risk at various heights in the occupancy zone, contaminant removal effectiveness and other relevant comfort or indoor air quality indices used in the study.

Thus, any difference in performance in terms of ventilation and comfort can be directly linked to the intrinsic characteristics of the ventilation system and their different velocity cases. This is a structured research framework that provides a clear and systematic approach to determining the most effective ventilation strategy for a classroom with a high number of occupants, as well as the role of a supply velocity for the thermal comfort and indoor air quality in a high occupancy room.

3.2 Numerical model

The numerical model used in this study was developed by validating results with previous work to simulate indoor airflow accurately and to allow the numerical assessment of classroom ventilation performance under the different ventilation approaches and their different supply velocity cases. Since the reliability of CFD predictions depends strongly on the appropriateness of the numerical procedure, the modeling work was divided into two main stages i.e. numerical model preparation and numerical model.

3.2.1 Numerical model preparation

Before applying the CFD approach to the actual classroom configuration and their different ventilation scenarios, the numerical procedure was validated against the experimental measurements reported by (Chen et al., 2020). For this purpose, the computational domain was defined according to the reduced-scale enclosure described in the reference study. The validation geometry consisted of a cubic chamber with

dimensions of 1 m × 1 m × 1 m. while both the inlet and outlet had dimensions of 0.18 m × 0.05 m at a room temperature of 20 °C. The configuration included a top inlet and a bottom outlet, providing a simple and well-defined benchmark case for CFD validation. The simulated airflow field obtained from this numerical setup was then compared with the corresponding experimental data reported by (Chen et al., 2020) to assess the reliability of the adopted CFD methodology.

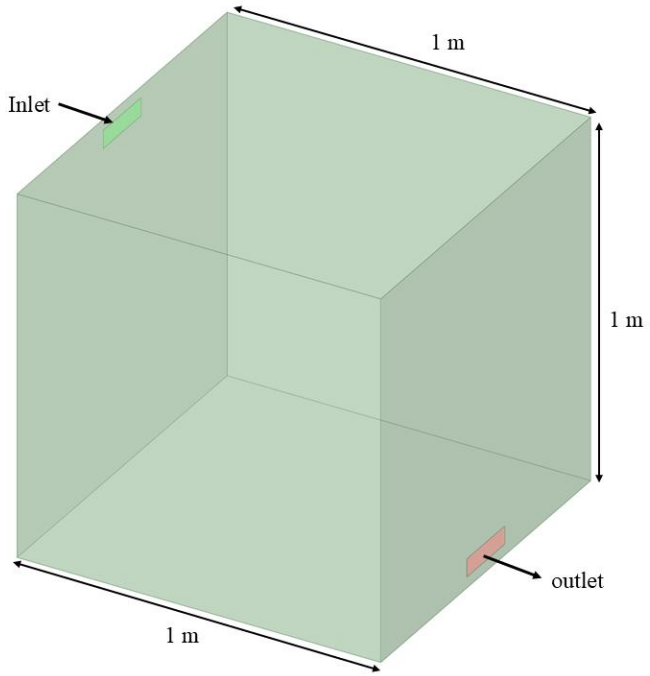

Figure 3.2: 3D model of the chamber

The validation process was mainly focused only on the three inlet-velocity cases reported in the benchmark study, namely 0.111 m/s, 0.278 m/s and 0.444 m/s. which corresponds to 4 ACH, 10 ACH and 16 ACH, respectively. These cases were selected because they were experimentally measured and numerically compared making them suitable for direct validation of the airflow field (Chen et al., 2020), making them suitable for direct validation of the airflow field.

The governing equations solved in the numerical model were the continuity and momentum equations for incompressible turbulent flow. In the reference study (Chen et al., 2020) airflow was modeled in CFD software using the RNG $k-\varepsilon$ turbulence model, which the authors reported to be more suitable than other tested models for indoor airflow prediction. The same turbulence-modeling approach was therefore adopted in the present validation setup to maintain consistency with the benchmark

case. The paper further reports the use of enhanced wall treatment, with $y^+ < 5$, a uniform velocity inlet, pressure outlet, turbulence intensity of 5 %, turbulence length scale of 0.01 m, turbulent Schmidt number of 0.7, the SIMPLE pressure-velocity coupling scheme, and second-order upwind discretization, with solution residuals controlled to 10^{-4}. These settings were reproduced as closely as possible in the present validation model to minimize methodological differences between the numerical reproduction and the benchmark study.

3.2.2 Numerical model validation

A structured validation procedure was then followed. First, the computational domain was discretized with sufficient refinement near the inlet, outlet, and wall regions to capture the developing jet and the near-wall velocity gradients. Second, steady-state simulations were performed for each of the three inlet velocities. Third, the velocity field was sampled along the same line used in the reference paper for comparison with the published experimental data. According to (Chen et al., 2020), one of the reported validation profiles was extracted on the xz-plane at $y = 0.5$ m, along the vertical line located at $(x, y) = (0.5\,, 0.5)$ m. The velocity was presented in normalized form as $u^* = u_x/u_{in}$, while the vertical coordinate was expressed as $z^* = z/H$, where $H = 1$ m. The same definitions were adopted in the present study for validation comparison.

The normalized x-velocity profiles along the chamber midline obtained from the simulation were compared with the corresponding experimental measurements. For this purpose, both velocity and spatial coordinates were nondimensionalized using the inlet velocity and chamber height, respectively, and are defined as follows:

$$u^* = \frac{u_x}{u_{in}}, \quad Z^* = \frac{z}{H} \tag{3.1}$$

where u^* represents the normalized velocity magnitude and Z^*denotes the normalized vertical position.

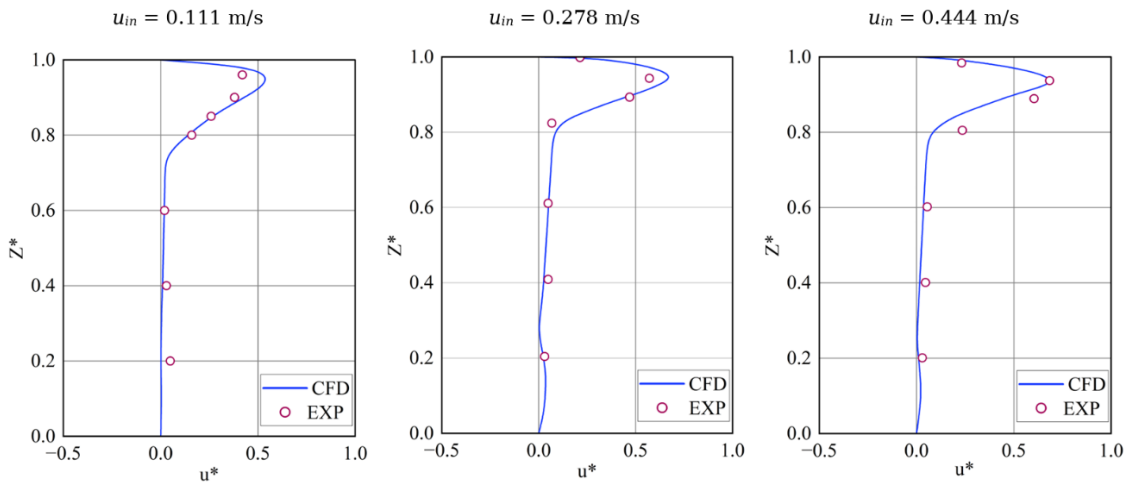

Figure 3.3: Experiments vs simulations

To quantitatively evaluate the difference between the numerical predictions and experimental measurements, the root-mean-square deviation (RMSD) was calculated using the following expression:

$$RMSD = \sqrt{\frac{\sum_{i=1}^{N}(\phi_{Exp,i} - \phi_{Num,i})^2}{N}} \tag{3.2}$$

where $\phi_{Exp,i}$ and $\phi_{Num,i}$ correspond to the experimental and numerical values at the i-th measurement point, respectively, and N denotes the total number of measurement locations. The RMSD values obtained for inlet velocities of 0.111 m/s, 0.278 m/s, and 0.444 m/s were 0.048, 0.064, and 0.079, respectively. These comparatively small deviations are indicative of good agreement between the CFD solutions and the experimental data and indicate that the CFD model is suitable for the representation of indoor airflow.

3.3 Classroom geometry and occupancy modelling

The three-dimensional model of a classroom dimension of 11m x 7m x 3.6 m was developed representing a realistic teaching environment with 48 students spaced uniformly with one teacher, the students and teacher were modeled with simplified block in order to facilitate mesh generation, numerical stability and reduce computational power throughout the different numerical simulations as shown in Figure 3.4. The classroom was also modeled with their windows of 2.90 m x 1.80 m which are responsible for adding heat to the classroom. The role of the windows could be

significant enough for thermal comfort but in this analysis same overall heat transfer coefficient and outdoor temperature was applied to ensure fair comparison of different ventilation approaches. Which only single outs the effect of different ventilation approaches and their different inlet supply velocities within.

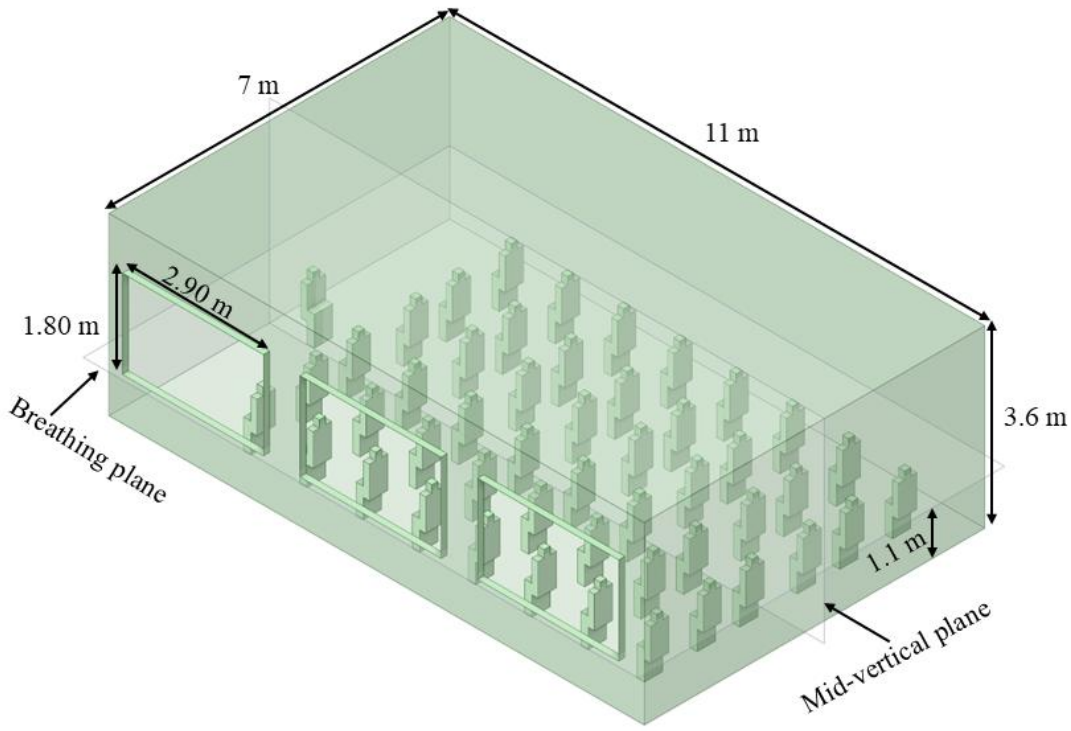

Figure 3.4: Physical model of the classroom

The occupied zone was defined as the region extending from the floor up to a height representative of seated occupants, considered up to 1.2 m from the floor level. The numerical analysis was mainly focused in two plane namely breathing plane and mid-vertical plane. Since the student are distributed uniformly across the classroom, analyzing different parameters like age of air, contaminant removal efficiency, velocity and temperature distribution etc. on these planes are enough to provide the thermal comfort and indoor air quality across the classroom.

Table 3.1: Detail information of classroom geometry and occupancy

	Parameters	Value
Geometry	Room length	11.0 m

	Parameters	Value
	Room width	7.0 m
	Room height	3.60 m
Windows	Window count	3
	Window size	2.90 m × 1.80 m
Occupancy	Number of students	48
	Number of teachers	1
	Student height (seated)	1.2 m
	Teacher height (seated)	1.2 m

Other occupancies such as classroom door, desks, bench, whiteboard etc. were excluded from the simulation to reduce computational cost was justified because the primary objective of this study was to evaluate ventilation effectiveness, thermal comfort indices, and draft risk at the room and occupied-zone scale. Detailed anatomical modeling of human bodies would significantly increase mesh resolution requirements without proportionally improving prediction of large-scale airflow patterns.

Recent indoor airflow CFD studies have shown that simplified block representations of occupants adequately reproduce obstruction effects for room-scale ventilation and contaminant transport analysis (Zhang, Chen, & S, 2018). Therefore, the adopted modeling strategy provides an appropriate balance between numerical accuracy and computational efficiency.

3.4 Indoor set-point conditions and outdoor boundary condition

The set of operating parameters and their different boundary conditions used in the present numerical analysis are shown in Table 3.2. The outdoor design condition was defined using an outside dry-bulb temperature of 302.85 K for the location 27.6°N, 85.359°E which corresponds to the 3 PM design condition in June 2025 and representing the ASHRAE 1% cooling design condition. This condition was selected to simulate a representative near-peak summer cooling scenario for the study location. The indoor design condition was fixed at 297.15 K and 50% relative humidity to represent the target thermal comfort condition inside the classroom. The classroom was

maintained at the supply of 6 ACH was used in the CFD simulation. The inlet carbon dioxide concentration was supplied at 420 ppm to represent outdoor air concentration. The ventilation rate was maintained at 6 ACH in all cases. This value was chosen based on published classroom ventilation guidance, which identifies about 6 ACH as an appropriate target for occupied school spaces. ASHRAE guidance for education facilities recommends that classroom systems should strive to achieve 3–6 ACH during occupied periods and 6–8 ACH where enhanced indoor air quality is desired, while other school ventilation guidance also uses 6 ACH as a practical classroom target. Accordingly, 6 ACH was considered suitable for the present classroom CFD analysis.

Table 3.2: Indoor set-point conditions and outdoor boundary conditions

S.N.	Parameters	Value	
1.	Analysis day	June 2025	
	Outside DB temperature	302.85 K	
2.	Target indoor condition	Temperature	297.15 K
		Relative Humidity	50 %
3.	Supply condition	Air change per hour	6
		Carbon dioxide	420 PPM

The spaces adjacent to the two end walls (7 m x 3.6 m) of the classroom and the floor below were assumed to be conditioned spaces; however, a boundary temperature of 298.15 K was assigned to these surfaces to represent a conservative worst-case condition. Whereas other walls, roof and is exposed to the outside temperature of 302.85 K.

The numerical analysis for ventilation and comfort analysis will be more occupancy centric as the major source of heat source with in the classroom.

3.5 Total cooling load formulation

The total cooling load of the space is defined as the summation of all sensible and latent heat gains entering the conditioned space at the design hour.

$$Q_{\text{total}} = Q_{\text{sensible}} + Q_{\text{latent}} \tag{3.3}$$

$$Q_{\text{sensible}} = \sum_{i,j} Q_{\text{wall},i,j} + \sum_{i,j} Q_{\text{window,cond},i,j} + Q_{\text{people,sensible}} \tag{3.4}$$

where Q_{sensible} is the total sensible heat gain in the classroom, $Q_{\text{wall},i,j}$ is the sensible heat gain through the i-th wall associated with the j-th corresponding outdoor temperature condition, $Q_{\text{window,cond},i,j}$ is the conductive sensible heat gain through the i-th window associated with the j-th corresponding outdoor temperature condition, and $Q_{\text{people,sensible}}$ is the total sensible heat released by the occupants.

$$Q_{\text{latent}} = \dot{m_{\text{H}_2\text{O}}}\, h_{fg} \tag{3.5}$$

The latent heat load was determined from the moisture generation rate of water vapor. As given in Eq 3.5, the latent heat load, Q_{latent}, is equal to the product of the water vapor generation rate, $\dot{m}_{\text{H}_2\text{O}}$, and the latent heat of vaporization, h_{fg}. This formulation was used to relate occupant moisture generation to its equivalent latent heat contribution within the classroom.

3.5.1 Envelope heat transfer

Heat transfer through opaque building elements was represented using a quasi-steady conduction approach to define the thermal behavior of the classroom envelope in the CFD model. In this approach, the thermal transmittance of each envelope element was calculated from steady-state one-dimensional conduction theory, while the actual heat transfer rate was allowed to vary according to the instantaneous temperature difference between the prescribed outdoor condition and the solution-dependent indoor-side temperature.

For each multilayer wall element i, the total thermal resistance was calculated as:

$$R_{\text{total},i} = R_{si} + \sum_{m=1}^{n} \frac{L_{m,i}}{k_{m,i}} + R_{so} \tag{3.6}$$

where R_{si} and R_{so} are the internal and external surface resistances, respectively, $L_{m,i}$ is the thickness of layer m in envelope element i (m), $k_{m,i}$ is the thermal conductivity of layer m in envelope element i (W/m·K), and n is the number of layers in that construction. The overall heat transfer coefficient of each element was then obtained as:

$$U_i = \frac{1}{R_{\text{total},i}} \tag{3.7}$$

Similarly, the thermal transmittance of each glazing element was determined from its corresponding window assembly properties. The calculated U-values of the classroom are shown in Table 3.3.

Table 3.3: Overall heat transfer coefficient

Surfaces	Values
Wall U-value (W/m²·K)	1.8
Ceiling U-value (W/m²·K)	2.0
Floor U-value (W/m²·K)	2.0
Windows U-value (W/m²·K)	5.0

Although the envelope U-values remained constant throughout the analysis, the heat transfer through walls and windows was not imposed as a fixed thermal load. Instead, a quasi-steady boundary treatment was adopted. Under this treatment, the outdoor thermal condition assigned to each surface remained prescribed, whereas the indoor-side temperature was obtained from the evolving CFD solution. As a result, the conductive heat flux across each envelope element varied during the simulation according to the local temperature difference across that surface.

For opaque surface i, the conductive heat transfer at simulation state j was expressed as:

$$Q_{\text{wall},i,j} = U_{\text{wall},i} A_{\text{wall},i} \left(T_{\text{out},i} - T_{\text{in},i,j}\right) \tag{3.8}$$

where $U_{\text{wall},i}$ is the overall heat transfer coefficient of wall i(W/m^2·K), $A_{\text{wall},i}$ is the exposed area of wall $i(m^2)$, $T_{\text{out},i}$ is the prescribed outdoor temperature corresponding to wall i(°C), and $T_{\text{in},i,j}$ is the indoor-side temperature of wall $i$obtained from the CFD solution at simulation state j.

For glazing element i, the conductive component was determined in the same manner:

$$Q_{\text{window,cond},i,j} = U_{\text{glass},i} A_{\text{window},i} \left(T_{\text{out},i} - T_{\text{in},i,j}\right) \tag{3.9}$$

where $T_{\text{out},i}$ represents the prescribed outdoor temperature for the corresponding glazed surface.

Thus, the thermal properties of the classroom envelope were treated as constant, but the associated heat transfer was resolved quasi-steadily during the CFD simulation. This means that the model did not solve transient heat storage within the wall layers; rather, it updated the conductive heat transfer continuously based on the instantaneous indoor-side temperature predicted by the airflow and energy solution.

3.5.2 Internal heat and contaminant generation

The internal heat gain from occupants was divided into sensible heat generation and moisture generation. Sensible heat released by occupants was calculated based on the number of occupants in each category and their corresponding sensible heat emission rate. Thus, the total sensible heat gain from occupants was determined as:

$$Q_{\text{people,sensible}} = \sum \left(N_i \times q_{\text{sensible},i}\right) \tag{3.10}$$

where $N_i$is the number of occupants of type i, and $q_{\text{sensible},i}$is the sensible heat generation rate per occupant (W). In the present study, sensible heat gains of 75 W per student and 100 W per teacher were used (ASHRAE Handbook—Fundamentals, Chapter 18).

Since moisture released by occupants was modeled in the CFD simulation as a water vapor mass source rather than as a direct latent heat input, the latent contribution was represented through the total water vapor generation rate:

$$\dot{m}_{\mathrm{H_2O,people}} = \sum\left(N_i \times \dot{m}_{\mathrm{H_2O},i}\right) \tag{3.11}$$

where $\boldsymbol{N_i}$ is the number of occupants of type $\boldsymbol{i}$, and $\boldsymbol{\dot{m}_{\mathrm{H_2O},i}}$is the water vapor generation rate per occupant (kg/s). In the present study, occupant moisture emission was represented with a water vapor generation rate of 0.022 g/s per student for an activity level of 1.2 met, while 0.024 g/s was assigned to the teacher to reflect an activity level of 1.6 met (ASHRAE 62.1 Handbook). Therefore, latent occupant effects were incorporated through species transport of water vapor in the CFD model rather than by imposing a separate latent heat source term.

$$\dot{m_{\mathrm{CO_2,people}}} = \sum\left(N_i\, \dot{m_{\mathrm{CO_2},i}}\right) \tag{3.12}$$

Similarly, Carbon dioxide generation from occupants was incorporated as an internal species source in the CFD model. CO_2 generation rate of 9.30×10^{-6} kg/s per student was adopted for students at 1.2 met, while a rate of 1.24×10^{-5} kg/s was used for the teacher at 1.6 met (ASHRAE 62.1 Handbook).

3.6 Governing equations

In the present simulation, the fluid mixture is assumed to behave as an incompressible ideal gas. This assumption is mathematically represented by the continuity equation for incompressible flow:

$$\nabla \cdot \boldsymbol{v} = 0 \tag{3.13}$$

where **v** is the velocity vector of the airflow.

This equation expresses the fact that the net volumetric flow into or out of any infinitesimal control volume is zero, or that the divergence of the velocity field is zero. Physically this means that the mass density at each point in the domain is constant, so that there is no local increase or decrease in mass within the domain.

From a practical perspective, this assumption helps to simplify the Navier–Stokes equations, thereby reducing computational complexity, allowing for the simulation to be more manageable and yet still give accurate airflow predictions in indoor scenarios at standard atmospheric conditions.

The turbulent airflow in the present study was modeled using the RNG k-ε turbulence model with enhanced wall treatment. The RNG k-ε model solves two additional transport equations: one for turbulent kinetic energy $(k)$and another for turbulent dissipation rate (ε). The transport equations are given as follows.

$$\frac{\partial}{\partial x_i}(\rho\varepsilon u_i) = \frac{\partial}{\partial x_j}\left(\alpha_\varepsilon \mu_{\text{eff}} \frac{\partial \varepsilon}{\partial x_j}\right) + C_{1\varepsilon}^{*}\frac{\varepsilon}{k}(G_k + C_{3\varepsilon}G_b) - C_{2\varepsilon}\rho\frac{\varepsilon^2}{k} - R_\varepsilon + S_\varepsilon \tag{3.14}$$

$$\frac{\partial}{\partial x_i}(\rho k u_i) = \frac{\partial}{\partial x_j}\left(\alpha_k \mu_{\text{eff}} \frac{\partial k}{\partial x_j}\right) + G_k + G_b - \rho\varepsilon - Y_M + S_k \tag{3.15}$$

where, ρ is the fluid density, u_i is the velocity component in the i-direction, k is the turbulent kinetic energy, $\varepsilon$is the turbulent dissipation rate, μ is the molecular viscosity, μ_t is the turbulent viscosity, and μ_{eff} is the effective viscosity. G_k represents the generation of turbulent kinetic energy due to mean velocity gradients, G_b is the generation of turbulent kinetic energy due to buoyancy, Y_M represents the contribution of fluctuating dilatation in compressible turbulence, and S_k and S_ε are user-defined source terms.

$$\mu_{eff} = \mu + \mu_t, \quad \mu_t = \rho C_\mu \frac{k^2}{\varepsilon} \tag{3.16}$$

The effective dynamic viscosity (μ_{eff}) represents the total viscosity used in turbulence modeling. It consists of the molecular (laminar) viscosity (μ) and the turbulent (eddy) viscosity (μ_t). This combined viscosity accounts for both molecular momentum diffusion and additional mixing caused by turbulence.

$$\frac{\partial \rho Y_i}{\partial t} + \nabla \cdot (\rho \vec{u} Y_i) = \nabla \cdot (\Gamma_i \nabla Y_i) + \dot{\omega}_\iota \tag{3.17}$$

$$\frac{\partial \rho Y_i}{\partial t} + \nabla \cdot (\rho \vec{u} Y_i) = \nabla \cdot (D_i \nabla Y_i) + \dot{\omega}_\iota \tag{3.18}$$

Equations (3.17) and (3.18) represent the general transient species transport equations used to model contaminant dispersion. These equations account for temporal variation, convection by airflow, diffusion due to molecular and turbulent mixing, and volumetric source terms ($\dot{\omega}_\iota$). The difference between the two forms lies in the representation of the diffusion coefficient (Γ_i or D_i), depending on modeling assumptions.

$$\frac{\partial \rho Y_{\mathrm{H_2O}}}{\partial t} + \nabla \cdot \left(\rho \vec{u} Y_{\mathrm{H_2O}}\right) = \nabla \cdot \left(D_{\mathrm{H_2O}} \nabla Y_{\mathrm{H_2O}}\right) + \dot{\omega_{\mathrm{H_2O}}} \tag{3.19}$$

$$\frac{\partial \rho Y_{\mathrm{air}}}{\partial t} + \nabla \cdot (\rho \vec{u} Y_{\mathrm{air}}) = \nabla \cdot (D_{\mathrm{air}} \nabla Y_{\mathrm{air}}) + \dot{\omega_{\mathrm{air}}} \tag{3.20}$$

$$\frac{\partial \rho Y_{Co2}}{\partial t} + \nabla \cdot (\rho \vec{u} Y_{Co2}) = \nabla \cdot (D_{Co2} \nabla Y_{Co2}) + \dot{\omega_{Co2}} \tag{3.21}$$

Equation (3.19), (3.20) and (3.21) represents the species transport of H_2O, Air and CO_2 respectively.

$$\Gamma_i = -D_i \nabla Y_i \tag{3.22}$$

Equation (3.22) represents the diffusive mass flux (Γ_i) based on Fick's law of diffusion. where D_i is the diffusive mass flux and ∇Y_i is the concentration gradient of species i. This relationship governs the diffusion driven transport of species in the flow domain.

3.7 Numerical analysis

The numerical analysis was carried out using a CFD-based methodology and with the help of CFD software to evaluate the indoor airflow, temperature field, and contaminant distribution in the classroom. After the solution convergence, the results were analyzed and assessed using a set of ventilation and comfort related performance indicators. The indoor air quality parameters were quantified using age of air and contaminant removal efficiency. The thermal comfort characteristics were evaluated using temperature distribution, velocity distribution, draft risk at different height level in the occupancy zone and air distribution index. The numerical analysis was structured to provide an integrated assessment of both ventilation effectiveness and indoor comfort performance for the investigated classroom ventilation strategies.

3.7.1 Indoor air quality

Indoor air quality parameters of each case were assessed using age of air and contaminant removal efficiency. These parameters were chosen to quantify the effectiveness of fresh air distribution and pollutant removal within the classroom. Age of air was used as an indicator of air freshness in the breathing plane of the occupancy zone. Contaminant removal efficiency was used to determine the ability of the ventilation system to extract internally generated pollutants i.e. carbon dioxide. Collectively, these parameters were used to compare the indoor air quality of the investigated air distribution strategies.

3.7.1.1 Age of air

The Age of air (AoA) is a widely used indoor air quality performance indicator that quantifies the average time required for fresh supply air to reach a specific location within an enclosed space. In this study we are mainly concerned with age of air in the breathing plane. It provides spatially resolved information about air renewal effectiveness and contaminant removal potential, making it particularly suitable for high-occupancy indoor environments such as classrooms. Unlike air change rate (ACH), which represents a global indicator, AoA shows local air quality performance variations and stagnation zones.

$$\nabla \cdot (\rho \vec{u} \varphi_i - \xi_i \nabla \varphi_i) = S_{\varphi_i} \tag{3.23}$$

The steady-state transport equation for a general scalar quantity (φ_i) in a fluid flow field is given in equation (3.23). It describes the net flow of the transported scalar quantity such as temperature, species concentration or age of air out of an infinitesimal control volume. Consists of both molecular diffusion and turbulence. S_{φ_i} is the source term, which is the volumetric generation/consumption of the scalar in the domain. ξ_i (Diffusion coefficient) represents the effective diffusion coefficient of the scalar variable. The Local mean age of air is determined in the present study by solving the general scalar transport equation in the CFD framework. The transported scalar variable represents the age of air (τ). We assume a unit source term (S = 1) over the entire domain of the room in order to calculate the residence time of air at every point in the room. This will allow the model to determine the time it takes for the provided outdoor air to

arrive at various points within the classroom. The lower the age of air, the fresher the air quality and the more effective the ventilation, while the higher the value, the slower the air renewal and the more stagnant the air quality.

$$\xi_i = (2.88 \times 10^{-5})\rho + \frac{\mu_{eff}}{Sc_t} \quad (3.24)$$

Equation (3.24) defines the effective diffusion coefficient (ξ_i) used in scalar transport modeling. The first term $(2.88 \times 10^{-5})\rho$ represents molecular diffusion scaled with fluid density. The second term, μ_{eff}/ Sc_t, accounts for turbulent diffusion, where μ_{eff} is the effective viscosity (sum of molecular and turbulent viscosity) and Sc_t is the turbulent Schmidt number. This formulation allows both molecular and turbulence-induced mixing to be considered in scalar transport.

3.7.2 Contaminant removal efficiency

To evaluate the indoor air quality in the in the classroom, Contaminant Removal Efficiency (CRE) was assessed within the breathing zone. CRE quantifies the effectiveness of the ventilation system in removing internally generated contaminant (CO_2) from occupied regions relative to the exhaust air, CRE provides a spatially resolved indicator of ventilation performance at occupant level.

$$\varepsilon_c = \frac{C_{out} - C_{in}}{C_{bz} - C_{in}} \times 100 \quad (3.25)$$

Where:

C_{out}= contaminant concentration at exhaust outlet

C_{in}= contaminant concentration at supply inlet

C_{bz}= area-weighted average contaminant concentration at breathing zone

Interpretation:

- $\varepsilon_c = 100 \rightarrow$ Perfect mixing ventilation
- $\varepsilon_c > 100 \rightarrow$ Efficient contaminant removal (e.g., displacement or stratified flow effect)

- $\varepsilon_c < 100 \rightarrow$ Poor ventilation performance or short-circuiting between supply and exhaust

A value greater than unity indicates that the breathing zone concentration is lower than the exhaust concentration, suggesting preferential removal of contaminants from occupied regions.

3.7.3 Comfort parameters

The thermal comfort performance of the classroom was evaluated using temperature and velocity distribution, draft risk, and air distribution index. These parameters were selected to assess the indoor thermal environment from both local and overall performance perspectives. Temperature distribution was used to examine the spatial variation of air temperature within the classroom and to identify thermal stratification or non-uniformity in the occupied zone. Draft risk was used to evaluate the likelihood of local discomfort caused by unwanted air movement at occupant level. The air distribution index was used as an integrated indicator combining thermal and ventilation performance, thereby providing an overall basis for comparing the effectiveness of the investigated ventilation strategies.

3.7.3.1 Temperature and velocity distribution

Air temperature and velocity fields were extracted directly from the CFD solution after convergence had been achieved for each ventilation configuration. Temperature and velocity magnitude contours were plotted on the vertical mid-plane of the classroom in order to evaluate the indoor airflow structure and thermal distribution. These contour plots were used to identify key characteristics such as supply jet development, airflow penetration into the occupied zone, thermal stratification, stagnant regions, and the general pattern of air circulation within the space. The temperature field provided information on the spatial distribution of thermal conditions and the effectiveness of sensible heat removal, while the velocity field illustrated the strength and direction of air movement generated by each ventilation strategy.

Special emphasis was placed on the air velocity at breathing height because of its direct relationship with both indoor air distribution and local thermal comfort. Excessive air velocity in the occupied zone can produce draft sensation and local discomfort, whereas insufficient air movement may reduce air renewal effectiveness and weaken

contaminant removal. Accordingly, the velocity magnitude at breathing level was examined as an important indicator of the balance between ventilation effectiveness and comfort performance in the classroom.

3.7.3.2 Draft Risk (DR)

Draft risk quantifies the percentage of occupants likely to feel local cooling discomfort due to unwanted air movement. It was calculated according to ISO 7730:

$$DR = (34 - T_a)\,(V - 0.05)^{0.62}\,(0.37\,V\,Tu + 3.14) \tag{3.26}$$

Where:

T_a= local air temperature (°C)

V= local mean air velocity (m/s)

Tu= turbulence intensity (%)

Draft risk was evaluated only for velocities between 0.05–0.5 m/s, as recommended by standards.

The turbulence intensity was obtained from CFD results using:

$$Tu = \frac{\sqrt{2k/3}}{V}\ 100\ \% \tag{3.27}$$

Where k is turbulent kinetic energy.

Spatial DR contours were plotted at breathing height, and area-weighted average DR values were calculated for each ventilation configuration.

Interpretation:

- DR < 10% → Low draft risk
- 10% < DR < 20% → Acceptable
- DR > 20% → High draft discomfort

3.7.3.3 Air distribution index

To evaluate the overall effectiveness of the ventilation system by combining both thermal comfort and ventilation performance, the Air Distribution Index (ADI) was

used. In indoor environmental studies, a single parameter such as temperature, velocity, or contaminant concentration alone may not fully describe the performance of a ventilation system. A system may provide good contaminant removal but poor thermal comfort, or it may provide acceptable thermal conditions while delivering fresh air inefficiently. Therefore, ADI is employed as a combined performance indicator to assess how well the ventilation system simultaneously satisfies these two important aspects.

The ADI used in the present study is expressed as

$$ADI = \left[\left(1 - \frac{|S|}{3}\right)\varepsilon_t + \frac{\varepsilon_c}{\tau^*}\right] \tag{3.28}$$

where:

- S= thermal sensation index
- ε_t= temperature effectiveness
- τ^*= normalized age of air
- $\boldsymbol{\varepsilon_c}$= contaminant removal effectiveness

$$\tau^* = \frac{\overline{\tau_{bz}}}{\tau_n} \tag{3.29}$$

Equation (3.29) defines the dimensionless age of air (τ^*), calculated as the ratio of the average breathing-zone age of air ($\overline{\tau_{bz}}$) to the nominal age of air (τ_n). This parameter provides a normalized measure of ventilation performance within the occupied zone.

Interpretation:

- $\tau^* = 1 \rightarrow$ Ideal mixing ventilation
- $\tau^* < 1 \rightarrow$ Better-than-mixing performance (efficient air renewal)
- $\tau^* > 1 \rightarrow$ Poor ventilation / stagnation regions

In this study, spatial contours of τ^*were plotted at breathing height (1.1 m) to evaluate ventilation performance within the occupied zone. Area-weighted averages of τ^*were used for quantitative comparison between cases.

$$\varepsilon_t = \frac{T_{\text{out}} - T_{\text{in}}}{T_{\text{oz}} - T_{\text{in}}} \tag{3.30}$$

where:

- T_{out}= exhaust or outlet air temperature
- T_{in}= supply air temperature
- T_{oz}= average temperature in the occupied zone

The temperature effectiveness, ε_t, represents the ability of the ventilation system to remove heat from the occupied zone. It is defined as the ratio of the temperature difference between outlet air and supply air to the temperature difference between occupied-zone air and supply air. Higher values of $\varepsilon_t$indicate more effective heat removal from the occupied zone.

Thermal comfort contribution

$$\left(1 - \frac{|\,S\,|}{3}\right)\varepsilon_t$$

The term *S*represents the thermal sensation of occupants. It indicates whether the indoor environment feels too cold, neutral, or too warm. In general, the thermal sensation scale ranges approximately from:

- $\boldsymbol{S = -3}\rightarrow$ cold
- $\boldsymbol{S = 0}\rightarrow$ neutral
- $\boldsymbol{S = +3}\rightarrow$ hot

In the ADI equation, the absolute value $|\,S\,|$is used because both excessive coldness and excessive warmth reduce comfort.

The term $\varepsilon_t$represents the temperature effectiveness, which indicates how efficiently the ventilation system removes excess heat from the occupied zone or maintains the desired thermal state.

It is used to evaluate whether the supplied air is effectively improving the thermal environment around occupants rather than simply mixing with the room air without

useful cooling or heating effect. A higher value of $\varepsilon_t$indicates that the system is more effective in controlling indoor thermal conditions.

In the ADI equation, ε_t is multiplied by the thermal sensation weighting term. This means that even if the system has high temperature effectiveness, its contribution to ADI is reduced if occupants still experience thermal discomfort. Therefore, the equation ensures that thermal performance is only rewarded when it is associated with acceptable human sensation.

Ventilation or air quality contribution

$$\frac{\varepsilon_c}{\tau^*}$$

The term τ^*represents the normalized age of air, which is a dimensionless form of local mean age of air. It describes how fresh or stale the air is in the breathing zone relative to the nominal room air age.

Age of air is the average time required for supply air to reach a certain location in the room. Lower age of air indicates fresher air and better air renewal. By normalizing it, the performance can be compared across different systems independently of airflow rate and room size.

In general:

- lower age of air means better ventilation
- better ventilation leads to faster delivery of fresh air to occupants
- normalized age helps compare actual air renewal against an ideal or nominal reference

In the ADI equation, $\tau^*$is included in the ventilation performance part because it reflects the freshness of air in the occupied zone.

The term ε_c represents the contaminant removal effectiveness, which indicates how effectively internally generated pollutants such as CO_2 are removed from the breathing zone.

It is commonly interpreted as:

- $\varepsilon_c > 1 \rightarrow$ better than perfect mixing, efficient contaminant removal

- $\varepsilon_c = 1 \rightarrow$ perfect mixing
- $\varepsilon_c < 1 \rightarrow$ poor removal performance or short-circuiting

A higher value of ε_c means that contaminants are more effectively displaced away from occupants and exhausted from the space. In the present study, this term is important because classroom occupants continuously generate CO_2, making contaminant removal a key indicator of ventilation quality.

When divided by τ^*, it forms the second part of ADI, which accounts for the system's ability to provide fresh air and remove pollutants from the occupied zone.

ADI reflects the combined ability of a ventilation system to maintain acceptable thermal conditions while also removing contaminants effectively from the occupied zone. Thus, ADI allows the four ventilation strategies to be assessed on a common basis by considering both thermal and contaminant-related aspects of indoor environmental quality.

Interpretation of ADI

A higher ADI value indicates better overall performance of the ventilation system. This means:

- acceptable or near-neutral thermal sensation
- effective temperature control
- fresher air in the occupied zone
- better contaminant removal

A lower ADI value indicates poorer overall performance, which may result from:

- thermal discomfort
- weak temperature effectiveness
- older air in the breathing zone
- poor contaminant removal efficiency

Therefore, ADI can be used as a comparative index to rank different ventilation strategies in terms of their combined indoor environmental performance.

Relevance to the present study

In the present study, ADI was used to compare the performance of displacement ventilation, ceiling diffuser ventilation, and wall grill ventilation in a high-occupancy classroom. Since the objective of the study was not only to assess ventilation effectiveness but also to evaluate thermal comfort within the breathing zone, ADI provides a suitable combined metric.

For classroom environments, this is particularly important because students are exposed for prolonged periods and require both:

- effective fresh air delivery for good indoor air quality, and
- acceptable thermal conditions for comfort and learning performance

3.7.4 The role of supply velocity on Archimedes number

The flow regime for each air distribution system was then assessed using the Archimedes number, which expresses the relative importance of buoyancy force to inertial force and is commonly written as.

$$Ar = \frac{g\,\beta\,\Delta T\,H}{U^2} \tag{3.31}$$

Where:

- g= gravitational acceleration (9.81 m/s²)
- β= thermal expansion coefficient of air (1/T)
- ΔT= temperature difference between supply air and room air (K)
- H= characteristic length (m)
- U= inlet air velocity (m/s)

The Archimedes number represents the ratio of buoyancy forces to inertial forces in the airflow. Its magnitude provides insight into the dominant airflow mechanism within the ventilated space.

- Ar << 1 → inertia dominated flow (mixing ventilation)
- Ar ≈ 1 → mixed influence of buoyancy and momentum
- Ar > 1 → buoyancy dominated flow (displacement ventilation)

Four diffusers were used for all ventilation systems (DV, SV, CD, and WG) to distribute the fixed 6 ACH supply airflow more uniformly because previous research has shown that, at the same supply air temperature and total airflow rate, increasing the number of diffusers improves the breathing-zone air distribution effectiveness (Lee et al., 2009).

The selected DV velocities of 0.17 m/s, 0.25 m/s, and 0.35 m/s represent different buoyancy-to-momentum conditions as shown in Table 3.4. The lower-velocity case of 0.17 m/s has a higher Archimedes number and represents stronger buoyancy-dominated displacement flow, while the higher-velocity case of 0.35 m/s has a lower Archimedes number and represents increased momentum influence. Hence, these cases were chosen to examine how changes in supply velocity alter the buoyancy-driven behavior of displacement ventilation under the same ACH and supply temperature.

Table 3.4: Supply cases for DV

Case No.	Face velocity (m/s)	No. of diffusers	Effective area per diffusers (m^2)	ACH
1.	0.17	4	0.67	6
2.	0.25	4	0.47	6
3.	0.35	4	0.33	6

The selected SV velocities of 0.5 m/s, 0.8 m/s, and 1.2 m/s represent different buoyancy-to-momentum conditions for stratum ventilation as shown in Table 3.5. Since the ACH and supply temperature were kept constant, changing the face velocity mainly changes the Archimedes number and the relative dominance of buoyancy and supply momentum. The lower-velocity case of 0.50 m/s has a higher Archimedes number and represents a stronger buoyancy-influenced condition, but with weaker horizontal jet penetration across the occupied zone. The intermediate-velocity case of 0.80 m/s provides a more balanced condition between buoyancy effect and supply momentum, allowing better air delivery at the breathing level. The higher-velocity case of 1.20 m/s has a lower Archimedes number and represents a more momentum-dominated flow, where stronger jet penetration may increase mixing and disturb the intended occupied-zone air distribution. Hence, these cases were chosen to examine how changes in supply velocity alter the buoyancy–momentum interaction and breathing-zone air distribution performance of stratum ventilation under the same ACH and supply temperature.

Table 3.5: Supply cases for SV

Case No.	Face velocity (m/s)	No. of diffusers	Effective area per diffusers (m^2)	ACH
1.	0.50	4	0.23	6
2.	0.80	4	0.15	6
3.	1.20	4	0.10	6

The selected CD velocities of 1.0 m/s, 1.4 m/s, and 2.0 m/s represent different momentum-dominated mixing conditions for the ceiling diffuser system as shown in Table 3.6. Since the ACH and supply temperature were kept constant, changing the face velocity mainly changes the Archimedes number and the relative strength of supply momentum compared with buoyancy. However, unlike DV and SV, the ceiling diffuser system is primarily a mixing ventilation strategy; therefore, the selected velocities were used to examine how different levels of supply momentum affect room air mixing, ceiling jet development, recirculation, and air distribution in the occupied zone. The lower-velocity case of 1.0 m/s has a relatively higher Archimedes number and weaker jet momentum, which may reduce mixing effectiveness and limit fresh-air distribution. The supply velocity of 1.40 m/s case can provide a more balanced mixing condition, where the supply jet has sufficient momentum to distribute air without excessive local disturbance. The higher velocity case of 2.00 m/s has a lower Archimedes number and stronger momentum dominance, which can intensify mixing and recirculation but may also increase draft risk and reduce local contaminant removal effectiveness. Hence, these cases of varying inlet supply velocity were chosen to evaluate how changes in supply velocity influence the mixing behavior and overall ventilation performance of the ceiling diffuser system under the same ACH and supply temperature.

Table 3.6: Supply cases for CD

Case No.	Face velocity (m/s)	No. of diffusers	Effective area per diffusers (m^2)	ACH
1.	1.00	4	0.12	6
2.	1.40	4	0.08	6
3.	2.00	4	0.06	6

The supply velocities at the wall grills of 1.40 m/s, 2.00 m/s, and 2.84 m/s reflect various flow regimes characterized by dominant momentum in the wall grill ventilation

scenario. As ACH and supply temperature remained unchanged throughout the numerical simulation, altering the supply velocity affects only the Archimedes number and momentum to buoyancy ratio. Yet, since the wall grill ventilation system belongs to the category of traditional mixing-type systems, the considered supply velocities were employed to investigate how the growing wall jet momentum influences room air circulation, recirculation efficiency, contaminant mixing, and draft potential within the breathing zone. In the low-velocity flow regime of 1.40 m/s, the higher value of the Archimedes number indicates a lower level of wall jet momentum and, consequently, a weak room air circulation and insufficient air distribution. The mid-velocity flow regime of 2.00 m/s ensures a stronger wall jet momentum, improving air mixing and distribution throughout the room. The high-velocity flow regime of 2.84 m/s features a lower Archimedes number and momentum domination, which can intensify mixing and recirculation but may also increase local air movement, draft risk, and contaminant redistribution near the breathing zone.

Table 3.7: Supply cases for WG

Case No.	Face velocity (m/s)	No. of diffusers	Effective area per diffusers (m^2)	ACH
1.	1.40	4	0.08	6
2.	2.00	4	0.06	6
3.	2.84	4	0.04	6

3.8 Selection of ventilation layouts for comparative analysis

In this particular research, only one layout per each of the four ventilation strategies was chosen in order to perform an equal evaluation of all the three parameters mentioned above: air flow, thermal comfort, and indoor air quality. It is worth saying that the purpose of this work was not to optimize several diffuser layouts for each ventilation approach, but to investigate the unique properties of each approach applied to a certain room layout. As such, the criterion for choosing just one layout for each particular ventilation system involved the consideration of the working principles of each approach, its applicability to the specified room geometry, as well as ensuring the necessary air velocity at the same boundaries conditions.

3.8.1 Displacement ventilation

For displacement ventilation strategy down-supply and up-exhaust ventilation configuration was selected in the present study because it has been reported to provide higher ventilation effectiveness and improved delivery of fresh air into the breathing zone compared to other supply arrangements (Jahanbin & Semprini, 2024).

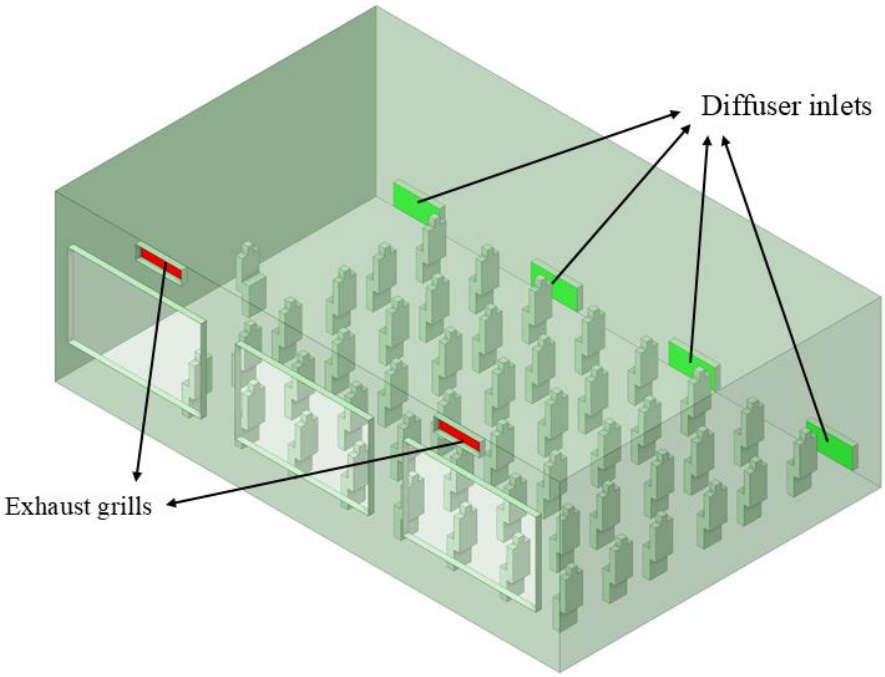

Figure 3.5: Displacement Ventilation

Additionally, this configuration conforms to the desired flow dynamics of stratified ventilation systems, whereby supply air is supplied from a lower elevation and exhausted from a higher elevation position to facilitate the upward buoyancy flow of pollutants and heat.

This flow dynamics is especially significant in densely populated classroom settings, where the creation of thermal plumes by individuals could facilitate vertical mixing of the room air. The flow dynamics also provide a unique and distinctive path for air distribution, which would enable the assessment of ventilation performance under prescribed conditions.

3.8.2 Stratum ventilation

For stratum ventilation a side wall supply arrangement at occupant level with upper-level exhaust was selected for the stratum ventilation system in the present study. Stratum ventilation is intended to deliver conditioned air directly into the occupied zone through horizontal.

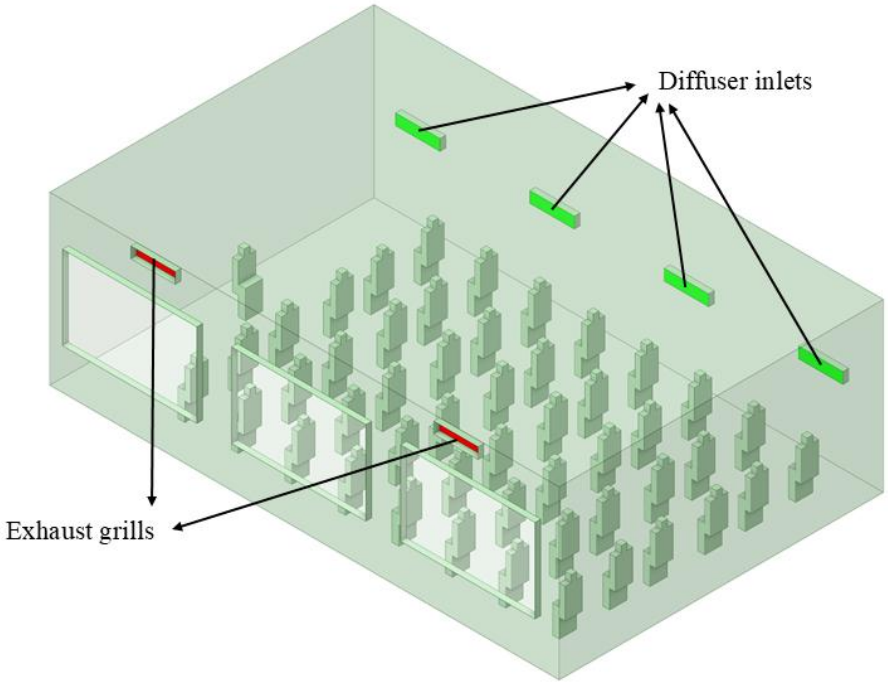

Figure 3.6: Stratum Ventilation

Air jets, thereby improving the removal of heat and internally generated contaminants from the breathing zone. Previous studies have shown that, when properly designed, stratum ventilation can provide acceptable thermal comfort and effective air distribution in classrooms and other densely occupied spaces, while also performing well in heat and contaminant removal.

Supplying air closer to seated occupants shortens the path to the breathing zone, reduces unnecessary upper-room mixing, and improves fresh air delivery where it is most needed. This makes the arrangement suitable for classrooms, where horizontal supply jets interact with occupant thermal plumes to carry heat and contaminants upward toward the exhaust. Therefore, the selected layout was considered appropriate for

representing the typical airflow behavior and ventilation performance of stratum ventilation in the present study.

3.8.3 Ceiling diffuser

Central supply with corner exhaust configuration was adopted for this ventilation system in this study because previous CFD investigations have shown that locating the air supply near the center of the room provides more uniform air and improved ventilation performance compared with other supply arrangements (Lin et al., 2005).

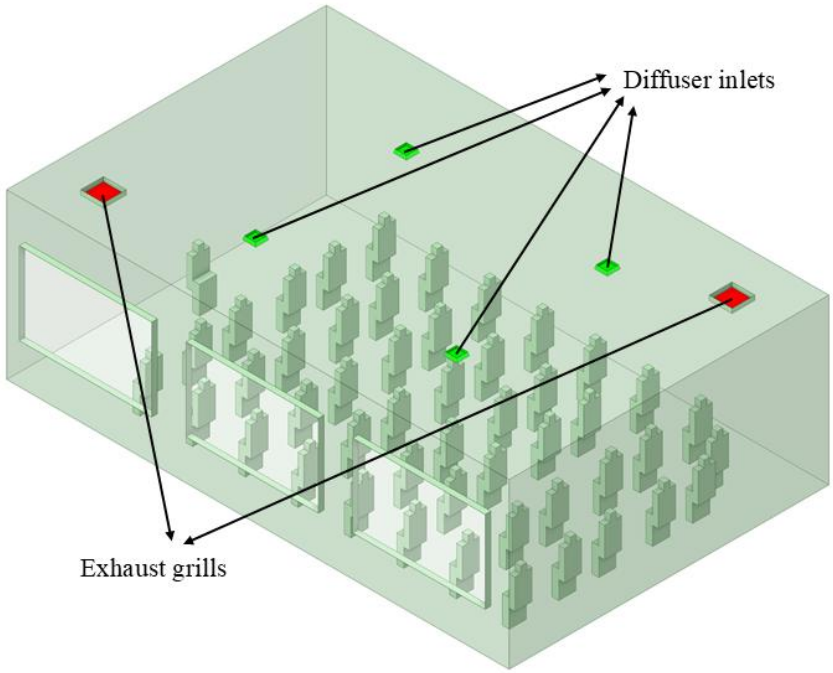

Figure 3.7: Ceiling diffusers

Also, central supply leads to a relatively balanced radial distribution of the supply air, which is beneficial for attaining the required well-mixed indoor conditions in conventional mixing ventilation.

The location of exhaust vents in the corners ensures the evacuation of the mixed room air while reducing local recirculation between the supply and return vents. This design configuration thus provides a reasonable representation of the physical arrangement that can be used in assessing the flow dynamics and ventilation performance of the mixed ventilation system under consideration.

3.8.4 Wall grills

High supply and low exhaust configuration have been selected for the wall grill ventilation system because previous studies have shown that supplying air from an elevated wall location and exhausting it at a lower level promotes effective air circulation and enhances ventilation performance in mechanically ventilated spaces (Awbi, 2003).

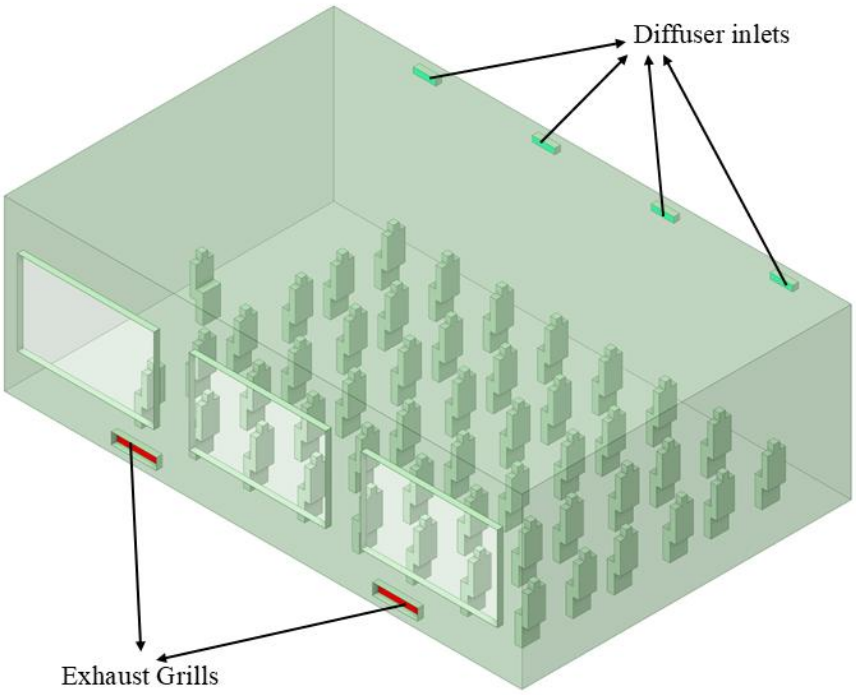

Figure 3.8: Wall grill system

Along with this, the raised wall supply can be utilized to disperse the air jet over the area of the room before it flows down into the area of occupancy; and the low-level exhaust will help evacuate cooler, contaminated air from the lower portion of the room. This helps to allow for continuous air flow throughout the class and may help to minimize stagnant areas around occupants. Hence, the selected configuration was deemed to be appropriate for typical airflow pattern and ventilation behavior of the wall grill system in the current study.

3.9 Mesh independence test

A mesh independence study was conducted to make sure that the numerical results are not strongly dependent upon the grid resolution. The poly-hexacore mesh was used together with tetrahedral surface elements to generate five different meshes with

varying numbers of elements. The number of cells in the meshes varied from about 2.14 million to 6.58 million cells. The air temperature and velocity magnitude distribution for each mesh case were assessed with air temperature at the occupied zone (0–1.2 m) and velocity magnitude being the two important parameters to consider for both ventilation performance and thermal comfort.

The difference in the temperature and velocity between mesh case 3 and the finer meshes was negligible, and mesh no. 3 (around 5.6 million elements) was chosen for the final simulations. Table 3.8. demonstrates that this mesh is grid independent.

Table 3.8: Mesh independence test

Mesh no.	Elements		T(°C)	v (m/s)
	Hex core	Tetrahedral		
1.	2,138,264	381,929	297.172	0.126
2.	3,435,583	556,681	297.113	0.122
3.	**4,778,592**	**850,589**	**297.061**	**0.110**
4.	5,497,438	904,569	296.971	0.109
5.	6,586,228	1,102,323	296.963	0.108

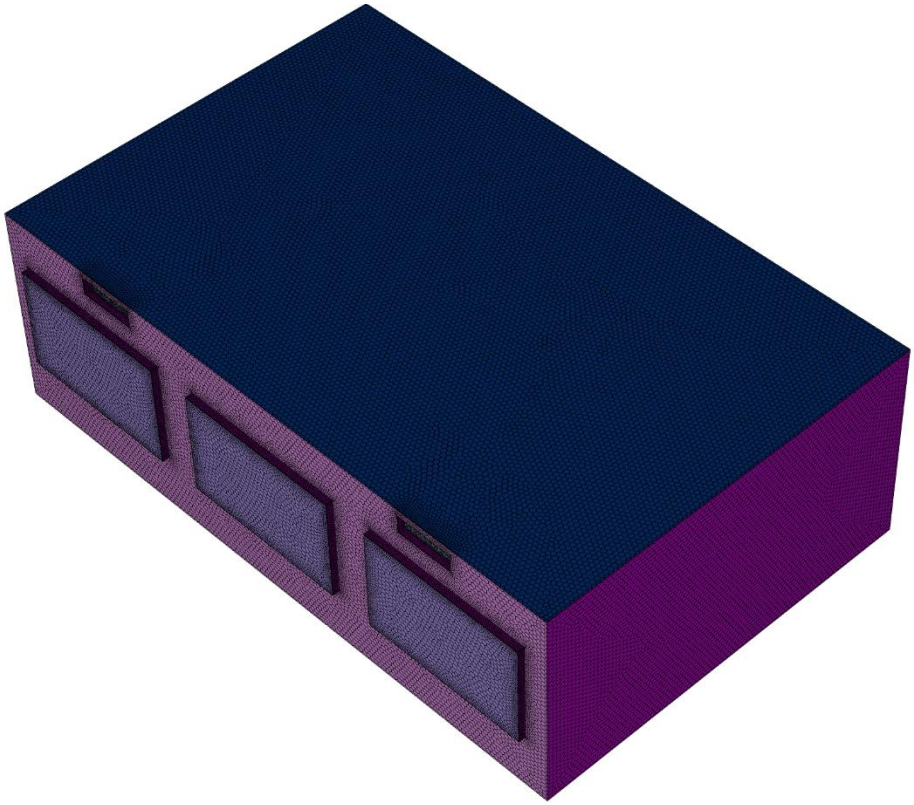

Figure 3.9: Displacement ventilation mesh

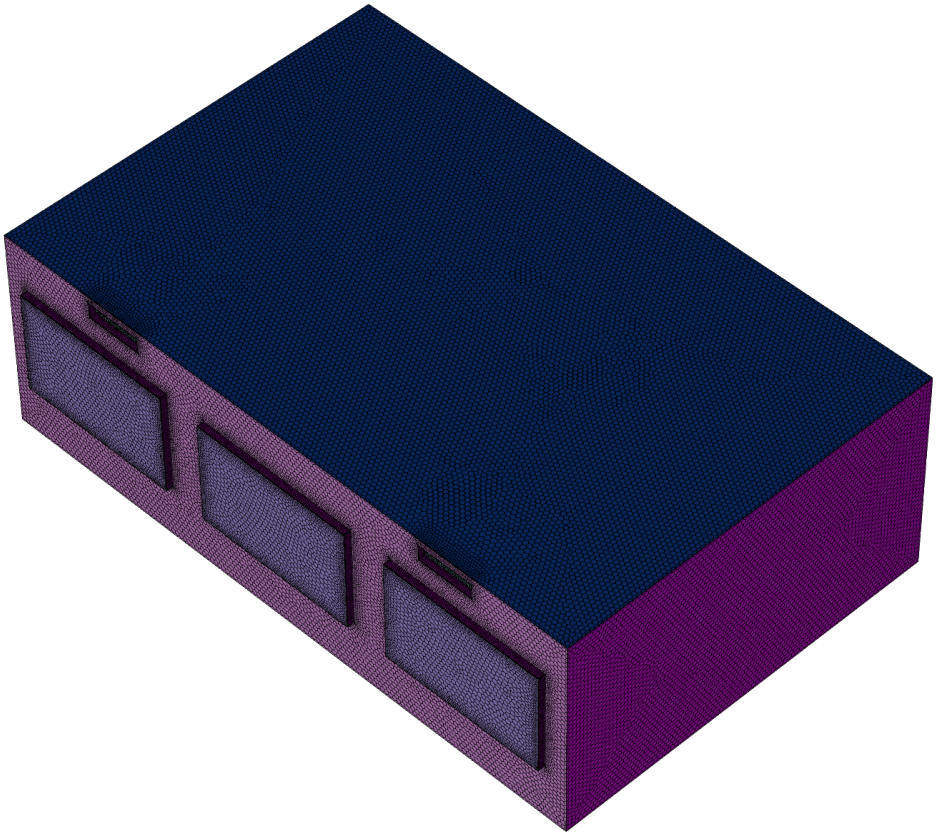

Figure 3.10: Stratum ventilation mesh

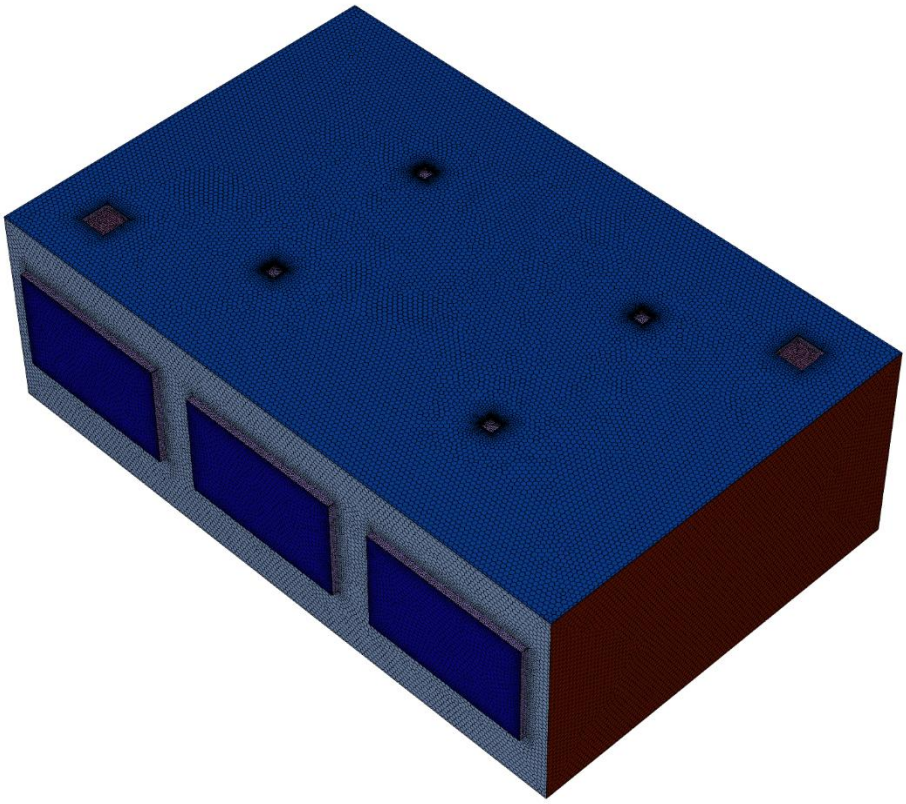

Figure 3.11: ceiling diffuser mesh

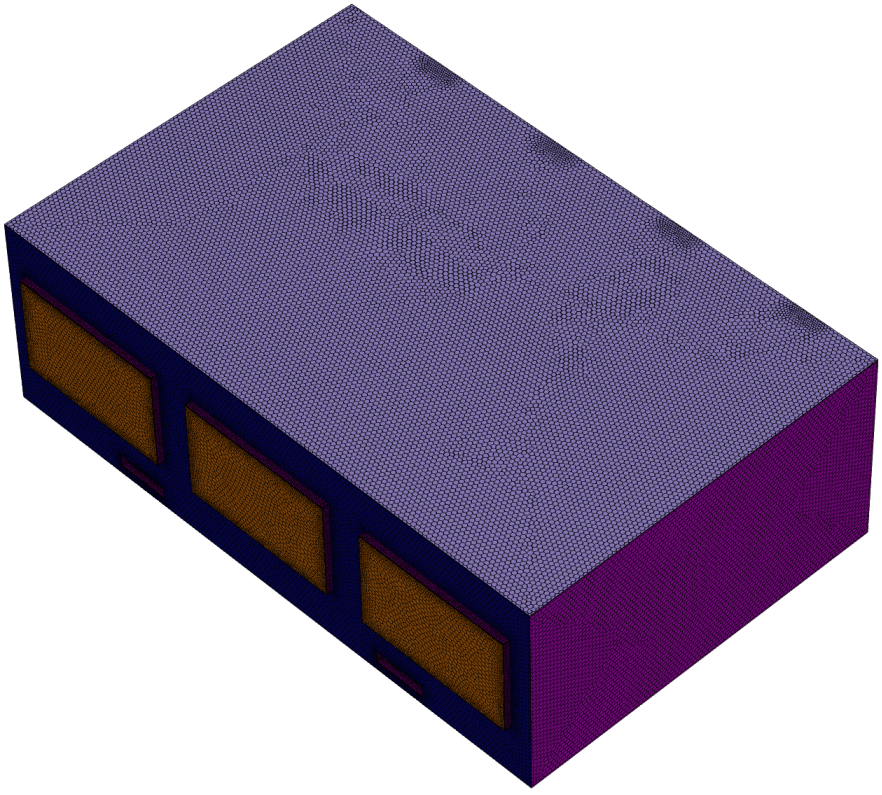

Figure 3.12: Wall grills mesh

The minimum orthogonal quality of the generated meshes was 0.64 and the maximum skewness was 0.48, which demonstrates a good mesh quality for all 12 cases. The generated meshes for the displacement ventilation, stratum ventilation, ceiling diffuser, and wall grill cases are shown in Figures 3.9, 3.10, 3.11, and 3.12, respectively.

The three-dimensional governing equations were solved using the FVM (Finite Volume Method) in CFD software. A pressure based second-order upwind scheme was used to discretize the convective terms in the governing equations. In the finite volume method, the transport equations are integrated over each control volume, and the values of transported variables such as velocity, temperature, turbulence quantities, and scalar concentration are required at the cell faces. In a first-order upwind scheme, the face value is taken directly from the upstream cell, which is stable but can introduce high numerical diffusion. In contrast, the second-order upwind scheme reconstructs the face value using a Taylor-series expansion from the upstream cell centroid. Therefore, both the upstream cell value and its spatial gradient are used to estimate the face value. This improves the accuracy of the solution, especially in regions with strong velocity, temperature, or contaminant gradients

The SIMPLE algorithm works through the following main steps. The first step is to make an initial assumption of pressure field. With this guessed pressure field, the momentum equations are solved to get some preliminary velocity components. These provisional velocities do not necessarily satisfy the mass conservation exactly. Thus, the continuity equation is used to obtain a pressure correction equation. The pressure field is then corrected and the velocity components are updated by using the corrected pressure field. This procedure is iterated until the difference in mass, momentum, energy and scalar transport equations is small enough.

Convergence was monitored using residual histories, with under relaxation applied to stabilize momentum and turbulence equations. Convergence criteria were set to 10^{-3} for momentum, 10^{-6} for energy, and 10^{-4} for user-defined scalars. Finally, the heat flux balance across domain boundaries was checked to ensure the overall error remained below 0.1%.

3.10 Supply scenario for comparative analysis

A supply air temperature of 291.15 K, supply relative humidity of 72%, and ventilation rate of 6 ACH were imposed for all four ventilation methods and total of 12 simulations. These boundary conditions were determined through a preliminary iterative assessment. During iterative approach, several trial cases were examined to achieve an air temperature of approximately 297.15 K in the breathing zone for the displacement ventilation case of 0.17 m/s inlet supply velocity. The selected supply condition was then maintained for the remaining ventilation methods and their various inlet velocity cases to provide a uniform basis for comparative evaluation.

CHAPTER FOUR: RESULTS AND DISCUSSION

This chapter presents the findings of the numerical analysis performed under identical supply conditions for all four ventilation methods and their different inlet velocity supply cases. A supply air temperature of 291.15 K, relative humidity of 72%, and ventilation rate of 6 ACH were maintained in every case to ensure a consistent basis for comparison.

4.1 Ventilation performance

The ventilation performance of the investigated cases was evaluated using age of air and contaminant removal efficiency. These parameters were selected to assess the effectiveness of fresh-air distribution, air renewal, and pollutant removal within the classroom. The results for each parameter are discussed in the following subsections to compare the ventilation behavior of the four air distribution strategies.

4.1.1 Age of air

Figure 4.5 shows the variation of age of air for displacement ventilation (DV), stratum ventilation (SV), ceiling diffuser (CD), and wall grill (WG) systems at the same air change rate of 6 ACH and the same supply air temperature. Since the nominal time constant at 6 ACH is approximately 600 s, values lower than 600 s indicate faster renewal of air in the evaluated zone, whereas values close to or above 600 s indicate slower local air replacement. The mean age of air is a widely used ventilation-performance indicator because it represents how long supplied fresh air takes to reach a given region inside the room (Davidson et al., 1987).

For displacement ventilation, the age of air increased from approximately 416 s at 0.17 m/s to 436 s at 0.25 m/s and 461 s at 0.35 m/s. The age of air distribution in the mid-vertical plane for different displacement cases is shown in Figure 4.1. Although all DV cases remained well below the nominal air-change time of 600 s, the increasing trend suggests that raising the supply velocity slightly weakened the ideal displacement-flow behavior. At lower velocity, the cool supply air spreads more gently near the floor and is lifted upward by thermal plumes generated by occupants, which improves fresh-air delivery to the occupied zone (Lin et al., 2005). This trend is consistent with displacement ventilation theory and CFD studies showing that supply location and

buoyancy-driven stratification strongly influence local mean age of air and indoor air quality performance (Lin et al., 2005).

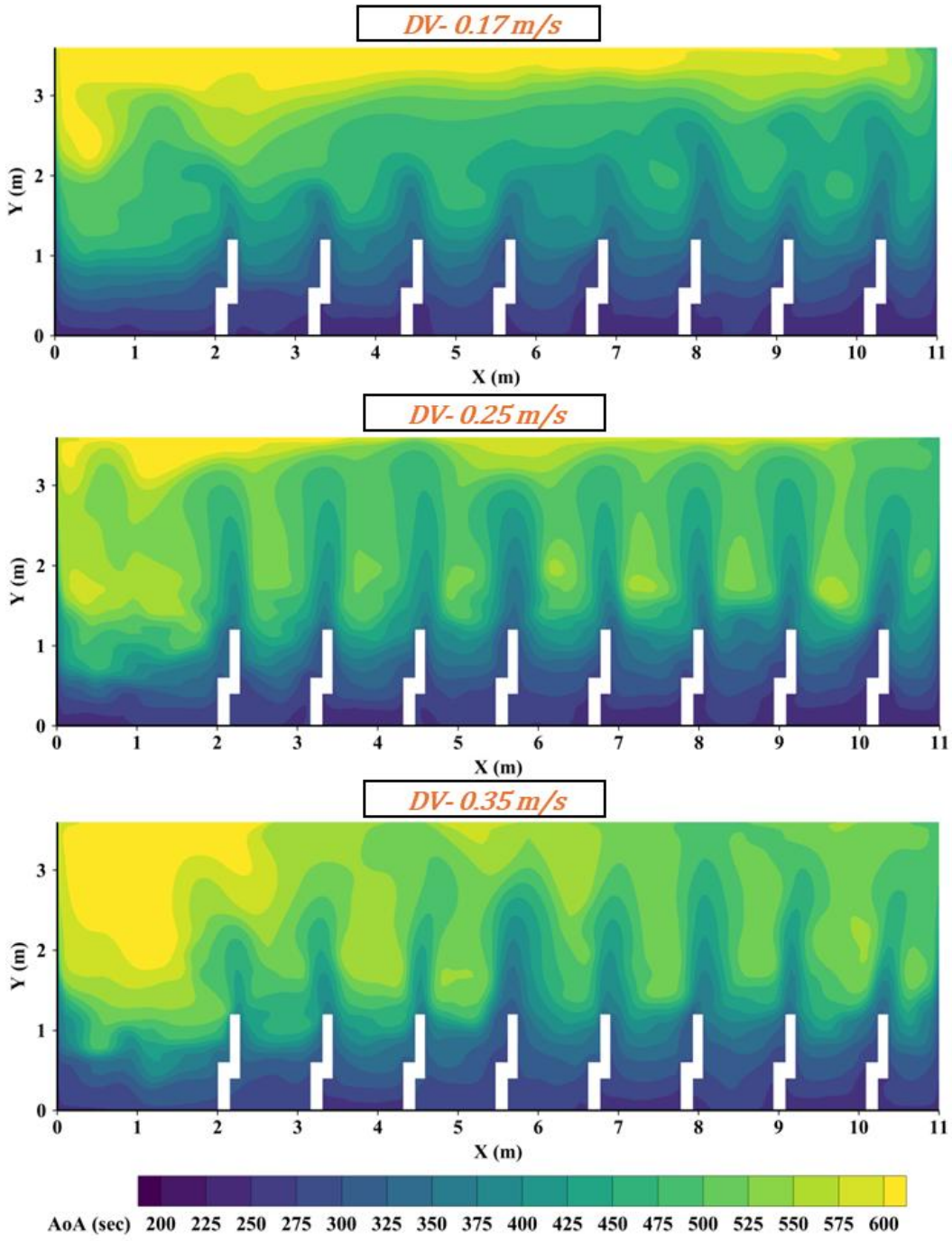

Figure 4.1: Age of air distribution in mid-vericle plane for DV cases

For stratum ventilation, the age of air was approximately 478 s at 0.5 m/s, decreased to 458 s at 0.8 m/s, and then increased to 502 s at 1.2 m/s. The age of air distribution in the mid-vertical plane for stratum displacement cases is shown in Figure 4.2. This indicates that the velocity of 0.8 m/s produced the most effective air renewal among the

SV cases. At very low velocity, the supply jet may not penetrate sufficiently across the occupied zone, while at higher velocity, excessive mixing can disturb the intended breathing-zone air layer (Lin et al., 2011).

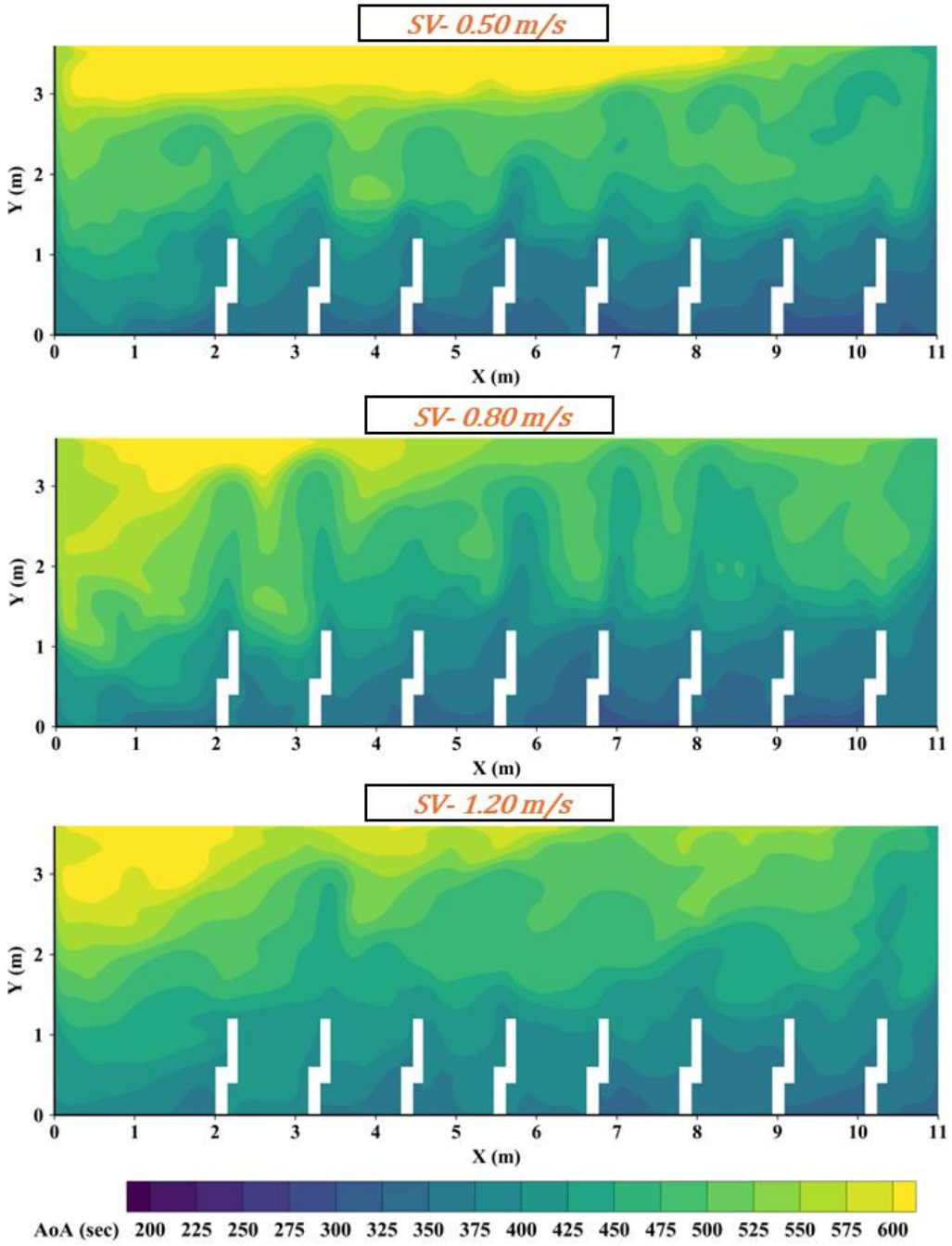

Figure 4.2: Age of air distribution in mid-vertical plane for SV cases

The result agrees with published studies on stratum ventilation, which show that air terminal type, supply jet behavior, and interaction between momentum and buoyancy

strongly affect local mean age of air, temperature distribution, and contaminant transport (Yao et al., 2014).

For the ceiling diffuser system, the age of air was approximately 612 s at 1.0 m/s, reduced to 579 s at 1.4 m/s, and increased again to about 632 s at 2.0 m/s.

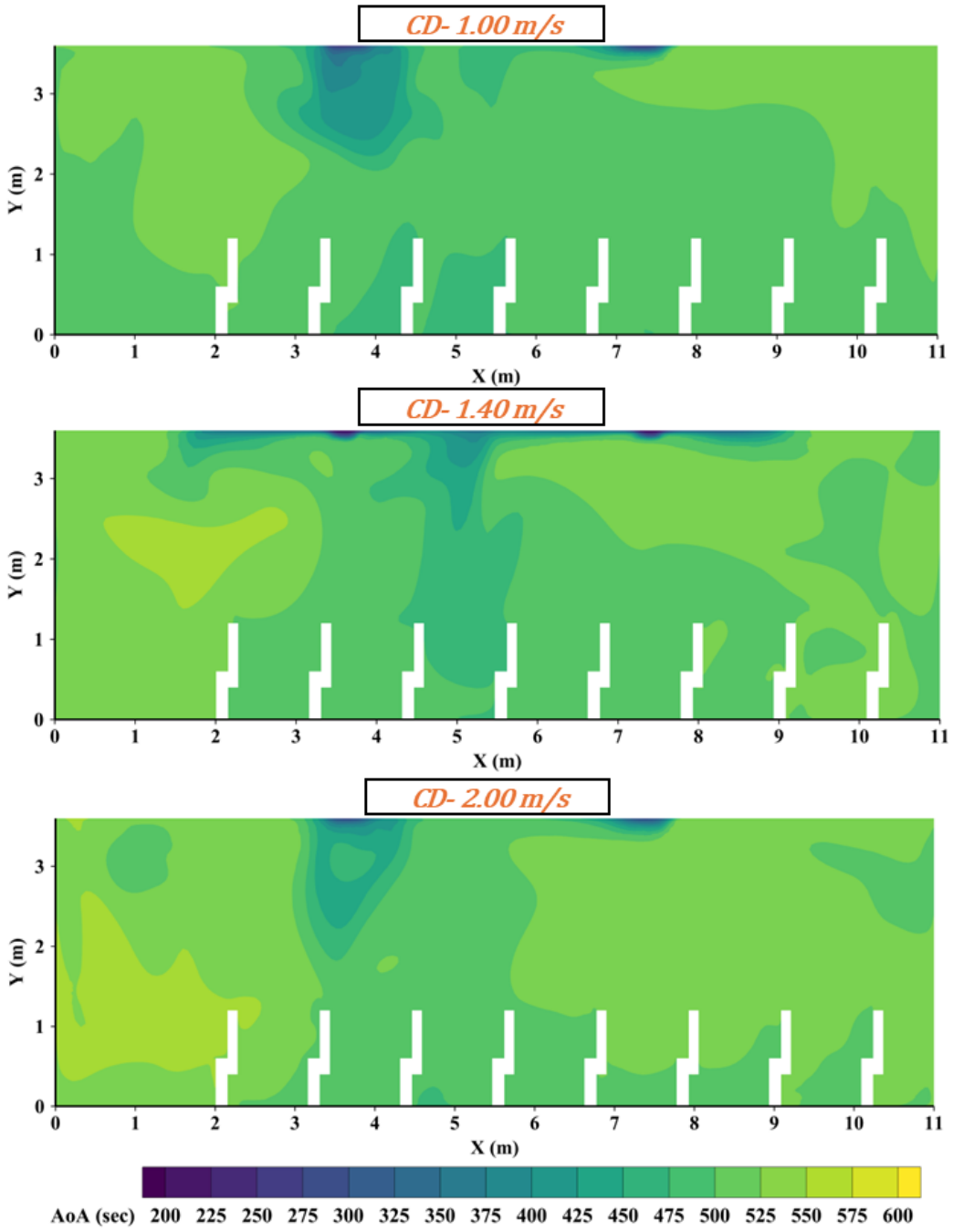

Figure 4.3: Age of air distribution in mid-vertical plane for CD cases

The age of air distribution in the mid-vertical plane for different ceiling diffusers cases is shown in Figure 4.3. The lowest value at 1.4 m/s suggests that a moderate supply

velocity improved room mixing and helped distribute fresh air more effectively. However, the higher value at 2.0 m/s indicates that increasing velocity further did not necessarily improve ventilation effectiveness, possibly because the ceiling jet promoted recirculation and non-uniform air replacement in the occupied zone (Aziz et al., 2012).

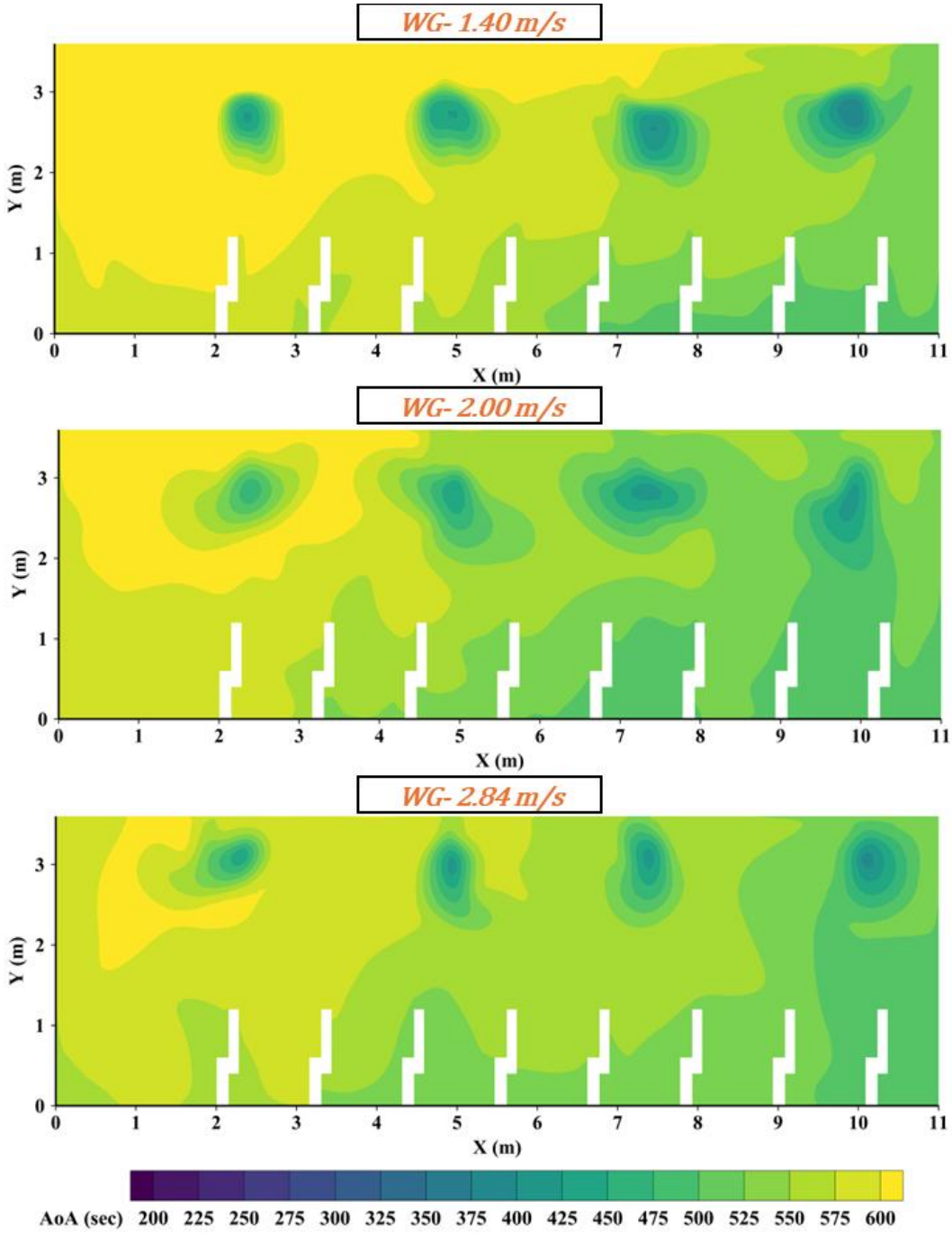

Figure 4.4: Age of air distribution in mid-vertical plane for WG cases

For the wall grill system, the age of air remained the highest among the four systems, with values of approximately 634 s at 1.4 m/s, 622 s at 2.0 m/s, and 661 s at 2.84 m/s.

The lowest WG value occurred at the intermediate velocity, but even this value was higher than the nominal time constant of 600 s. This indicates that, under the present layout, the wall grill system was less effective in renewing air in the evaluated zone. The high supply momentum likely promoted bulk mixing and recirculation rather than direct fresh-air delivery to the occupied zone. This is consistent with comparisons between displacement and mixing ventilation, where mixing-based systems generally provide more uniform room conditions but can show weaker local ventilation effectiveness in the breathing zone than stratified or non-uniform systems (Cheng et al., 2015).

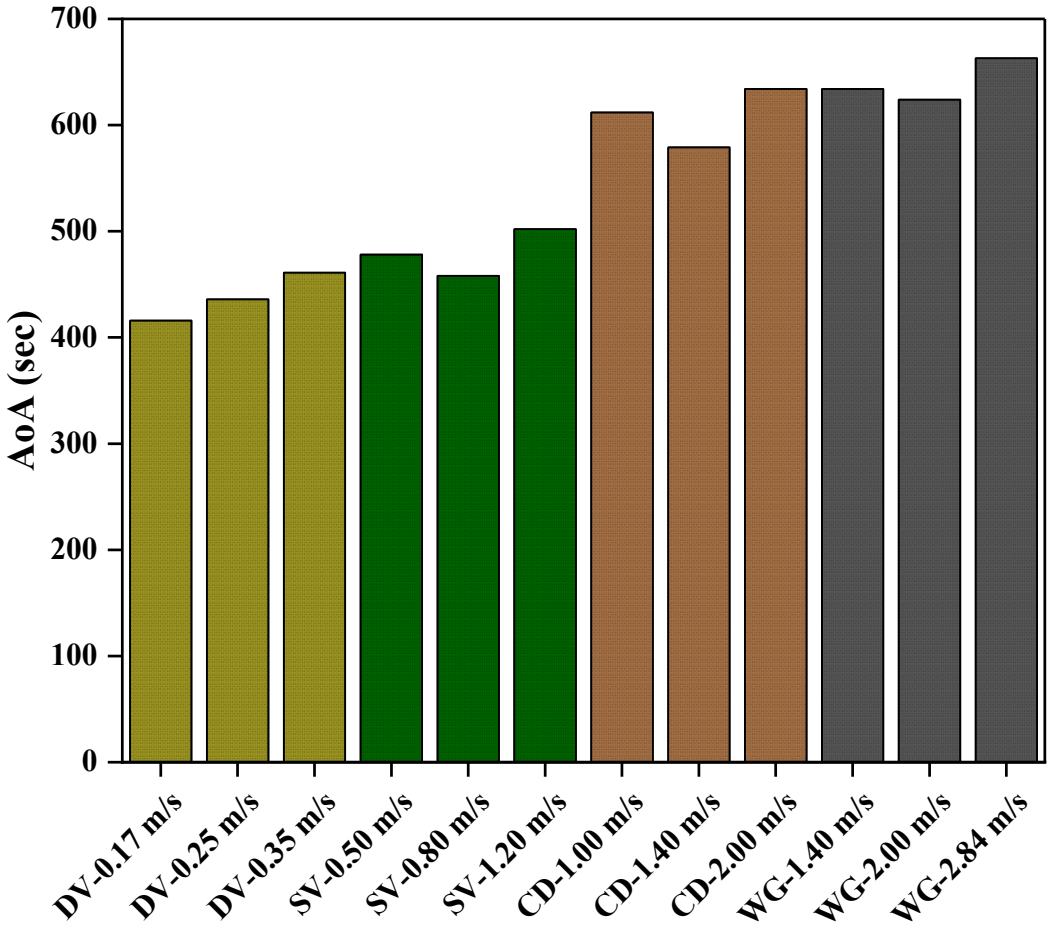

Figure 4.5: Age of air in the breathing plane

Overall, the results show that DV provided the lowest age of air, followed by SV, while CD and WG showed higher values. Based on the approximate average values, DV achieved an average age of air of about 438 s, SV about 479 s, CD about 608 s, and WG about 639 s. Thus, DV reduced the age of air by roughly 28% compared with CD

and 31% compared with WG, confirming its stronger fresh-air delivery performance under the same ACH and supply temperature. SV also performed better than the two mixing-based systems, but its performance was slightly weaker than DV because the horizontal supply jet introduced more mixing in the occupied zone (Lin et al., 2015). These findings are physically reasonable, which generally reports that non-uniform systems such as displacement and stratum ventilation can reduce mean age of air and improve breathing-zone air quality compared with conventional mixing systems (Fan et al., 2022).

4.1.2 Contaminant removal efficiency

The contaminant removal efficiency (CRE) at the breathing height for the four ventilation strategies analyzed under the same air change rate of 6 ACH and the same supply air temperature of 291.15 K is shown in Figure 4.6.

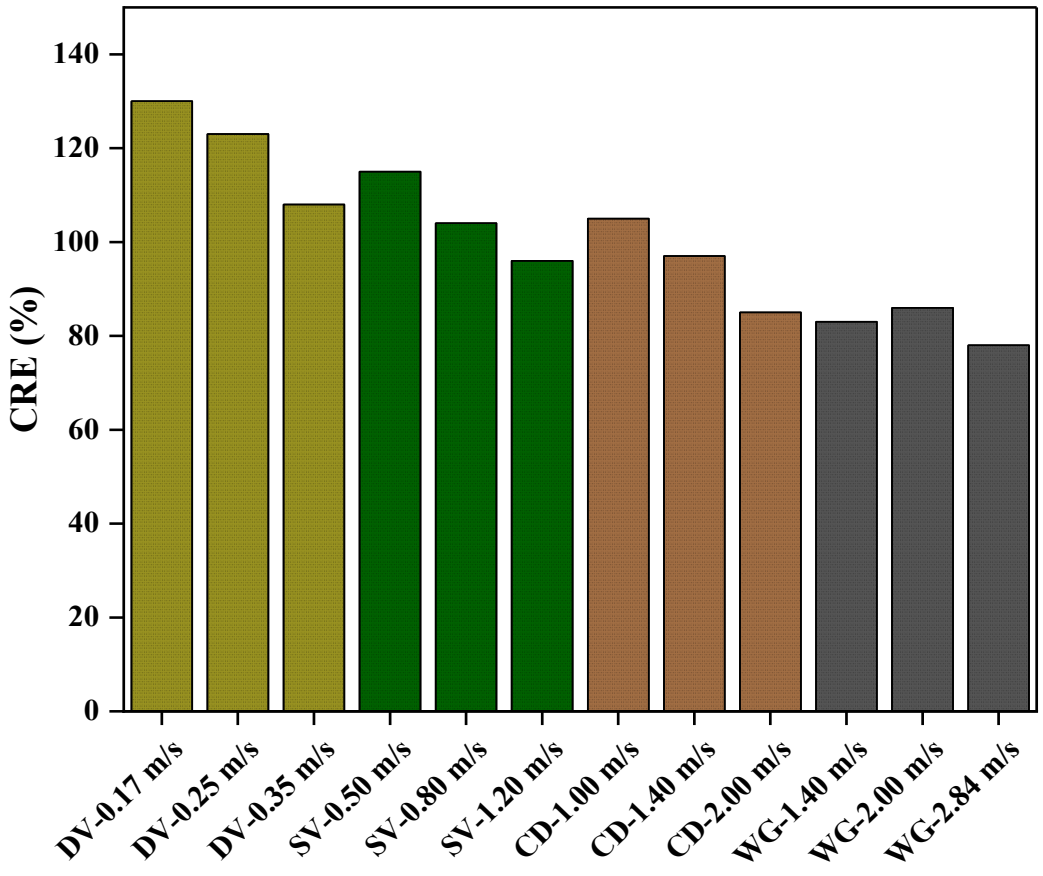

Figure 4.6: Contaminant removal efficiency

CRE is an important indoor air quality indicator because it describes how effectively contaminants generated inside the room are removed by the ventilation system. In

general, CRE values above 100% indicate better contaminant removal than complete mixing, whereas values below 100% indicate weaker contaminant removal from the evaluated.

For displacement ventilation, the CRE decreased from approximately 147% at 0.17 m/s to 134% at 0.25 m/s and 113% at 0.35 m/s. All DV cases were above 100%, however the downward trend was an indication that the more of the contaminant was supplied the more effective the removal was, but at a steady rate. This may be due to the reduced stable stratification at higher supply velocity as it could induce momentum to break the upward displacement flow and enhance partial mixing in the occupied zone. When the supply air entered at the lowest velocity, it flowed slowly near the floor where contaminants were carried upward by thermal plumes to the exhaust, leading to the largest CRE. This behavior was observed and found to be in accord of the displacement ventilation study conducted, which indicates that the location of the air supply source and buoyancy-driven airflow significantly influence the distribution of pollutants and performance of the building ventilation system (Lin et al.,2014). The CRE increased from about 107% at a inlet velocity of 0.5 m/s to 115% at 0.8 m/s and then dropped to 96% at 1.2 m/s when stratum ventilation was considered. This revealed that the intermediate supply velocity gave the best contamination removal performance for the cases tested for supply velocity. At low velocity, the horizontal supply jet might not have reached far enough across the occupied area, and at high velocity, the momentum of the jet may be excessive and cause greater mixing, which may limit the concentration of contaminants removed directly from the breathing zone. Thus, the 0.8 m/s case seems to be the better compromise between jet penetration and controlled mixing. This trend is consistent with previous research on stratum ventilation, which found that the velocity of supply air is heavily affected by the effectiveness of the stratum ventilation and the behavior of horizontal jets, and that these parameters also significantly impact the transport of contaminants and the effectiveness of ventilation in the occupied zone (Cheng & Lin, 2015). The CREs, in the case of the ceiling diffuser system, decreased to about 105% at 1.0 m/s, 97% at 1.4 m/s, and 85% at 2.0 m/s. The reduction observed in this case indicates that the contaminants were not removed more efficiently with an increase in the velocity of the ceiling diffuser in the present configuration. While ceiling diffusers can improve mixing, excessive supply momentum can result in more uniform

contaminant distribution, which can lead to more recirculation and less direct movement from the occupied zone. This results in a relatively high concentration of the contaminant in the breathing zone as compared to the exhaust concentration and thus lower CRE. The same results have been reported in the study of ceiling diffusers, which shows that the indoor air quality performance and ventilation effectiveness vary significantly according to ceiling diffuser type, the momentum of the ceiling diffusers and the airflow structure of the room (Aziz et al., 2012). The CRE values of wall grill system were the lowest among all the systems, and the values were about 83% at 1.4 m/s, 86% at 2.0 m/s and 78% at 2.84 m/s. In all of the WG cases, intermediate velocity resulted in slightly lower removal, but still below 100%, showing that less contamination was removed than was complete mixing. This implies that the wall grill system was not as successful in removing contaminants from the occupied area for the current boundary conditions. The direct transport to the exhaust was possibly short-circuited by the high momentum wall jet as it may have caused recirculation and mixing of fresh and contaminated air. This behavior agrees with the one found in the comparison of displacement and mixing ventilation (Fan et al., 2022), which indicates that the mixing ventilation system may have a lower effectiveness of breathing zone contaminant removal compared to the stratified system. Overall, the results indicate that the displacement ventilation system achieved the greatest removal effectiveness, followed by the stratum ventilation system, ceiling diffuser system and wall grill system. The average values were used for the above approximate average CRE values: DV 131%, SV 106%, CD 96%, and WG 82%. As a result, the removal of contaminants was enhanced by about 37% by DV over CD and 60% over WG. The primary advantage of DV is its ability to create an upward airflow pattern, which is buoyancy driven and removes contaminants from the occupied area to the top exhaust. Although the effectiveness of SV was highly dependent on supply velocity, this method was also found to be more effective than the two mixing based systems due to the introduction of the supply air close to the breathing level. Lower CRE was obtained in CD and WG systems due to their mixing dominated flow patterns which facilitated more recirculation of contaminants and less direct removal out of the occupied zone. The results are physically reasonable and consistent with published ventilation studies that found, under appropriate operating conditions, non-uniform ventilation systems

(displacement and stratum ventilation) may be more effective at removing the contaminant than mixing-based systems (Fan et al., 2022).

4.2 Thermal comfort

The thermal comfort performance of the analyzed cases was evaluated using temperature and velocity distributions in the vertical mid-plane, draft risk, and air distribution index. These parameters were used to assess the indoor thermal condition, local airflow behavior, and overall air distribution quality within the classroom.

4.2.1 Temperature distribution

The temperature gradient for different DV supply cases and the temperature contours for different displacement ventilation cases at same supply temperature of 291.15 K and same ACH of 6 are shown in Figure 4.7 and Figure 4.8 respectively.

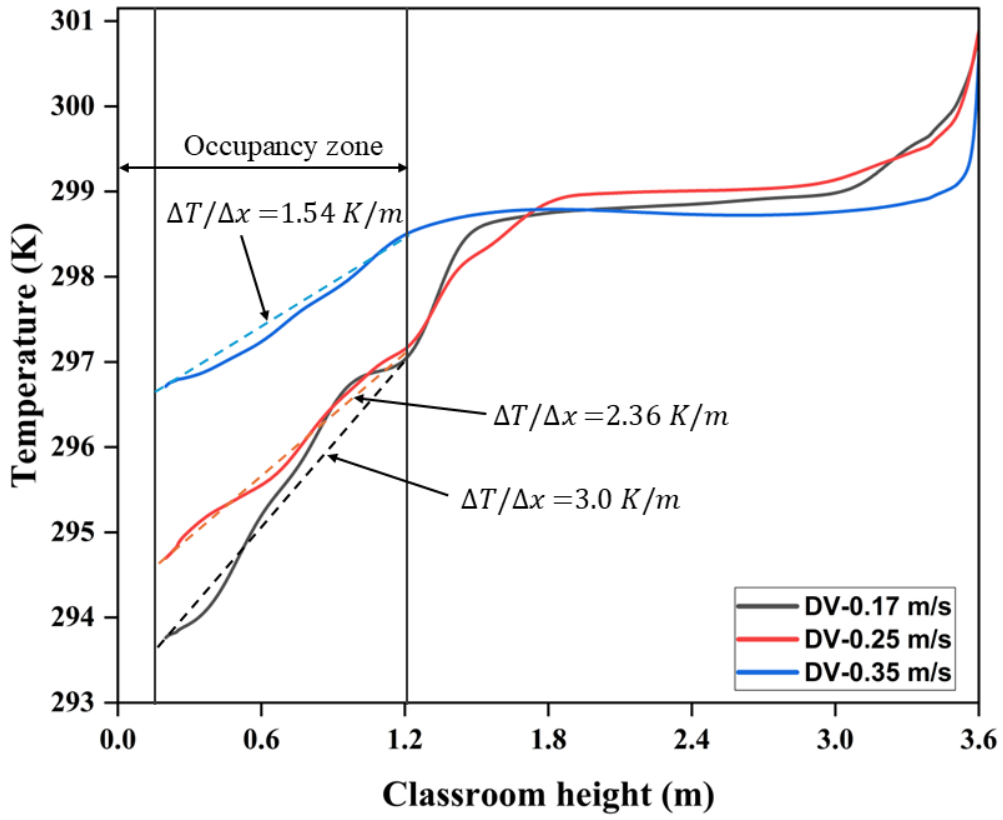

Figure 4.7: Temperature gradient for different DV cases

The contours clearly show the typical thermal stratification pattern of displacement ventilation, where cooler supply air remains in the lower occupied zone while warmer air rises upward due to buoyancy and occupant-generated thermal plumes. Since, the

supply conditions were varied by changing the supply velocities only i.e. 0.17 m/s, 0.25 m/s and 0.35m/s the role of Archimedes number played a big role in temperature distribution in the classroom.

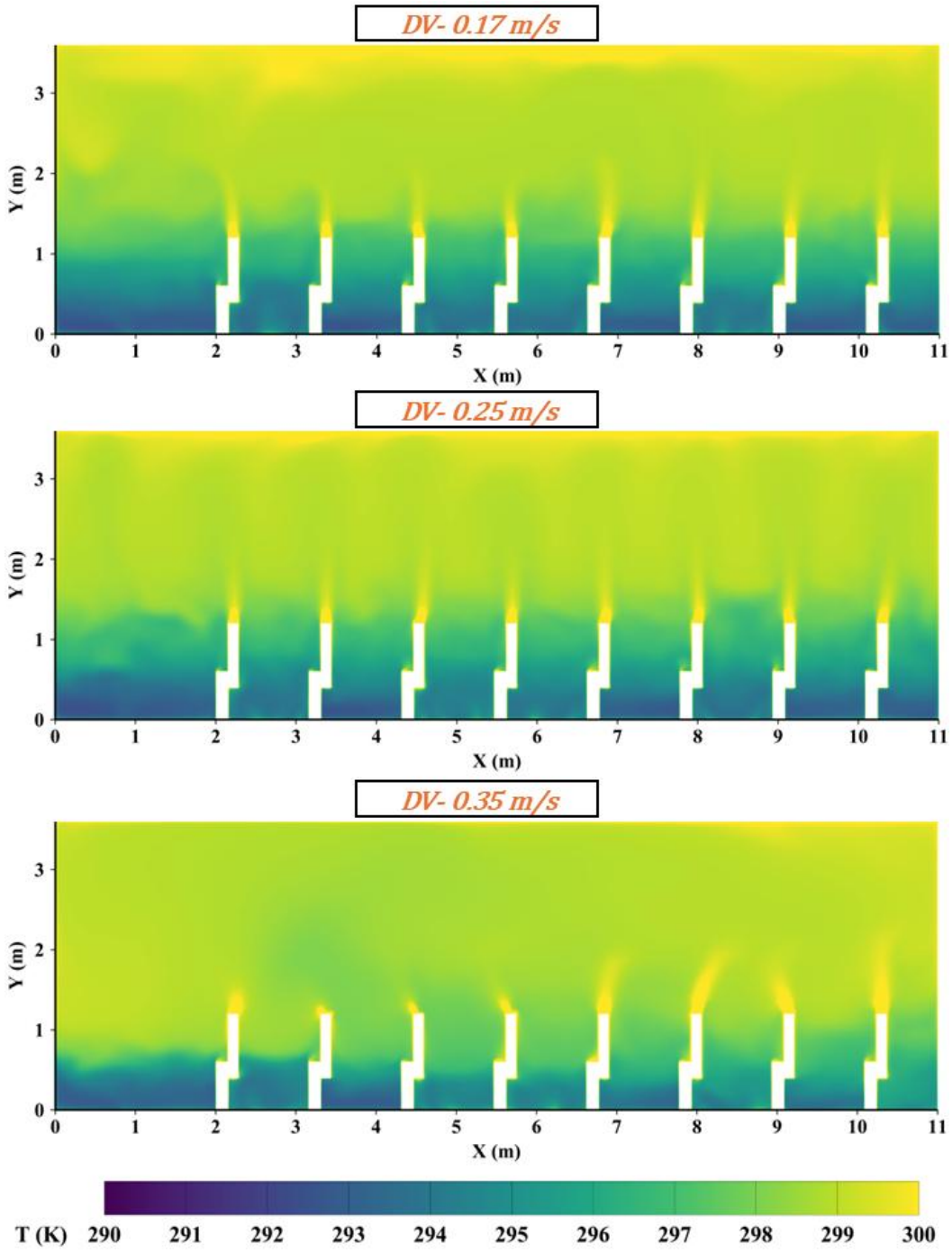

Figure 4.8: Temperature contour at mid-vertical plane DV cases

As the supply velocity decreased the temperature gradient was found to be increased, at the supply condition of 0.17 m/s the temperature gradient of 3 K/m was observed

which accounts for 293.7 K at the foot level of 0.1m from the ground and 297 K at the head height of 1.2 m from the ground level , this is mainly due to strong buoyancy force at higher Archimedes number.

When the supply velocity was increases to 0.25 m/s the temperature gradient was also decreases to 2.36 K/m. Which accounts for 294.66 K at the foot level of 0.1 m from the ground and 297.26 K at the head height of 1.2 m from the ground level, the buoyancy force seems still strong even at 0.25 m/s.

When the supply velocity was increases to 0.35 m/s the temperature gradient was also decreases to 1.54 K/m. Which accounts for 296.75 K at the foot level of 0.1 m from the ground and 298.45 K at the head height of 1.2 m from the ground level, the buoyancy force seems to be at the transitional phase towards mixing ventilation at 0.35 m/s and beyond.

Thus, stronger inlet velocity causes greater mixing in the occupied zone, reducing the stability of the thermal stratification and spreading warmer air downward in some regions. Overall, the temperature contours indicate that lower supply velocity supports better displacement ventilation performance by maintaining a cooler occupied zone and a warmer upper zone, whereas increasing the velocity weakens the buoyancy-driven stratification and increases mixing between the lower and upper air layers.

The temperature gradient for different stratum ventilation supply cases and the temperature contours for different stratum ventilation cases at same supply temperature of 291.15 K and same ACH of 6 are shown in Figure 4.9 and Figure 4.10 respectively.

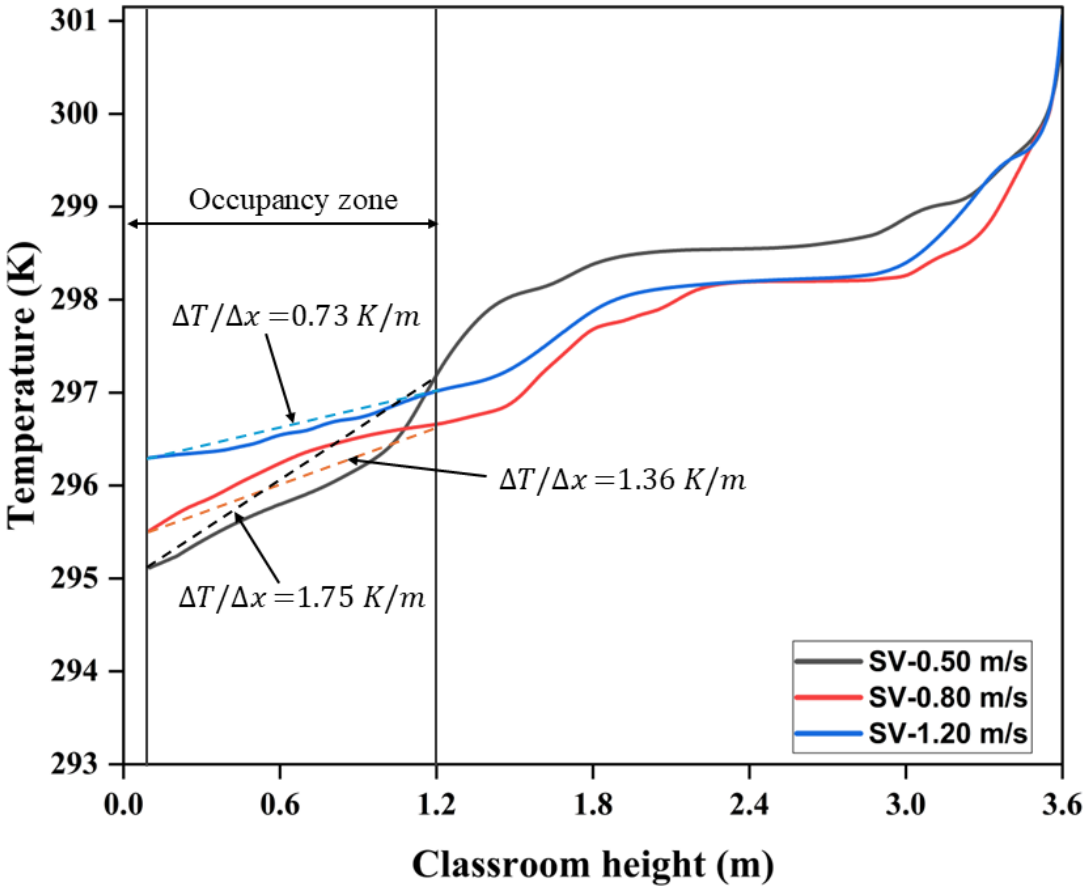

Figure 4.9: Temperature gradient for different SV cases

As the supply velocity increased the temperature gradient was found to be decreased, at the supply condition of 0.50 m/s the temperature gradient of 1.75 K/m was observed which accounts for 295.10 K at the foot level of 0.1m from the ground and 297.05 K at the head height of 1.2 m from the ground level , this is mainly due to buoyancy force at lower Archimedes number.

When the supply velocity was increases to 0.80 m/s the temperature gradient was also decreases to 1.36 K/m. Which accounts for 295.50 K at the foot level of 0.1 m from the ground and 297.0 K at the head height of 1.2 m from the ground level, the buoyancy force seems still strong even at 0.80 m/s.

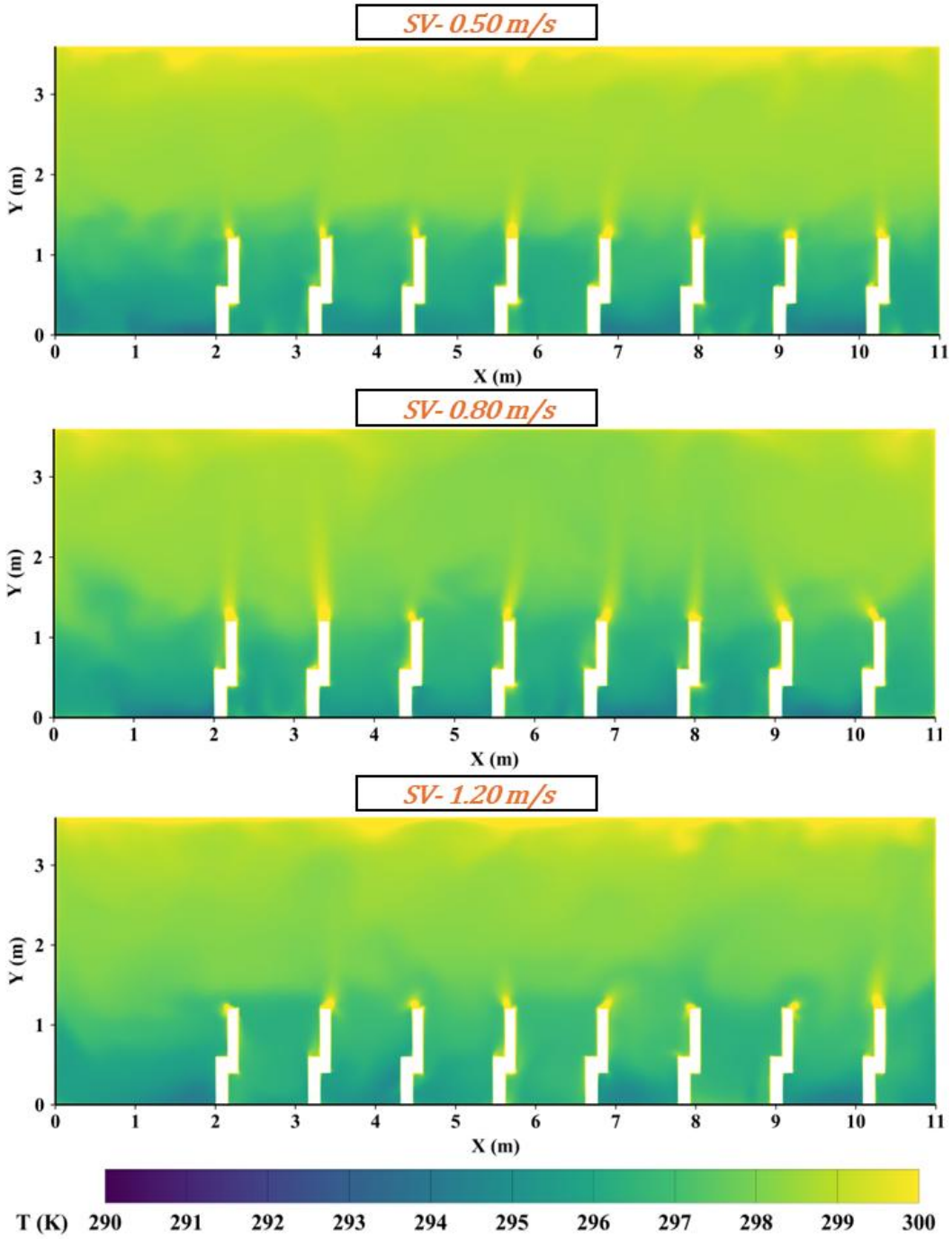

Figure 4.10: Temperature contour at mid-vertical plane SV cases

When the supply velocity was increases to 1.20 m/s the temperature gradient was also decreases to 0.73 K/m. Which accounts for 296.45 K at the foot level of 0.1 m from the ground and 297.25 K at the head height of 1.2 m from the ground level, the temperature gradually seems to decreases from the supply condition of 0.50 m/s to 1.20 m/s. As the velocity of supply increased the Archimedes number and its significant towards the

buoyancy effect began to diminish. As a result, the flow in the classroom became mixing dominated rather than buoyancy dominated at the supply of 1.20 m/s.

At lower supply of 0.50 m/s the temperature at the floor and the feet level was lower as compared to the supply of 0.80 m/s and 1.20 m/s. At supply of 0.8 m/s it was found that air distribution and thermal comfort parameters showed the most favorable conditions as confirmed by age of air and contaminant removal efficiency mainly because it provided more uniform and balanced air distribution than the other two supply velocities of 0.8 m/s and 1.20 m/s respectively.

Figure 4.12 shows the temperature contours for the ceiling diffuser system at supply velocities of 1.0 m/s, 1.4 m/s, and 2.0 m/s under the same ACH and supply temperature.

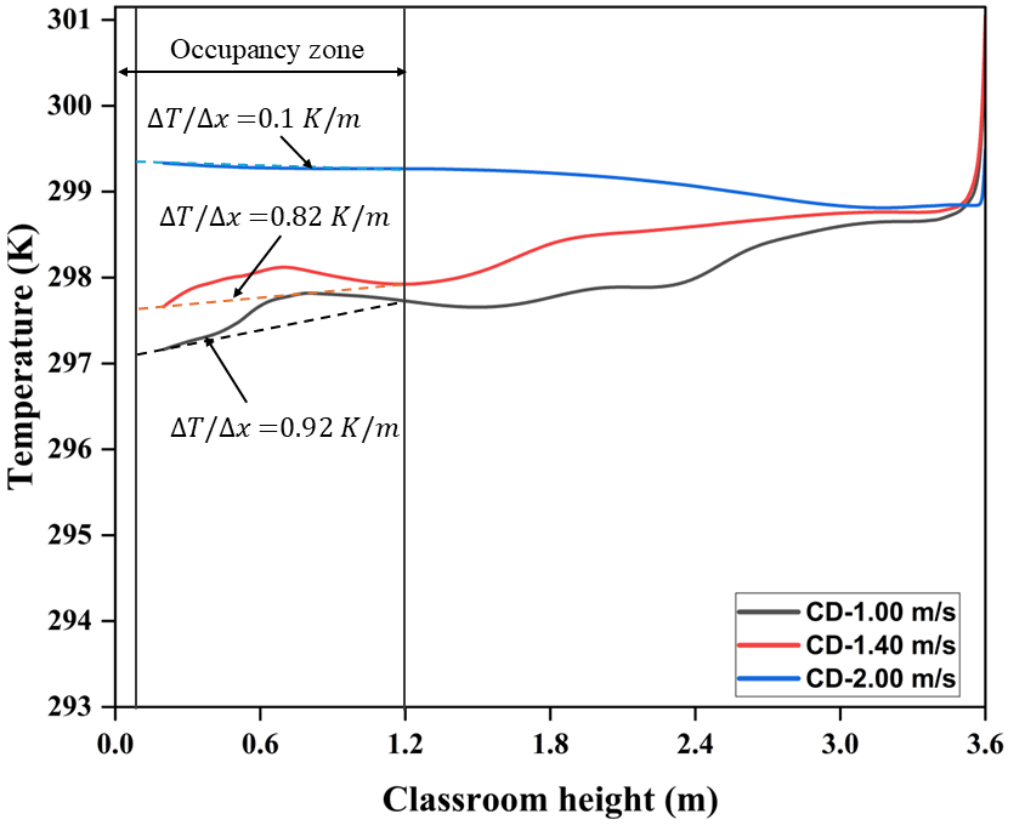

Figure 4.11: Temperature gradient for different CD cases

The contours indicate that the ceiling diffuser system produces a more mixing-dominated thermal field compared with stratified systems such as displacement or stratum ventilation, because the supply air is introduced from the upper region and is distributed through room-scale circulation. At 1.0 m/s, the room temperature remains mostly within the green-to-yellow range, indicating moderate thermal mixing, but a

localized cooler region is observed near the upper central zone, suggesting that the supply jet does not fully mix with the room air before descending

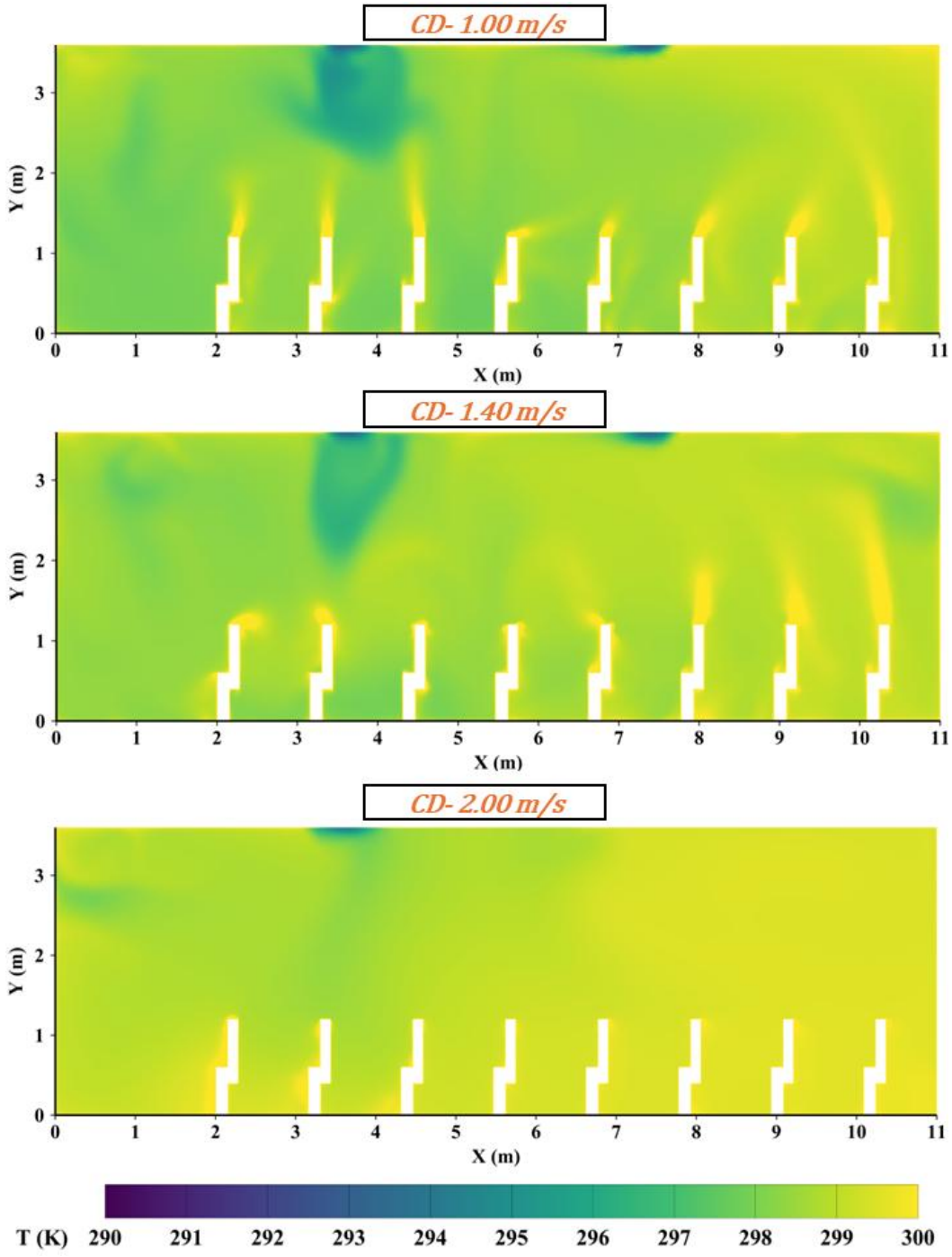

Figure 4.12: Temperature contour at mid-vertical plane CD cases

At 1.4 m/s, the temperature distribution becomes slightly more uniform across the occupied zone, showing that the increased supply momentum improves air mixing and reduces local temperature variation. However, small cooler pockets are still visible near

the ceiling, indicating the influence of the ceiling supply jet. At 2.0 m/s, the thermal field becomes the most uniform, with most of the room approaching the yellow range, showing stronger mixing and reduced vertical thermal stratification. Although this improves temperature uniformity, it also indicates that the system relies mainly on dilution and mixing rather than maintaining a cooler lower occupied zone. Overall, the temperature contours show that increasing the ceiling diffuser velocity enhances thermal uniformity, with CD-1.4 m/s providing a more balanced condition, while CD-2.0 m/s produces stronger mixing that reduces stratification but may also increase local air movement and draft risk in the occupied zone.

As the supply velocity increased the temperature gradient was found to be decreased even though due to the nature of mixing nature rather than buoyancy dominated air distribution in a classroom in ceiling diffusers cases. at the supply condition of 1.00 m/s the temperature gradient of 0.92 K/m was observed which accounts for 297.00 K at the foot level of 0.1m from the ground and 298.01 K at the head height of 1.2 m from the ground.

When the supply velocity was increases to 1.40 m/s the temperature gradient was also decreases to 0.82 K/m. Which accounts for 297.60 K at the foot level of 0.1 m from the ground and 298.21 K at the head height of 1.2 m from the ground level

When the supply velocity was increases to 2.00 m/s the temperature gradient was also decreases to 0.10 K/m. Which accounts for 299.20 K at the foot level of 0.1 m from the ground and 299.09 K at the head height of 1.2 m from the ground level.

The overall temperature in the classroom gradually seems to increase from the supply condition of 1.00 m/s to 2.00 m/s. At supply velocity of 1.4 m/s it shows the better age of air and contaminant removal efficiency as compared to other two supply conditions. Even though the temperature distribution in the classroom was not governed by the buoyancy force, the supply velocity played a big role for the temperature obtained in the occupancy zone. Therefore, even for a mixing dominated air distribution system with very small temperature gradient across the occupancy zone, supply velocity plays a crucial role to provide better air distribution and indoor air quality t as confirmed by age of air, contaminant removal efficiency.

.

Figure 4.14 shows the temperature contours for wall grill ventilation at supply velocities of 1.4 m/s, 2.0 m/s, and 2.84 m/s under the same ACH and supply temperature.

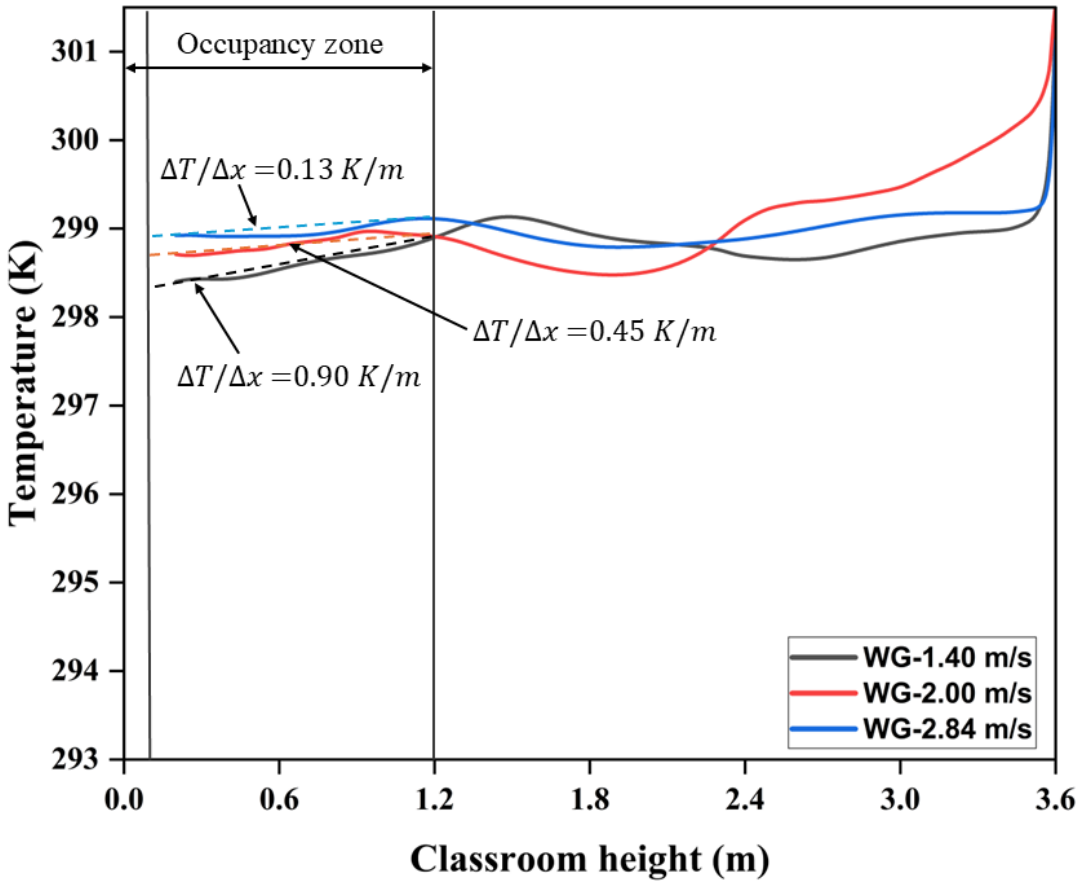

Figure 4.13: Temperature gradient for different WG cases

Unlike DV and SV, the WG system shows a more mixing-dominated thermal field, where the temperature distribution is relatively uniform across the room and the vertical stratification is weaker. At 1.4 m/s, warmer air occupies most of the upper and middle regions, while some localized cooler zones appear around the occupied area due to the interaction between supply jets and occupant thermal plumes. At 2.0 m/s, the higher supply momentum improves mixing and spreads conditioned air more widely, but it also weakens the separation between the cooler occupied zone and warmer upper zone. At 2.84 m/s, the temperature field becomes more uniformly mixed, with less clear stratification and stronger disturbance of the thermal plume structure.

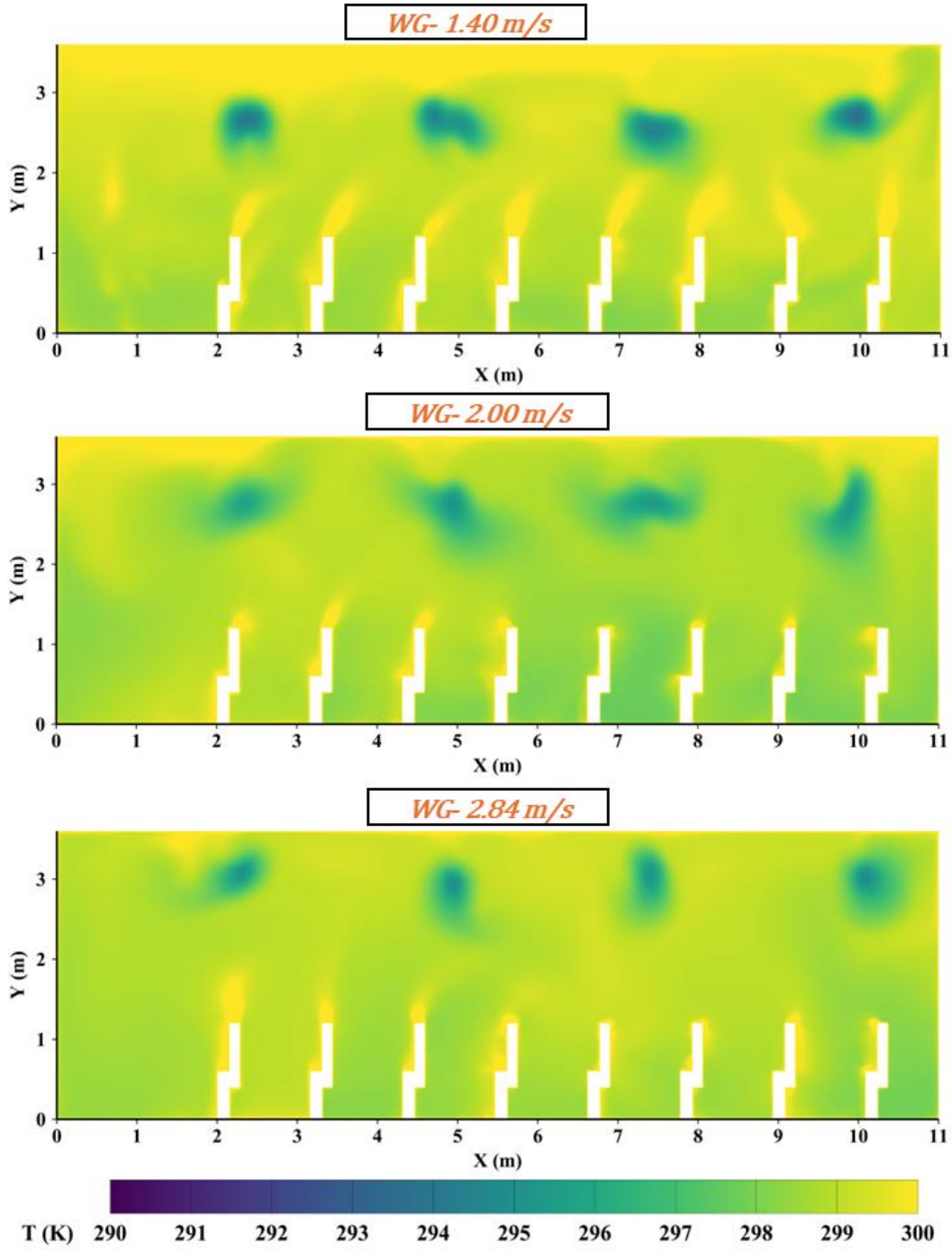

Figure 4.14: Temperature contour at mid-vertical plane WG cases

As the supply velocity increased the temperature gradient was found to be decreased even though due to the nature of mixing nature rather than buoyancy dominated air distribution in a classroom in wall grill cases. At the supply condition of 1.40 m/s the temperature gradient of 0.90 K/m was observed which accounts for 298.30 K at the foot level of 0.1m from the ground and 299.21 K at the head height of 1.2 m from the ground.

When the supply velocity was increases to 2.84 m/s the temperature gradient was also decreases to 0.45 K/m. Which accounts for 298.75 K at the foot level of 0.1 m from the ground and 299.25 K at the head height of 1.2 m from the ground level.

When the supply velocity was increases to 2.00 m/s the temperature gradient was also decreases to 0.13 K/m. Which accounts for 298.90 K at the foot level of 0.1 m from the ground and 299.05 K at the head height of 1.2 m from the ground level.

This indicates that increasing wall grill velocity enhances bulk mixing rather than maintaining a stable thermal layer in the occupied zone. Overall, the temperature contours confirm that the WG system provides more uniform thermal distribution than stratified systems.

4.2.2 Velocity distribution

Figure 4.15 shows the velocity contours for displacement ventilation velocity contours at supply velocities of 0.17 m/s, 0.25 m/s and 0.35 m/s for the same ACH of 6 and supply temperature of 291.15 K. The contours show a significant impact of the supply velocity on the airflow field particularly in the lower occupied zone and in the vicinity of the thermal plumes of the occupant.

At 0.17 m/s, the magnitude of velocity is low in most of the room, but there are local upward plume regions above the occupants indicating a dominance of buoyancy driven flow over supply momentum. This supports the use of stable displacement ventilation with gentle distribution of fresh air near the floor and mainly rising through occupant thermal plumes.

At 0.17 m/s, the magnitude of the velocity is generally low throughout much of the room, with the presence of localized upward plume regions evident above the occupants, indicating that buoyancy-driven flow dominates over supply momentum. This helps in stable displacement ventilation whereby the fresh air flows slowly at the floor level, and ascends chiefly by the occupant thermal plumes. At 0.25 m/s, the air flow is again slightly more disturbed, with a larger velocity change in the occupied zone, and more lateral spreading of air, demonstrating that the higher inlet momentum is already beginning to interact more strongly with the thermal plumes.

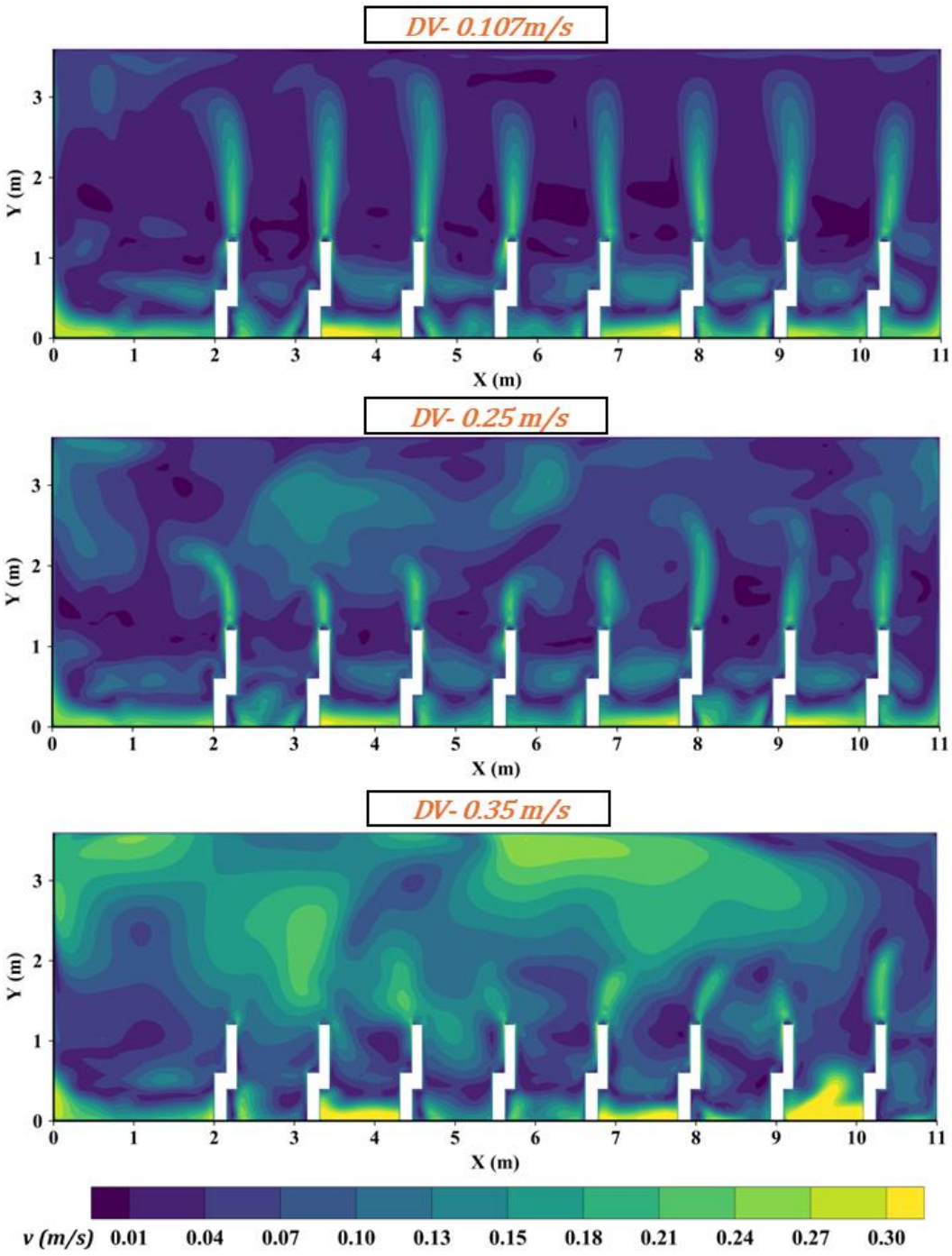

Figure 4.15: Velocity contour at mid-vertical plane for DV cases

Faster velocity areas become more extensive at higher velocities, particularly in the lower zone and around occupied area, which means that the dispersion of velocity is stronger and the displacement behavior of the stratified layer is weaker. In general, the contours of the velocity confirm that decreasing the supply velocity keeps the displacement-flow structure more stable, whereas increasing the supply velocity enhances the local air movement and mixing.

Figure 4.16 shows all the velocity magnitude contours of stratum ventilation of supply velocities of 0.5 m/s, 0.8 m/s, and 1.2 m/s with the same ACH and supply temperature of 291.15 K.

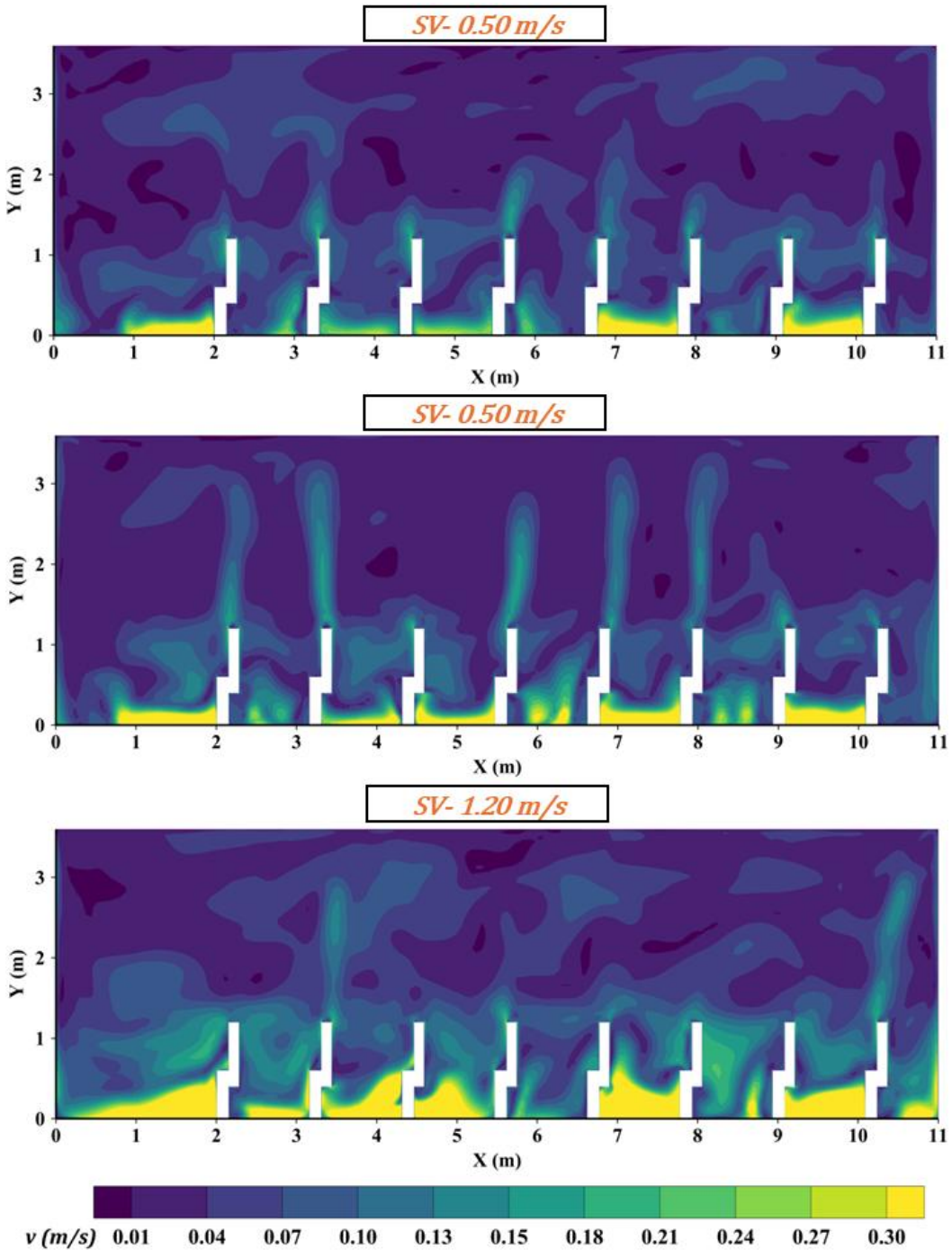

Figure 4.16: Velocity contour at mid-vertical plane for SV cases

The velocity scale is between 0.01 m/s and 0.25 m/s with dark purple areas indicating almost no air movement or low speed air movement whereas the green to yellow

regions indicates high local air movement. Most of the room in the case of 0.5 m/s falls within the low-velocity range, particularly in the upper zone, suggesting that the supply momentum is not very strong. Concentration of the airflow is primarily focused around the lower occupied area and around the occupants, with plume-like structures visible vertically above the heat sources. This indicates that effects of occupants on buoyancy have a significant role to play in the upward movement of air. Nevertheless, due to the low inlet momentum, the supplied air does not spread intensively throughout the entire occupied zone, which could be one of the reasons behind the relatively poor performance of the supplied air in removing contaminants compared to the intermediate case. The velocity distribution is more structured and the regions of upward flows above occupants are more differentiated in the case of 0.8 m/s. The moderate velocity zones pass through the occupied area and indicate that the supply jet has the necessary momentum to dispense fresh air in a more efficient manner without creating a lot of mixing throughout the entire room. The case indicates a superior equilibrium of supplying jet penetration and buoyancy-induced transportation, which contributes to enhanced air renewal and elimination of contaminants in the breathing zone. The higher velocity regions, in the case of 1.2 m/s, are more pronounced towards the lower and middle occupied regions, and the airflow field seems to be more disturbed than in the case of 0.8 m/s. The increase in supply momentum enhances local air movement around the occupants and enhances more mixing between the lower occupied area and the upper room air. This can lead to better air circulation, but it can also destabilize the desired stratum ventilation pattern and raise the risk of local drafts, particularly around seated and breathing heights. Generally, the velocity contours show that the 0.5 m/s has inadequate jet penetration, the 0.8 m/s provides the most optimal structure of airflow and the 1.2 m/s yields more intense mixing and higher local velocities. Hence, the contour reinforces the quantitative findings whereby the intermediate SV velocity provides better overall performance through the delivery of effective occupied-zone air and avoiding excessive mixing and draft.

Figure 4.17 shows the contours of the velocity magnitude of the ceiling diffuser (CD) cases at the supply velocities of 1.0 m/s, 1.4 m/s and 2.0 m/s at the same ACH and supply temperature. The ceiling diffuser system exhibits a more mixing-dominated

airflow pattern, in which the air supplied is dispersed throughout the room by momentum driven flow and recirculation unlike displacement or stratum ventilation.

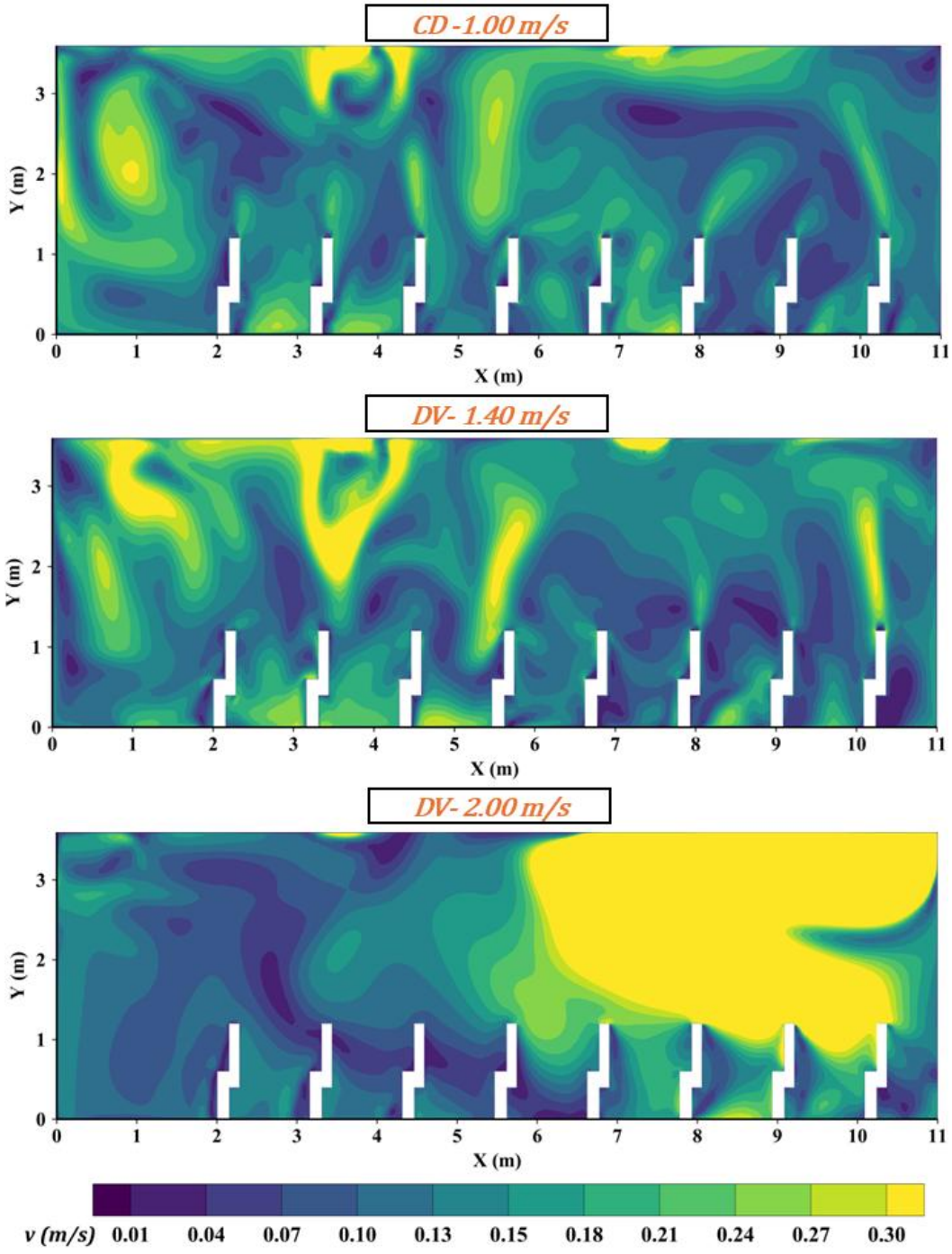

Figure 4.17: Velocity contour at mid-vertical plane for CD cases

In the 1.0 m/s case, the velocity field is more or less uniform, with a few high-velocity zones at the top and in the occupied area, but much of the available space lies in the low-to-medium velocity range. This means that the supply momentum is adequate to

provide room circulation, but not high enough to provide highly uniform mixing all the way through the entire space. Consequently, certain stagnant pockets of low velocity might be found between occupant areas, which may raise the local residence time of air and reduce ventilation performance. In the 1.4 m/s case, the velocity distribution becomes more active and widespread, the downward and recirculating flow structures extending downwards and upwards respectively are stronger and more widespread. This implies that the intermediate velocity promotes air mixing and increases the distribution of the supplied air in the room. The regions with higher velocity are more evenly distributed as compared to the case of 1.0 m/s and this explains why this case gave the lowest age of air among the CD cases and the highest ADI of the best ceiling diffuser system. Nevertheless, the air is still momentum driven instead of stratified, so the enhanced air renewal is accomplished primarily through mixing, rather than through direct displacement of contaminants. In the 2.0 m/s case, the velocity field has become significantly more dominated by the high-speed areas, particularly on the upper and right-side sides of the room, where large yellow areas indicate velocities near the upper end of the plotted scale. This demonstrates that the high supply momentum generates excellent circulation and potential over-mixing, causing the natural upwards movement of thermal plumes by occupants to be disturbed. Though the stronger mixing can lead to the reduction of the stagnant zones, the excess momentum can also increase the recirculation, the local draft risk, and the redistribution of the contaminants within the occupied zone instead of eliminating them efficiently. Thus, the results obtained through the contour results show that the most balanced airflow structure is provided by 1.4 m/s, and the poorest mixing and the largest low-velocity pockets are produced by 1.0 m/s, and excessive high-velocity mixing can be produced by 2.0 m/s. This graphical interpretation complements the quantitative findings, whereby the intermediate ceiling diffuser velocity presented better overall air distribution performance, as compared to the highest velocity that increased draft risk and weakened the overall ventilation effectiveness.

Figure 4.18 shows the contours of velocity magnitude velocity at the wall grill ventilation (WG) cases at supply velocity of 1.4 m/s, 2.0 m/s and 2.84 m/s and constant ACH and supply temperature. The velocity scale is between 0.01 m/s and 0.25 m/s with purple areas indicating low-velocity or poorly ventilated areas and green to yellow areas

indicating that the area has a higher local velocity. In the 1.4 m/s case, the airflow field is very non-uniform with several pockets of low velocity in the occupied field and localized high velocity zones near the upper part of the room. This implies that the wall grill jet generates circulation structures, instead of a steady stratified flow.

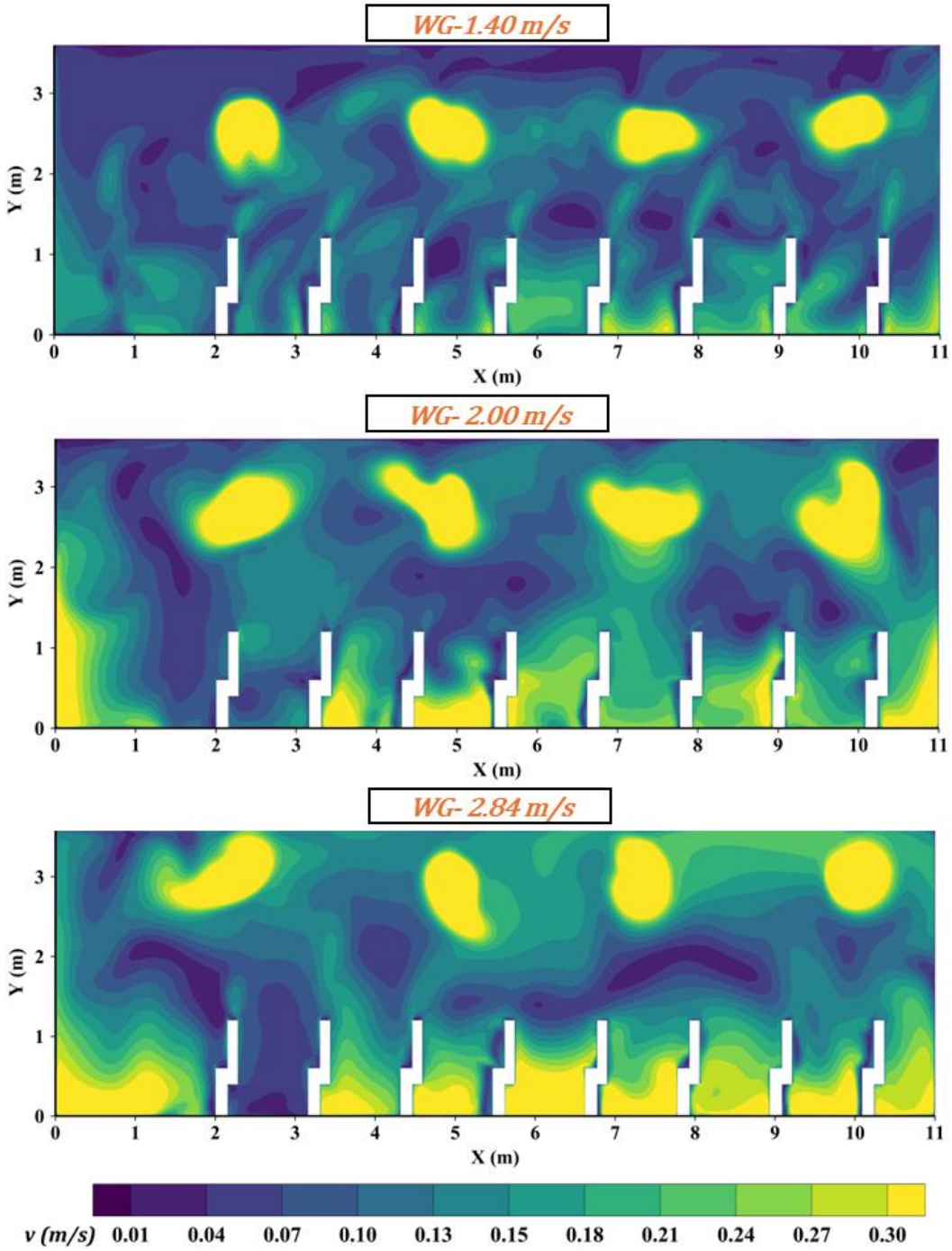

Figure 4.18: Velocity contour at mid-vertical plane for WG cases

Whereas certain circulatory is present in the vicinity of the lower zone, the distribution of velocity is not uniformly distributed throughout the breathing area, which can result

in local recirculation and inefficient contaminant removal. The magnitude of velocity in the 2.0 m/s case, is more widespread, particularly around the lower occupied zone and in the upper recirculation regions. The larger yellow and green areas reveal that the higher the supply velocity, the stronger the wall jet, the more the mix of space. But this increase in circulation does not always imply an increase in the ventilation effectiveness, since the flow is still mixing-dominated, and may redistribute contaminants within the occupied zone rather than eliminate them. The case of high-velocity regions becomes even more vivid in the 2.84 m/s case, demonstrating that the strong wall jet is even deeper into the room, and it causes even more local air movement. This is the reason why the WG system has been found to have higher draft risk, especially at seated and breathing heights. The presence of the strong high-velocity regions as well as low-velocity pockets indicate the absence of the dynamic air balance and evenly distributed air layers in the atmosphere. On the whole, the velocity contours affirm that when the wall grill supply velocity is increased, mixing and recirculation, as opposed to the establishment of an organized clean-air delivery path. Thus, the WG system demonstrates the poorest airflow structure in the among the studied ventilation strategies, with high local velocities, high draft potential, and low effective contaminant removal in comparison with displacement and stratum ventilation.

4.2.3 Draft risk

Draft risk represents the percentage of occupants likely to feel local discomfort due to unwanted cooling caused by air movement; therefore, lower values indicate better thermal comfort and a lower probability of draft sensation.

In displacement ventilation, the draft risk was the highest near the floor, and the least near the ceiling. At 0.1 m, Draft risk increased from approximately 8.7% at 0.17 m/s to 9.4% at 0.25 m/s and 13.4% at 0.35 m/s. At 0.6 m. which corresponds to values decreased to about 4.6%, 5.1%, and 8.8%, while at 1.1 m, they remained low at approximately 4.3%, 4.7%, and 8.7%. This trend suggests that the primary draft issue in DV is that cool supply air is added at the low level and then rises upwards through the buoyancy-driven thermal plumes. The increase in DR with supply velocity is physically reasonable, because higher inlet momentum increases near-floor air movement and local convective cooling. This agrees with studies showing that displacement and underfloor air distribution systems can create ankle-level draft

discomfort if local air movement near the floor is not properly controlled (Liu et al., 2017).

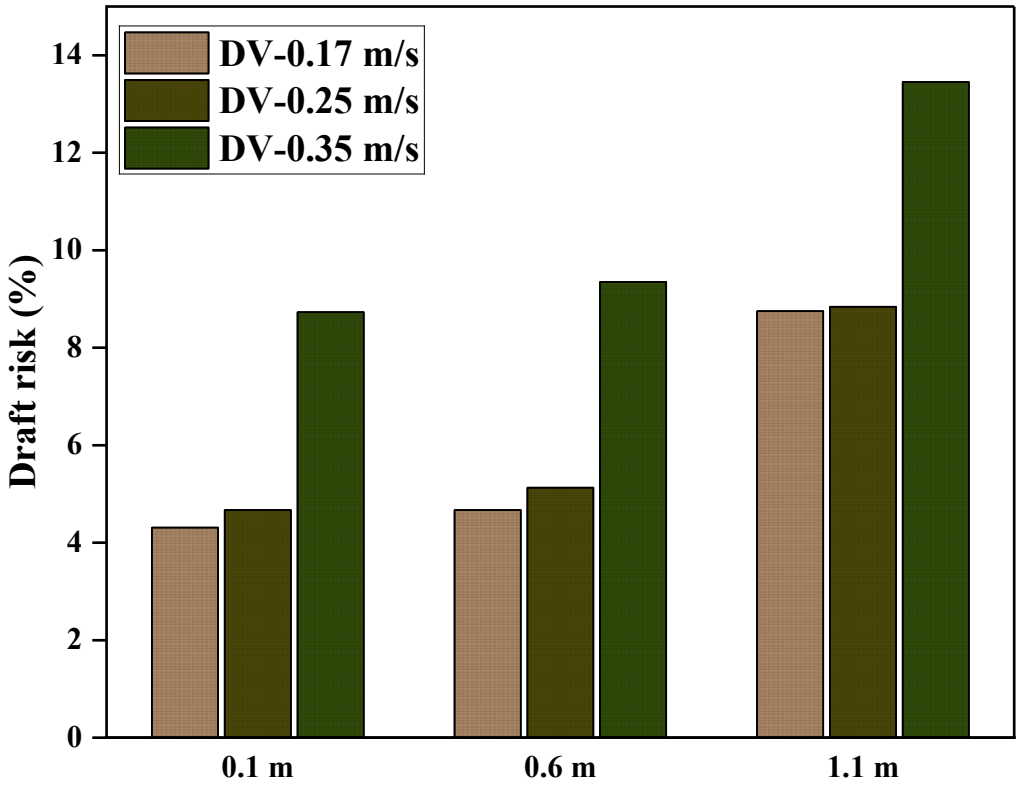

Figure 4.19: Draft risk at mid-vertical plane for DV cases

In terms of stratum ventilation, the risk of draft was proportionate to the supply velocity and height. At 0.1 m, Draft risk increased from approximately 7.2% at 0.5 m/s to 8.1% at 0.8 m/s and 9.4% at 1.2 m/s. At 0.6 m. The values increased to around 7.8%, 8.4%, and 10.3%, while at 1.1 m, they further increased to approximately 9.5%, 10.7%, and 12.7%. In contrast to DV, the maximum Draft risk (in SV) was at the levels near the upper occupied zone since the supply air is introduced nearer to the breathing level. This implies that increasing the SV velocity can not only enhance the delivery of air but might also result in local discomfort in the upper body and head area. Stratum ventilation created higher draft risk at the upper heights in the occupancy zones as compared to feet level. This is mainly due to the supply of diffusers inlet positioned at 1.8 m from the ground level. This behavior is consistent with stratum ventilation studies, which show that supply-jet characteristics, turbulence intensity, and interaction with the human thermal plume strongly affect local comfort and airflow distribution (Tian et al., 2019).

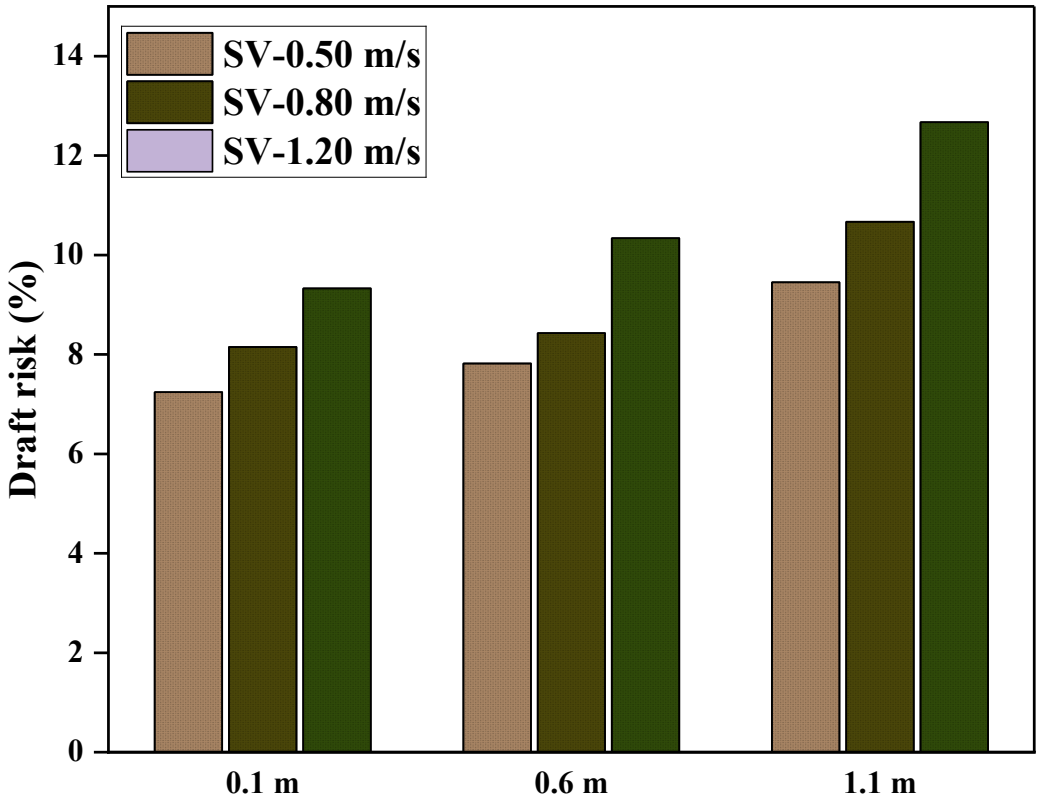

Figure 4.20: Draft risk at mid-vertical plane for SV cases

In the case of the ceiling diffuser system, draft risk generally increased with height and was greatest when the supply velocity was the highest. At 0.1 m, Draft risk was approximately 8.3% at 1.0 m/s, 8.1% at 1.4 m/s, and 11.5% at 2.0 m/s. At 0.6 m, the values were about 8.7%, 8.3%, and 12.3%, while at 1.1 m, they increased to approximately 10.3%, 9.1%, and 14.1%, respectively. The fact that the relatively lower values at 1.4 m/s may indicate that moderate ceiling-diffuser velocity created a more balanced mixing condition, as compared to the highest velocity that increased local air movement within the occupied zone. Ceiling diffuser systems created higher draft risk at 1.1 m as compared to 0.6 m and higher draft at 0.6 m as compared to 0.1 m, which suggest that when the supply is at the ceiling occupant feel higher draft at their head level as compared to their feet level. This agrees with ventilation literature showing that diffuser type, supply momentum, and airflow pattern strongly influence local comfort and ventilation performance (Fan et al., 2022).

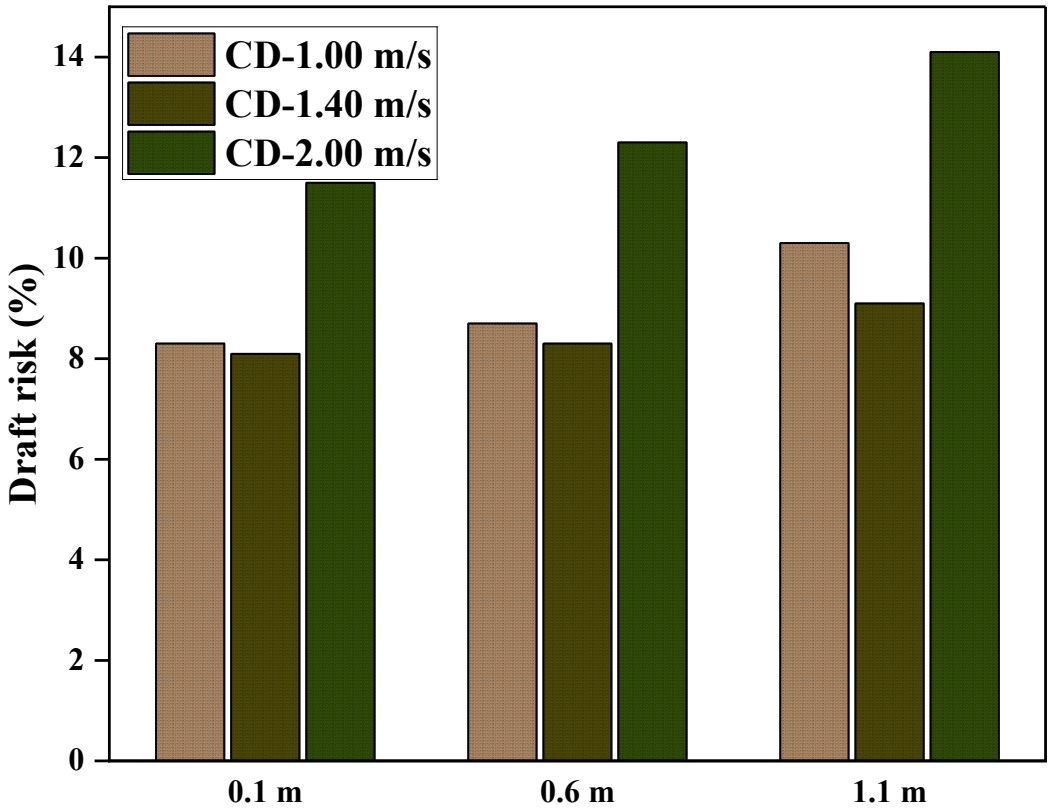

Figure 4.21: Draft risk at mid-vertical plane for CD cases

In the case of the wall grill system draft risk was the highest of all systems. It was greatly dependent on the height and supply velocity. Since, wall grill systems produce higher jet velocity and higher turbulent intensity as compared to other three systems, the draft risk was on the higher side as well. At 0.1 m, the Draft risk increased from approximately 9.8% at 1.4 m/s to 11.4% at 2.0 m/s and 14.2% at 2.84 m/s. At 0.6 m, the values increased to around 10.7%, 13.1%, and 15.7%, while at 1.1 m, they reached approximately 12.8%, 18.7%, and 24.5%, respectively. This implies that the wall grill system generated high local air movement in the upper occupied area and more so at the highest supply velocity. The large Draft risk of 1.1 m indicates that the wall jet was still maintaining significant momentum across the occupied zone and thus the probability of discomfort along the breathing and head plane. This result is consistent with the draft-risk model, where higher local velocity and turbulence intensity increase the percentage of occupants dissatisfied due to draft (Griefahn et al., 2002). The draft risk was mainly very high on the occupants which were near the supply inlet because wall grill system can create bathing of air jet in to the human bodies in the occupancy zone.

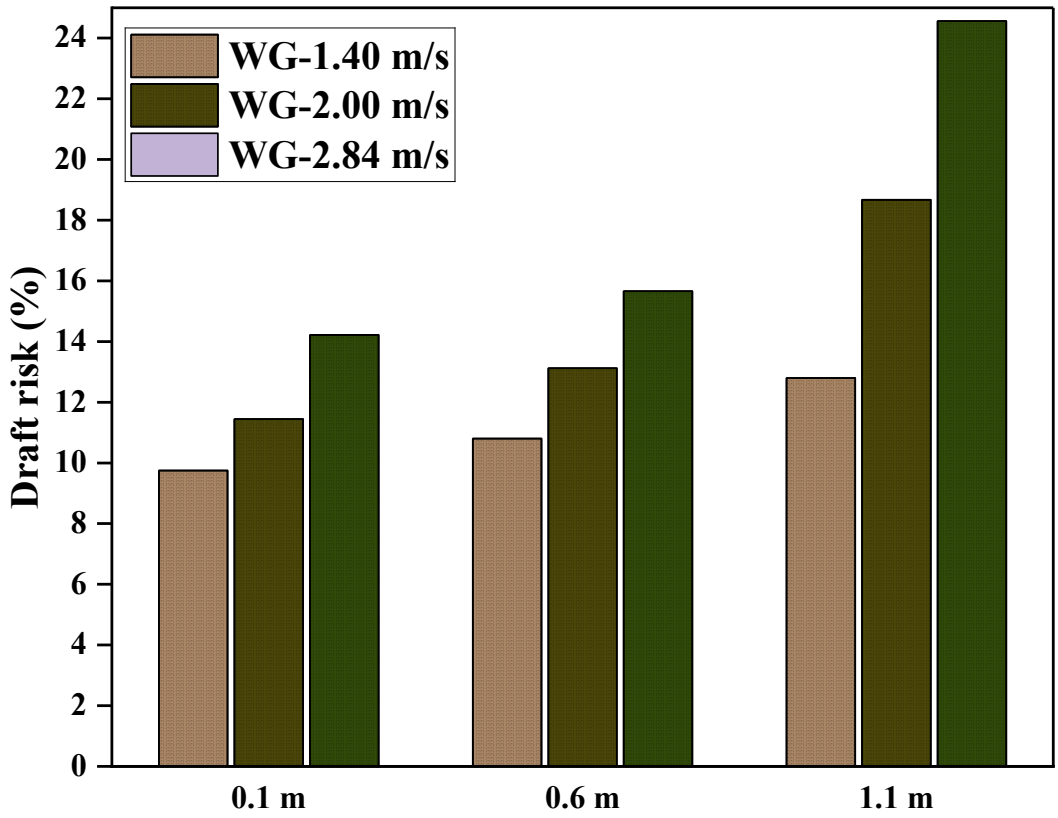

Figure 4.22: Draft risk at mid-vertical plane for WG cases

4.2.4 Air distribution index

The variation of the Air distribution index (ADI) for the four ventilation strategies investigated systems under the same air change rate of 6 ACH and the same supply air temperature of 291.15 K in this study is shown in Figure 4.23. ADI is a combined indicator that reflects the overall air distribution performance by incorporating both ventilation effectiveness and thermal comfort conditions within the occupied zone.

ADI is where thermal comfort is combined with temperature effectiveness, contaminant removal effectiveness and normalized age of air in a single performance indicator. Thus, an increased ADI indicates improved overall performance in terms of air distribution since it implies a better balance between thermal comfort and indoor air quality (Almesri et al., 2013). The published studies that define ADI as a combination index to assess thermal comfort, air quality, ventilation effectiveness and energy-related performance of ventilation systems are consistent with this use of ADI as an integrated air-distribution-performance index.

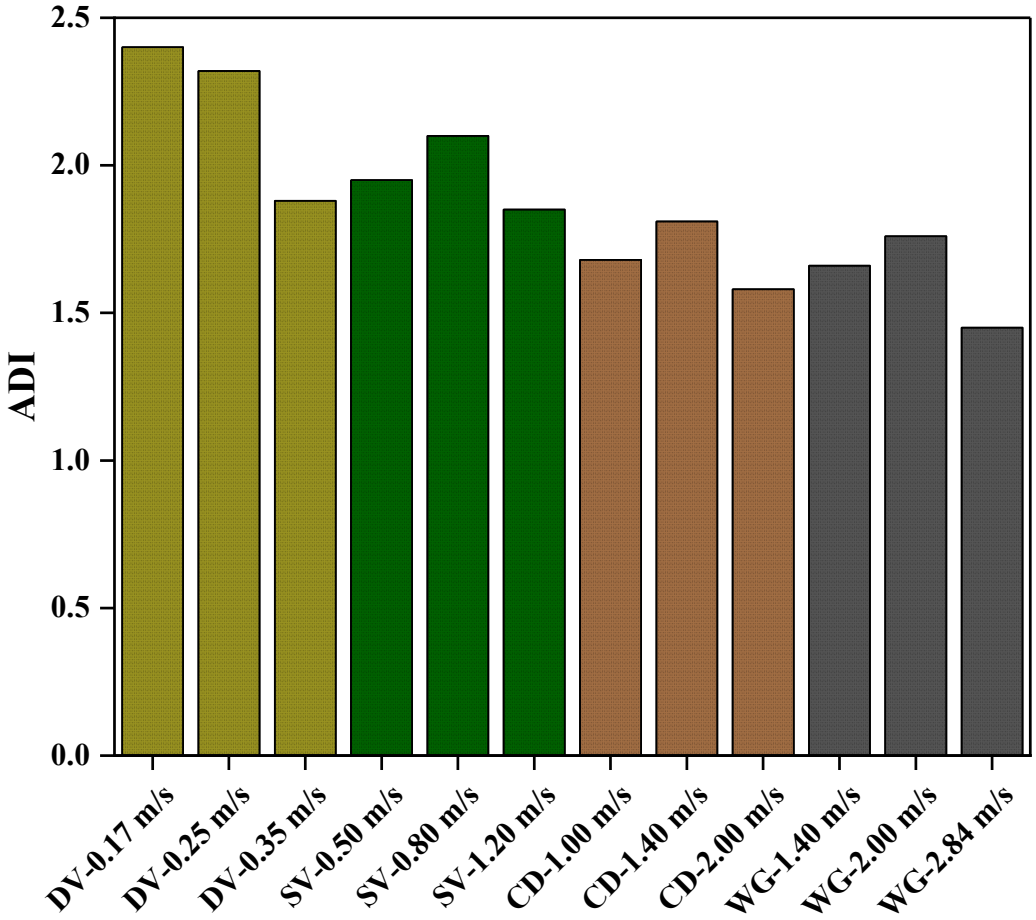

Figure 4.23: Air distribution index

In the case of displacement ventilation, the ADI decreased as follows: at 0.17 m/s, the value was approximately 2.40, then the value at 0.25 m/s was 2.32 and further to 1.88 at 0.35 m/s. The fact that all DV cases had relatively high ADI values, however, shows that the inverse relationship between increasing the supply velocity and the overall performance of the system was observed. This finding is understandable since the supply of low velocity in DV contributes to stable stratification, low age of air, and effective upward contaminant transport by the occupant thermal plumes. But it is possible that, as the supply velocity rises, the pattern of displacement-flow through occupied zone becomes more disturbed and the combined value of contaminant removal and freshness of air in occupied zone is diminished. This kind of behavior has also been noted in the research which revealed that floor level and displacement type supply systems could be used to improve the quality of the indoor air as well as the comfort of people when the supply momentum is effectively managed (Karimipanah et al., 2007). To achieve stratum ventilation, the ADI rose to about 1.85 at 1.2 m/s as

compared to 1.95 at 0.5 m/s. This demonstrates that the intermediate supply velocity gave the overall most effective performance of the SV cases. In low velocity the jet momentum of the supplied air may be insufficient to cause mixing across the occupied zone, whereas in high velocity the jet momentum of the supplied air may be too large to cause mixing across the occupied zone. Thus, the case of 0.8 m/s seems to offer a more balanced approach to the problem of air distribution, elimination of contaminants, and thermal comfort. This trend concurs with the body of literature on stratum ventilation that indicates that the velocity of supply, jet development and terminal configuration has a strong impact on local performance of comfort and air quality (Cheng & Lin, 2015). In the case of the ceiling diffuser system, the ADI varied between about 1.68 at 1.0 m/s and 1.81 at 1.4 m/s and slightly decreasing to 1.58 at 2.0 m/s. This implies that the highest CD performance was attained with the moderate supply velocity of 1.4 m/s. The ceiling diffuser, at this speed, was most likely more effective in mixing and distributing the fresh air in the room. But further acceleration to 2.0 m/s did not further enhance the ADI, so it is possible that excessive ceiling-jet momentum increased recirculation or local non-uniformity and reduced the combined effect of ventilation effectiveness and comfort. The same has been reported in the studies of ceiling diffusers, where the type of diffuser used, the supply momentum and the structure of the room airflow have a significant influence on the mean age of air, the effectiveness of ventilation, and the quality of indoor environment (Aziz et al., 2012). In the case of the wall grill system, the ADI was seen to be approximated as 1.66 at 1.4 m/s, 1.72 at 2.0 m/s, and then as 1.45 at 2.84 m/s. The intermediate velocity once again gave the best result, although the overall value of ADI was lower compared to those of DV and SV. This implies that the wall grill design was not as efficient in getting an optimal combined ratio of thermal comfort and contaminant removal. The strong wall jet at maximum velocity was likely to enhance mixing and recirculation, which diminished the advantage of fresh-air delivery to the occupied space. This is in line with literature where conventional mixing-based systems can show higher uniformity of room conditions with a reduction in local air quality performance when compared to stratified or non-uniform ventilation systems (Fan et al., 2022). In general, the ADI results indicate that DV exhibited the best overall performance in air distribution, then SV, and CD and WG had lower combined performance. According to the approximate average values, DV attained an average ADI of approximately 2.20, SV about 1.97, CD about

1.67 and WG about 1.61. Thus, DV enhanced ADI by about 12 percent as compared to SV, 32 percent as compared to CD, and 37 percent as compared to WG. The high ADI of DV can be largely attributed to its low age of air and high effectiveness in removing contaminants, with SV also performing well because the supply air was delivered at a low age of air and high efficiency of removing contaminants. Conversely, low ADI values were observed in CD and WG systems due to the fact that their airflow patterns were dominated by mixing, thus the collective benefits of freshness of air and elimination of contaminants in the occupied area was lower. These physical conclusions are physically sensible and consistent with published studies of ventilation using non-uniform systems, such as displacement and stratum ventilation which can achieve higher combined indoor air quality and thermal comfort performance than traditional mixing-based systems under appropriate operating conditions (Fan et al., 2022).

CHAPTER FIVE: CONCLUSIONS AND RECOMMENDATIONS

5.1 Conclusions

- Among the displacement ventilation cases, the lowest supply velocity at 0.17 m/s, gave the best ventilation performance, with the lowest age of air and highest contaminant removal effectiveness, indicating that lower supply momentum helps maintain stable buoyancy-driven stratification
- Stratum ventilation performed best at the supply velocity of 0.8 m/s, where the system achieved a better balance between horizontal jet penetration and controlled mixing, resulting in improved air renewal and contaminant removal compared with the lower and higher velocities cases for stratum ventilation
- Contaminant removal effectiveness was highest for displacement ventilation, with an average CRE of about 131%, followed by stratum ventilation at about 106%, ceiling diffuser at about 96%, and wall grill ventilation at about 82%, showing that stratified and occupied-zone supply systems removed contaminants more effectively than mixing-based systems
- The temperature contours indicated that the displacement and stratum ventilation systems preserved the clear thermal stratification with cooler air in the occupied zone and warmer air in the upper zone, while ceiling diffuser and wall grill systems generated more even temperature fields, but with the stratification increasingly influenced by mixing effects.
- Draft risk results showed that displacement ventilation had the lowest discomfort risk at seated and breathing heights, while wall grill ventilation produced the highest draft risk, especially at 1.1 m, where the highest WG velocity reached approximately 24.5 percentage
- Based on the Air Distribution Index, displacement ventilation provided the best overall performance, with an average ADI of approximately 2.20, followed by stratum ventilation at 1.97, ceiling diffuser at 1.67, and wall grill ventilation at 1.61
- Stratum ventilation can be a great alternative to displacement ventilation in a classroom where the space constraints exist, for mixed-based ventilation system ceiling diffusers could be a better choice

5.2 Recommendations

- The study should be conducted to different classroom geometries, room heights, and occupancy densities to examine whether the same ventilation ranking remains valid for other classrooms
- Experimental comfort surveys or PMV/PPD-based occupant response studies should be conducted to confirm whether the predicted draft risk and temperature distribution agree with actual occupant comfort perception

REFERENCES

Al-Rikabi, I. J., Karam, J., Alsaad, H., Ghali, K., Ghaddar, N., & Voelker, C. (2024). The impact of mechanical and natural ventilation modes on the spread of indoor airborne contaminants: A review. *Journal of Building Engineering*, *85*, 108715. https://doi.org/10.1016/j.jobe.2024.108715

Awwad, A., Mohamed, M. H., & Fatouh, M. (2017). Optimal design of a louver face ceiling diffuser using CFD to improve occupant's thermal comfort. *Journal of Building Engineering*, *11*, 134–157. https://doi.org/10.1016/j.jobe.2017.04.009

Branco, P. T. B. S., Sousa, S. I. V., Dudzińska, M. R., Ruzgar, D. G., Mutlu, M., Panaras, G., Papadopoulos, G., Saffell, J., Scutaru, A. M., Struck, C., & Weersink, A. (2024). A review of relevant parameters for assessing indoor air quality in educational facilities. *Environmental Research*, *261*, 119713. https://doi.org/10.1016/j.envres.2024.119713

Cabovská, B., Bekö, G., Teli, D., Ekberg, L., Dalenbäck, J.-O., Wargocki, P., Psomas, T., & Langer, S. (2022). Ventilation strategies and indoor air quality in Swedish primary school classrooms. *Building and Environment*, *226*, 109744. https://doi.org/10.1016/j.buildenv.2022.109744

Cetin, Y. E., Yuce, B. E., Kriegel, M., Wargocki, P., & Nielsen, P. V. (2025). Optimization of classroom window design using CFD and the Taguchi method. *Journal of Building Engineering*, *106*, 112580. https://doi.org/10.1016/j.jobe.2025.112580

Charres, I., Furst, L., Vicente, E. D., Soares, M., Viegas, C., Cervantes, R., Pena, P., Cerqueira, M., Feliciano, M., & Alves, C. (2025). School air quality and thermal

comfort: A multi-pollutant seasonal assessment. *Journal of Building Engineering*, *113*, 113997. https://doi.org/10.1016/j.jobe.2025.113997

Chen, T., Feng, Z., & Cao, S.-J. (2020). The effect of vent inlet aspect ratio and its location on ventilation efficiency. *Indoor and Built Environment*, *29*(2), 180–195. https://doi.org/10.1177/1420326X19865930

Cheng, F., Li, Y., Wu, Y., Cheng, Y., & Lin, Z. (2023). Experimental study of air distribution and heating performances of deflection ventilation. *Energy and Buildings*, *282*, 112800. https://doi.org/10.1016/j.enbuild.2023.112800

Cheng, F., Wu, Y., Gao, S., Liao, C., & Cheng, Y. (2022). Experimental study of thermal comfort in a field environment chamber with stratum ventilation system in winter. *Building and Environment*, *207*, 108445. https://doi.org/10.1016/j.buildenv.2021.108445

Collison, A. K., Byrne, M. A., & McGrath, J. A. (2025). Indoor air quality in naturally ventilated classrooms and offices in Ireland. *Building and Environment*, *279*, 113023. https://doi.org/10.1016/j.buildenv.2025.113023

Djunaedy, E., & Cheong, K. W. D. (2002). Development of a simplified technique of modelling four-way ceiling air supply diffuser. *Building and Environment*, *37*(4), 393–403. https://doi.org/10.1016/S0360-1323(01)00038-5

Eldanaf, T. S., Stefanic, P., Dagher, R., Altemnah, O., Saraiji, R., Langer, S., & Bekö, G. (2025). Indoor air quality in primary school classrooms in Sweden, Slovakia, and the United Arab Emirates. *Journal of Building Engineering*, *111*, 113151. https://doi.org/10.1016/j.jobe.2025.113151

Hatif, I. H., Kamar, H. M., Kamsah, N., & Wong, K. Y. (2023). Comparative evaluation of air distribution systems for controlling the airborne infection risk in indoor environments. *Journal of Building Engineering*, *79*, 107913. https://doi.org/10.1016/j.jobe.2023.107913

Huan, C., Wang, F. H., Lin, Z., Wu, X. Z., Ma, Z. J., Wang, Z. H., & Zhang, L. H. (2016). An experimental investigation into stratum ventilation for the cooling of an office with asymmetrically distributed heat gains. *Building and Environment*, *110*, 76–88. https://doi.org/10.1016/j.buildenv.2016.09.031

Hwang, R.-L., Lu, Y.-J., & Chen, W.-A. (2025). Thermal comfort and indoor air quality challenges in mixed-mode classrooms: Year-Round field study insights from a hot-humid climate. *Case Studies in Thermal Engineering*, *74*, 107031. https://doi.org/10.1016/j.csite.2025.107031

Jia, L.-R., Han, J., Chen, X., Li, Q.-Y., Lee, C.-C., & Fung, Y.-H. (2021). Interaction between Thermal Comfort, Indoor Air Quality and Ventilation Energy Consumption of Educational Buildings: A Comprehensive Review. *Buildings*, *11*(12), 591. https://doi.org/10.3390/buildings11120591

Kabirikopaei, A., Lau, J., Nord, J., & Bovaird, J. (2021). Identifying the K-12 classrooms' indoor air quality factors that affect student academic performance. *Science of The Total Environment*, *786*, 147498. https://doi.org/10.1016/j.scitotenv.2021.147498

Kristensen, M. H., Jensen, J. S., & Heiselberg, P. K. (2017). Field study evaluation of diffuse ceiling ventilation in classroom during real operating conditions. *Energy and Buildings*, *138*, 26–34. https://doi.org/10.1016/j.enbuild.2016.12.017

Lee, H., & Rim, D. (2024). Assessment of airborne transmitted infection risk in classrooms using computational fluid dynamics and machine learning-based surrogate modeling. *Journal of Building Engineering*, *97*, 110760. https://doi.org/10.1016/j.jobe.2024.110760

Li, H., Liu, M., Kong, X., Wang, L., Li, J., & Fan, M. (2025). Experimental research on energy utilization, aerosol transmission and thermal comfort under different ventilation strategies: Densely-occupied classrooms as a case study. *Building and Environment*, *270*, 112523. https://doi.org/10.1016/j.buildenv.2025.112523

Li, Y., Pan, Y., Huang, Z., Liang, Y., & Yuan, X. (2024). Simplified Simulation Method of Diffusers for Indoor Non-Uniform Temperature Distribution: A Case Study in Shanghai. *Buildings*, *14*(1), 206. https://doi.org/10.3390/buildings14010206

Lin, Z., Chow, T. T., Tsang, C. F., Fong, K. F., & Chan, L. S. (2009). Stratum ventilation – A potential solution to elevated indoor temperatures. *Building and Environment*, *44*(11), 2256–2269. https://doi.org/10.1016/j.buildenv.2009.03.007

Lin, Z., Wang, J., Yao, T., & Chow, T. T. (2012). Investigation into anti-airborne infection performance of stratum ventilation. *Building and Environment*, *54*, 29–38. https://doi.org/10.1016/j.buildenv.2012.01.017

Liu, Y., Liu, Y., Shao, X., Liu, Y., Huang, C.-E., & Jian, Y. (2022). Demand-oriented differentiated multi-zone thermal environment: Regulating air supply direction and velocity under stratum ventilation. *Building and Environment*, *219*, 109242. https://doi.org/10.1016/j.buildenv.2022.109242

Liu, Y., Pan, W., & Long, Z. (2021). Optimization of air supply parameters for stratum ventilation based on proper orthogonal decomposition. *Sustainable Cities and Society*, *75*, 103291. https://doi.org/10.1016/j.scs.2021.103291

Lu, Y., Liu, J., & Lin, Z. (2023). Impact of different supply modes of stratum ventilation on airflow and contaminant distribution characteristics. *Building and Environment*, *236*, 110303. https://doi.org/10.1016/j.buildenv.2023.110303

Maiques, M., Tarragona, J., Gangolells, M., & Casals, M. (2025). Energy implications of meeting indoor air quality and thermal comfort standards in Mediterranean schools using natural and mechanical ventilation strategies. *Energy and Buildings*, *328*, 115076. https://doi.org/10.1016/j.enbuild.2024.115076

Mateus, N. M., & Carrilho Da Graça, G. (2015). A validated three-node model for displacement ventilation. *Building and Environment*, *84*, 50–59. https://doi.org/10.1016/j.buildenv.2014.10.029

Miao, S., Gangolells, M., & Tejedor, B. (2023). A Comprehensive Assessment of Indoor Air Quality and Thermal Comfort in Educational Buildings in the Mediterranean Climate. *Indoor Air*, *2023*, 1–25. https://doi.org/10.1155/2023/6649829

Murga, A., Bale, R., Ito, K., & Tsubokura, M. (2024). Ventilation strategies for inhalation exposure risk mitigation: Eulerian-Lagrangian LES analysis of particle-laden turbulent flow applying virtual manikins. *Building and Environment*, *266*, 112149. https://doi.org/10.1016/j.buildenv.2024.112149

Olivas, A. C., & Yee, J.-J. (2025). Towards the use of data-driven methods for indoor airflow field reconstruction: A systematic review. *Journal of Building Engineering*, *106*, 112581. https://doi.org/10.1016/j.jobe.2025.112581

Peng, P., Zhang, C., Li, W., Pomianowski, M., Gong, G., Fang, X., Chun, L., & Guo, R. (2023). Investigation on indoor airflow and contaminant dispersion of diffuse ceiling ventilation in heating and cooling modes. *Journal of Building Engineering*, *80*, 107972. https://doi.org/10.1016/j.jobe.2023.107972

Pollozhani, F., McLeod, R. S., Schwarzbauer, C., & Hopfe, C. J. (2024). Assessing school ventilation strategies from the perspective of health, environment, and energy. *Applied Energy*, *353*, 121961. https://doi.org/10.1016/j.apenergy.2023.121961

Rawat, N., Kumar, P., Hama, S., Williams, N., & Zivelonghi, A. (2025). Improving classroom air quality and ventilation with IoT-driven acoustic and visual CO_2 feedback system. *Science of The Total Environment*, *980*, 179543. https://doi.org/10.1016/j.scitotenv.2025.179543

Saad, M., William, M. A., Hassan, A. A., & Hanafy, A. A. (2023). Influence of air ceiling diffusers in enclosed spaces: An experimental and numerical investigation. *Energy Reports*, *9*, 59–71. https://doi.org/10.1016/j.egyr.2023.05.253

Shan, X., Zhou, J., Chang, V. W.-C., & Yang, E.-H. (2016). Comparing mixing and displacement ventilation in tutorial rooms: Students' thermal comfort, sick building syndromes, and short-term performance. *Building and Environment*, *102*, 128–137. https://doi.org/10.1016/j.buildenv.2016.03.025

Shrestha, M., Rijal, H. B., Kayo, G., & Shukuya, M. (2022). An investigation on CO_2 concentration based on field survey and simulation in naturally ventilated Nepalese school buildings during summer. *Building and Environment*, *207*, 108405. https://doi.org/10.1016/j.buildenv.2021.108405

Son, S., & Jang, C.-M. (2022). Effects of internal airflow on IAQ and cross-infection of infectious diseases between students in classrooms. *Atmospheric Environment*, *279*, 119112. https://doi.org/10.1016/j.atmosenv.2022.119112

Tian, X., Zhang, S., Lin, Z., Li, Y., Cheng, Y., & Liao, C. (2019). Experimental investigation of thermal comfort with stratum ventilation using a pulsating air supply. *Building and Environment*, *165*, 106416. https://doi.org/10.1016/j.buildenv.2019.106416

Tikul, N., Hokpunna, A., & Chawana, P. (2022). Improving indoor air quality in primary school buildings through optimized apertures and classroom furniture layouts. *Journal of Building Engineering*, *62*, 105324. https://doi.org/10.1016/j.jobe.2022.105324

Tognon, G., & Zarrella, A. (2024). Displacement ventilation: A systematic review of the interactions with indoor environment and simplified modelling approaches. *Journal of Building Engineering*, *96*, 110474. https://doi.org/10.1016/j.jobe.2024.110474

Vasquez, N. G., Bekö, G., Wargocki, P., Cabovska, B., Teli, D., Dalenbäck, J.-O., Ekberg, L., Psomas, T., & Langer, S. (2023). Ventilation strategies and children's perception of the indoor environment in Swedish primary school classrooms. *Building and Environment*, *240*, 110450. https://doi.org/10.1016/j.buildenv.2023.110450

Villafruela, J. M., Olmedo, I., Ruiz De Adana, M., Méndez, C., & Nielsen, P. V. (2013). CFD analysis of the human exhalation flow using different boundary conditions and ventilation strategies. *Building and Environment*, *62*, 191–200. https://doi.org/10.1016/j.buildenv.2013.01.022

Wachenfeldt, B. J., Mysen, M., & Schild, P. G. (2007). Air flow rates and energy saving potential in schools with demand-controlled displacement ventilation. *Energy and Buildings*, *39*(10), 1073–1079. https://doi.org/10.1016/j.enbuild.2006.10.018

Wang, X., Yang, L., Gao, S., Zhao, S., & Zhai, Y. (2021). Thermal comfort in naturally ventilated university classrooms: A seasonal field study in Xi'an, China. *Energy and Buildings*, *247*, 111126. https://doi.org/10.1016/j.enbuild.2021.111126

Wang, Y., Zhao, F.-Y., Kuckelkorn, J., Spliethoff, H., & Rank, E. (2014). School building energy performance and classroom air environment implemented with the heat recovery heat pump and displacement ventilation system. *Applied Energy*, *114*, 58–68. https://doi.org/10.1016/j.apenergy.2013.09.020

Wargocki, P., Porras-Salazar, J. A., Contreras-Espinoza, S., & Bahnfleth, W. (2020). The relationships between classroom air quality and children's performance in school. *Building and Environment*, *173*, 106749. https://doi.org/10.1016/j.buildenv.2020.106749

Xu, R., Wu, F., Shen, L., Pan, X., Huang, Z., Yu, J., & Huang, Y. (2025). Investigation of airborne transmission and thermal comfort in a train cabin: Effects of air change rate and supply mode. *Case Studies in Thermal Engineering*, *76*, 107387. https://doi.org/10.1016/j.csite.2025.107387

Yao, T., & Lin, Z. (2014). An experimental and numerical study on the effect of air terminal layout on the performance of stratum ventilation. *Building and Environment*, *82*, 75–86. https://doi.org/10.1016/j.buildenv.2014.08.016

Yau, Y. H., Rodzi, M. A. M., & Nik Ghazali, N. N. (2024). Numerical simulation on supply air of high sidewall grille with retrofitted energy recovery ventilator system for thermal comfort in the tropics. *Journal of Building Engineering*, *89*, 109281. https://doi.org/10.1016/j.jobe.2024.109281

Zhang, S., Cheng, Y., Oladokun, M. O., Huan, C., & Lin, Z. (2019). Heat removal efficiency of stratum ventilation for air-side modulation. *Applied Energy*, *238*, 1237–1249. https://doi.org/10.1016/j.apenergy.2019.01.148

Zhang, S., & Lin, Z. (2026). Review and prospect on advanced ventilation strategies for livable and sustainable buildings. *Building and Environment*, *289*, 114122. https://doi.org/10.1016/j.buildenv.2025.114122

Zhao, W., Lestinen, S., Mustakallio, P., Kilpeläinen, S., Jokisalo, J., & Kosonen, R. (2021). Experimental study on thermal environment in a simulated classroom with different air distribution methods. *Journal of Building Engineering*, *43*, 103025. https://doi.org/10.1016/j.jobe.2021.103025

ANNEXES

Annex-1: Height vs Temperature (CD cases)

Height (m)	1.00 m/s (K)	1.40 m/s (K)	2.00 m/s (K)
0.10000	297.132	297.531	299.217
0.20000	297.162	297.661	299.333
0.20190	297.166	297.6701	299.333
0.26543	297.225	297.796	299.321
0.32943	297.277	297.8951	299.31
0.39343	297.319	297.9334	299.299
0.45743	297.391	297.9931	299.291
0.52143	297.502	298.0172	299.284
0.52143	297.502	298.0127	299.284
0.58543	297.6558	298.0608	299.278
0.64943	297.747	298.113	299.274
0.71343	297.776	298.126	299.272
0.77743	297.824	298.091	299.27
0.84143	297.814	298.052	299.269
0.90543	297.803	298.016	299.269
0.90543	297.803	298.016	299.269
0.96943	297.793	297.983	299.269
1.03343	297.78	297.954	299.269
1.09743	297.763	297.933	299.269
1.16143	297.742	297.922	299.268
1.22543	297.719	297.924	299.267
1.22543	297.719	297.924	299.267
1.28943	297.695	297.938	299.265
1.35343	297.675	297.962	299.263
1.41743	297.661	297.996	299.259
1.48143	297.654	298.043	299.255
1.54543	297.656	298.102	299.25
1.60943	297.669	298.174	299.243
1.67343	297.693	298.253	299.236
1.73743	297.727	298.33	299.227
1.80143	297.769	298.397	299.217
1.86543	297.813	298.446	299.206
1.92943	297.851	298.478	299.194
1.99343	297.877	298.499	299.181
2.05743	297.888	298.513	299.166
2.12143	297.888	298.526	299.15

Height (m)	1.00 m/s (K)	1.40 m/s (K)	2.00 m/s (K)
2.18543	297.885	298.54	299.132
2.24943	297.89	298.555	299.113
2.31343	297.913	298.571	299.093
2.37743	297.964	298.589	299.071
2.44143	298.047	298.607	299.047
2.50543	298.153	298.626	299.022
2.56943	298.259	298.645	298.996
2.63343	298.345	298.663	298.97
2.69743	298.407	298.681	298.943
2.76143	298.454	298.699	298.916
2.82543	298.496	298.715	298.891
2.82543	298.496	298.715	298.891
2.88943	298.536	298.729	298.867
2.95343	298.574	298.742	298.847
3.01743	298.606	298.752	298.83
3.08143	298.63	298.759	298.818
3.14543	298.646	298.763	298.812
3.20943	298.652	298.764	298.812
3.27343	298.653	298.761	298.819
3.33743	298.655	298.759	298.829
3.36402	298.664	298.762	298.832
3.40170	298.673	298.767	298.837
3.40170	298.673	298.767	298.837
3.48953	298.763	298.826	298.846
3.51972	298.838	298.899	298.842
3.51972	298.838	298.899	298.842
3.54212	298.918	299.014	298.839
3.56076	299.033	299.194	298.84
3.57629	299.285	299.474	298.843
3.58922	299.92	300.088	298.907
3.60000	300.934	301.053	299.492

Annex-2: Height vs Temperature (SV cases)

Height (m)	1.20 m/s (K)	0.80 m/s (K)	0.50 m/s (K)
0.10000	296.301	295.517	295.114
0.20000	296.331	295.692	295.234
0.20339	296.332	295.697	295.239
0.25441	296.343	295.776	295.33
0.31841	296.36	295.843	295.434
0.38241	296.376	295.936	295.531
0.44641	296.42	296.035	295.618
0.51041	296.453	296.121	295.698
0.57441	296.528	296.207	295.771
0.63841	296.569	296.292	295.84
0.70241	296.584	296.364	295.908
0.76641	296.659	296.418	295.985
0.83041	296.705	296.466	296.077
0.89441	296.72	296.513	296.174
0.95841	296.772	296.554	296.277
1.02241	296.845	296.586	296.411
1.08641	296.913	296.615	296.633
1.15041	296.976	296.64	296.95
1.21441	297.028	296.665	297.266
1.27841	297.067	296.703	297.53
1.34241	297.102	296.751	297.747
1.40641	297.151	296.791	297.914
1.47041	297.227	296.844	298.023
1.53441	297.335	296.988	298.083
1.59841	297.463	297.198	298.122
1.66241	297.601	297.352	298.188
1.72641	297.738	297.516	298.286
1.79041	297.865	297.684	298.375
1.85441	297.967	297.74	298.434
1.91841	298.037	297.767	298.473
1.98241	298.082	297.842	298.498
2.04641	298.112	297.879	298.516
2.11041	298.135	297.977	298.528
2.17441	298.153	298.085	298.536
2.23841	298.168	298.146	298.54
2.30241	298.182	298.176	298.543
2.36641	298.193	298.189	298.546
2.43041	298.203	298.195	298.55
2.49441	298.211	298.197	298.556

Height (m)	1.20 m/s (K)	0.80 m/s (K)	0.50 m/s (K)
2.55841	298.218	298.198	298.566
2.62241	298.225	298.199	298.582
2.68641	298.231	298.2	298.603
2.75041	298.24	298.202	298.63
2.81441	298.252	298.205	298.659
2.87841	298.275	298.211	298.699
2.87841	298.275	298.22	298.699
2.94241	298.319	298.233	298.779
3.00641	298.402	298.251	298.894
3.07041	298.532	298.37	298.983
3.13441	298.704	298.473	299.025
3.19841	298.892	298.54	299.05
3.26241	299.108	298.64	299.136
3.32641	299.345	298.84	299.317
3.39041	299.508	299.17	299.493
3.44754	299.573	299.47	299.626
3.48103	299.634	299.65	299.712
3.51987	299.792	299.85	299.867
3.54221	299.955	299.93	300
3.56082	300.16	300.14	300.159
3.57632	300.424	300.43	300.356
3.58924	300.74	300.74	300.596
3.6	301.063	300.96	300.842

Annex-3: Height vs Temperature (DV cases)

Height (m)	0.17 m/s (K)	0.25 m/s (K)	0.35 m/s (K)
0.2000	293.7670	294.1640	296.3176
0.2134	293.7885	294.1700	296.3445
0.2457	293.8376	294.1760	296.4516
0.2479	293.8409	294.1760	296.4592
0.2572	293.8548	294.1780	296.4911
0.3212	293.9592	294.2090	296.6578
0.3852	294.1131	294.2810	296.7778
0.4492	294.3848	294.4310	296.8947
0.5132	294.7607	294.7220	296.9993
0.5772	295.1160	295.1260	297.1917
0.6412	295.3766	295.5080	297.2992
0.7052	295.5837	295.7970	297.4799
0.7692	295.8095	296.0290	297.6088

Height (m)	0.17 m/s (K)	0.25 m/s (K)	0.35 m/s (K)
0.8332	296.1427	296.2670	297.7237
0.8972	296.5042	296.4910	297.8328
0.9612	296.7398	296.6350	297.9510
1.0252	296.8414	296.7910	298.1052
1.0892	296.8894	296.9840	298.2820
1.1532	296.9387	297.0880	298.4246
1.2172	297.0363	297.1440	298.5195
1.2812	297.3350	297.3820	298.5874
1.3452	297.8641	297.7800	298.6413
1.4092	298.3136	298.0800	298.6842
1.4732	298.5272	298.2250	298.7192
1.5372	298.6154	298.3110	298.7451
1.6012	298.6613	298.4550	298.7651
1.6652	298.6942	298.6270	298.7791
1.7292	298.7222	298.7600	298.7870
1.7932	298.7472	298.8690	298.7910
1.8572	298.7651	298.9350	298.7900
1.9212	298.7781	298.9580	298.7870
1.9852	298.7881	298.9700	298.7810
1.9852	298.7881	298.9700	298.7810
2.0492	298.7981	298.9790	298.7739
2.1132	298.8091	298.9870	298.7649
2.1772	298.8191	298.9930	298.7569
2.2412	298.8281	298.9990	298.7489
2.3052	298.8361	299.0030	298.7410
2.3692	298.8451	299.0060	298.7340
2.4332	298.8551	299.0090	298.7280
2.4972	298.8681	299.0130	298.7240
2.5612	298.8821	299.0170	298.7210
2.6252	298.8971	299.0230	298.7210
2.6892	298.9121	299.0300	298.7220
2.7532	298.9251	299.0400	298.7250
2.8172	298.9341	299.0540	298.7310
2.8812	298.9421	299.0730	298.7381
2.9452	298.9572	299.1010	298.7481
3.0092	298.9844	299.1410	298.7611
3.0732	299.0367	299.1990	298.7761
3.1372	299.1321	299.2720	298.7941
3.2012	299.2812	299.3390	298.8162
3.2652	299.4349	299.4010	298.8442

Height (m)	0.17 m/s (K)	0.25 m/s (K)	0.35 m/s (K)
3.3292	299.5519	299.4640	298.8793
3.3932	299.6650	299.5490	298.9264
3.4041	299.6877	299.5710	298.9375
3.4357	299.7649	299.6350	298.9698
3.4967	299.9735	299.8260	299.0605
3.5231	300.1184	299.9810	299.1195
3.5446	300.2538	300.1590	299.2034
3.5624	300.3924	300.3590	299.3354
3.5773	300.5405	300.5590	299.5662
3.5897	300.6933	300.7380	300.0032
3.6000	300.8320	300.8850	300.6090

Annex-4: Height vs Temperature (WG cases)

Height (m)	1.40 m/s (K)	2.00 m/s (K)	2.84 m/s (K)
0.1000	298.4190	298.6180	298.8670
0.2000	298.5160	298.7090	298.9739
0.2024	298.5122	298.7080	298.9723
0.2550	298.4577	298.6900	298.9395
0.3190	298.4310	298.6920	298.9169
0.3830	298.4262	298.7300	298.9100
0.4470	298.4424	298.7540	298.9111
0.5110	298.4775	298.7590	298.9140
0.5750	298.5225	298.7810	298.9140
0.6390	298.5694	298.8300	298.9162
0.7030	298.6114	298.8500	298.9243
0.7670	298.6473	298.8700	298.9416
0.8310	298.6752	298.8970	298.9687
0.8950	298.6982	298.9607	299.0048
0.9590	298.7223	298.9780	299.0457
1.0230	298.7544	298.9550	299.0815
1.0870	298.7965	298.9390	299.1072
1.1510	298.8497	298.9260	299.1169
1.2150	298.9147	298.9070	299.1106
1.2790	298.9877	298.8710	299.0914
1.3430	299.0576	298.8120	299.0622
1.4070	299.1123	298.7460	299.0241
1.4710	299.1379	298.6860	298.9801
1.5350	299.1286	298.6320	298.9341
1.5990	299.0925	298.5850	298.8912
1.6630	299.0435	298.5450	298.8544

1.7270	298.9915	298.5130	298.8256
1.7910	298.9436	298.4900	298.8048
1.8550	298.9047	298.4770	298.7929
1.9190	298.8758	298.4770	298.7901
1.9830	298.8549	298.4910	298.7932
2.0470	298.8399	298.5220	298.8012
2.1110	298.8259	298.5720	298.8133
2.1750	298.8108	298.6450	298.8273
2.2390	298.7927	298.7430	298.8413
2.3030	298.7624	298.8730	298.8563
2.3670	298.6999	299.0420	298.8734
2.4310	298.6785	299.1520	298.8945
2.4950	298.6621	299.2360	298.9206
2.5590	298.6507	299.2680	298.9507
2.6230	298.6493	299.3040	298.9837
2.6870	298.6628	299.3100	299.0187
2.7510	298.6914	299.3320	299.0537
2.8150	298.7350	299.3600	299.0866
2.8790	298.7786	299.3920	299.1155
2.9430	298.8222	299.4260	299.1394
3.0070	298.8608	299.4710	299.1572
3.0710	298.8923	299.5560	299.1691
3.1350	298.9179	299.6490	299.1760
3.1990	298.9405	299.7264	299.1780
3.2630	298.9601	299.8327	299.1780
3.3270	298.9681	299.9377	299.1780
3.3910	298.9812	300.0470	299.1802
3.4351	299.0017	300.1400	299.1857
3.4994	299.0739	300.2750	299.2058
3.5248	299.1509	300.3820	299.2242
3.5458	299.2765	300.4813	299.2647
3.5632	299.4833	300.6400	299.3640
3.5778	299.8491	300.7900	299.6343
3.5899	300.5199	301.3200	300.2587
3.6000	301.4100	301.5300	301.1390

Annex-5: ADI calculation

Case	|S|	ε_t	ε_c	$\tau*$
DV- 0.17 m/s	0.23	1.49	1.47	0.69
DV- 0.25 m/s	0.22	1.45	1.34	0.72
DV- 0.35 m/s	0.42	1.18	1.13	0.77
SV- 0.50 m/s	0.29	1.22	1.07	0.79
SV- 0.80 m/s	0.22	1.33	1.15	0.76
SV- 1.20 m/s	0.30	1.17	0.96	0.83
CD- 1.00 m/s	0.83	0.85	1.05	1.02
CD- 1.40 m/s	0.33	0.98	0.97	0.97
CD- 2.00 m/s	0.65	0.87	0.85	1.05
WG- 1.40 m/s	0.32	0.88	0.83	1.05
WG- 2.00 m/s	0.30	0.90	0.86	1.03
WG- 2.84 m/s	0.67	0.76	0.78	1.09

Annex-6: IOE GC acceptance letter

त्रिभुवन विश्वविद्यालय
TRIBHUVAN UNIVERSITY
इन्जिनियरिङ्ग अध्ययन संस्थान
INSTITUTE OF ENGINEERING
पुल्चोक क्याम्पस
PULCHOWK CAMPUS
Accredited by University Grants Commission (UGC) Nepal 2020
5-521260
5-521611
5-522104
5-522809
पुल्चोक, ललितपुर।
Pulchowk, Lalitpur

त्रिभुवन विश्वविद्यालय
इन्जिनियरिङ्ग अध्ययन संस्थान
पुल्चोक क्याम्पस

Date: May 8, 2026

To Whom It May Concern:

This is to certify that the paper titled "*Numerical Comparison of Ventilation Approaches for Thermal Comfort and Air Distribution in a Classroom*" (Submission ID #845), with **Binod KC** as the first author, was accepted through the peer-review process and has been presented at the 18th IOE Graduate Conference, organized at Pulchowk Campus, Lalitpur, Nepal, from May 7 to 9, 2026.

Please note that inclusion of the accepted manuscript in the conference proceedings is contingent upon timely compliance with any further editorial requirements during the publication process.

Prof. Sangeeta Singh
Convener
18th IOE Graduate Conference

Annex-7: Plagiarism check

Binod KC

Numerical Comparison of Ventilation Approaches for Thermal Comfort and Air Distribution in a Classroom

Tribhuvan University

Document Details

Submission ID
trn:oid:::3117:586998507

Submission Date
May 6, 2026, 4:57 PM GMT+5:45

Download Date
May 6, 2026, 5:00 PM GMT+5:45

File Name
Final_thesis_Binod_KC (updated) mod 1.docx

File Size
7.7 MB

108 Pages

24,174 Words

138,180 Characters

iThenticate Page 1 of 122 - Cover Page Submission ID trn:oid:::3117:586998507

13% Overall Similarity

The combined total of all matches, including overlapping sources, for each database.

Filtered from the Report

- Bibliography
- Quoted Text
- Cited Text
- Small Matches (less than 8 words)

Custom Section Exclusions

{titlesCount} Section Titles, {keywordsCount} Keywords

Section title	No. of Section Starters	Section Starters			
"Acknowledgements"	4	Acknowledgements	Acknowledgement	Acknowledgment	Acknowledgments

Match Groups

- **282** Not Cited or Quoted **13%**
  Matches with neither in-text citation nor quotation marks
- **0** Missing Quotations **0%**
  Matches that are still very similar to source material
- **0** Missing Citation **0%**
  Matches that have quotation marks, but no in-text citation
- **0** Cited and Quoted **0%**
  Matches with in-text citation present, but no quotation marks

Top Sources

9% Internet sources
11% Publications
0% Submitted works (Student Papers)

Integrity Flags

0 Integrity Flags for Review

No suspicious text manipulations found.

Our system's algorithms look deeply at a document for any inconsistencies that would set it apart from a normal submission. If we notice something strange, we flag it for you to review.

A Flag is not necessarily an indicator of a problem. However, we'd recommend you focus your attention there for further review.

iThenticate Page 2 of 122 - Integrity Overview Submission ID trn:oid:::3117:586998507

Match Groups

- **282** Not Cited or Quoted 13%
  Matches with neither in-text citation nor quotation marks
- **0** Missing Quotations 0%
  Matches that are still very similar to source material
- **0** Missing Citation 0%
  Matches that have quotation marks, but no in-text citation
- **0** Cited and Quoted 0%
  Matches with in-text citation present, but no quotation marks

Top Sources

9% Internet sources
11% Publications
0% Submitted works (Student Papers)

Top Sources

The sources with the highest number of matches within the submission. Overlapping sources will not be displayed.

1	Internet	
elibrary.tucl.edu.np		2%
2	Internet	
www.mdpi.com		<1%
3	Publication	
"Proceedings of the 11th International Symposium on Heating, Ventilation and Ai...		<1%
4	Internet	
diva-portal.org		<1%
5	Internet	
researchportaltest.northumbria.ac.uk		<1%
6	Internet	
studentsrepo.um.edu.my		<1%
7	Publication	
Xue Tian, Yong Cheng, Jian Liu, Zhang Lin. "Evaluation of sidewall air supply with ...		<1%
8	Publication	
Xue Tian, Yong Cheng, Zhang Lin. "An experimental investigation of the airborne ...		<1%
9	Internet	
internationalscienceindex.org		<1%
10	Publication	
Aminhossein Jahanbin, Giovanni Semprini. "On the optimisation of age of the air i...		<1%

iThenticate Page 3 of 122 - Integrity Overview Submission ID trn:oid:::3117:586998507

11	Publication	Sheng Zhang, Dun Niu, Zhang Lin. "Extending effective draft temperature to cove... <1%
12	Publication	Sheng Zhang, Jinghua Jiang, Yong Cheng, Zhang Lin. "Ventilation Performance In... <1%
13	Publication	Teng Li, Emmanuel A. Essah, Yuxin Wu, Chunhui Liao, Yong Cheng. "Evaluation of ... <1%
14	Publication	Fangning Shi, Nianping Li, Haiyan Yan. "The Influence of Thermal History and Air ... <1%
15	Publication	Fariborz Haghighat. "The Influence of Office Furniture, Workstation Layouts, Diff... <1%
16	Publication	Lin, Zhang, C. F. Tsang, T. T. Chow, K. F. Fong, and Ting Yao. "A Case Study of the E... <1%
17	Publication	Ya-Chi Chen, Chung-Lung Chen, Qimin Dong. "CFD modeling for motor fan syste... <1%
18	Internet	core.ac.uk <1%
19	Internet	backend.orbit.dtu.dk <1%
20	Publication	Jianchao Ma, Hua Qian, Fan Liu, Cong Liu, Xiaohong Zheng, Fujiang Chen. "Person... <1%
21	Publication	Brockmann, Gerrid. "Exhaust Positioning and Stagnation Risk in Mixing Ventilatio... <1%
22	Publication	Ching-Jen Chen, Chiang Shih, Jeffrey Lienau, Robin J. Kung. "Flow Modeling and Tu... <1%
23	Internet	open.library.ubc.ca <1%
24	Internet	www.db-thueringen.de <1%

25 Publication
Chen Wang, Ke Hu, Yin Liu. "A novel ventilation method: Experimental measurem... <1%

26 Internet
acris.aalto.fi <1%

27 Internet
aplusbe.eu <1%

28 Internet
www.aivc.org <1%

29 Internet
www.lib.uidaho.edu <1%

30 Internet
convin.gr <1%

31 Publication
Weijia Zhang, Weirong Zhang, Yifei Bai, Shuqing Wen. "Enhancing indoor environ... <1%

32 Publication
Amin Heidarpour, Xiao-Ling Zhao. "Tubular Structures XVI", CRC Press, 2017 <1%

33 Publication
Zhang Lin, Jinliang Wang, Ting Yao, T.T. Chow. "Investigation into anti-airborne in... <1%

34 Publication
Han Li, Musong Liu, Xiangfei Kong, Leilei Wang, Jinchao Li, Man Fan. "Experiment... <1%

35 Publication
Yalin Lu, Zhang Lin. "Chapter 16 Reducing Exposure Risk in Hospital Wards by Ap... <1%

36 Publication
Zhijian Liu, Chaofan Lin, Jie Shi, Mingtao Ding et al. "Evaluation of upper-room ult... <1%

37 Internet
c.coek.info <1%

38 Publication
Ghogare Abhijeet Ganesh, Shobha Lata Sinha, Tikendra Nath Verma, Satish Kuma... <1%

39 Internet
etkhpcorderapi.extweb.sp.se <1%

40 Internet
link.springer.com <1%

41 Internet
xdocs.net <1%

42 Publication
Zhixi Qing, Weirong Zhang, Weijia Zhang, Haotian Zhang, Yingli Xuan. "Influence ... <1%

43 Internet
aaltodoc.aalto.fi <1%

44 Publication
Jun Hu, Meiyu Sun, Tao Ren, Yihang Lu, Jia Yu, Jing Xie. "A comparative study of ex... <1%

45 Publication
Pei Peng, Michal Pomianowski, Chen Zhang, Rui Guo, Rasmus Lund Jensen, Kim Tr... <1%

46 Publication
Sheng Zhang, Xia Zhang, Zhang Lin. "Concept and ventilation performance demo... <1%

47 Publication
Yin, Haiguo, Angui Li, Zhiyong Liu, Yixiang Sun, and Ting Chen. "Experimental stu... <1%

48 Internet
epdf.tips <1%

49 Publication
Hamid Motamedi, Mohammadreza Shirzadi, Yoshihide Tominaga, Parham A. Mirz... <1%

50 Publication
J.H.W. Lee, A.W. Jayawardena, Z.Y. Wang. "Environmental Hydraulics", CRC Press, ... <1%

51 Publication
Michal Krajčík, Angela Simone, Bjarne W. Olesen. "Air distribution and ventilation... <1%

52 Publication
Wojciech Cepiński, Paweł Szałański, Magdalena Orłowska, Sylwia Janta-Lipińska, ... <1%

53	Internet	
deepblue.lib.umich.edu		<1%
54	Internet	
kth.diva-portal.org		<1%
55	Internet	
repository.londonmet.ac.uk		<1%
56	Internet	
www.globalscientificjournal.com		<1%
57	Internet	
www.researchgate.net		<1%
58	Internet	
smartech.gatech.edu		<1%
59	Internet	
www.iaeng.org		<1%
60	Internet	
www.sciencegate.app		<1%
61	Publication	
Mohammed M. Farid. "Mathematical Modeling of Food Processing", CRC Press, 20...		<1%
62	Internet	
eprints.whiterose.ac.uk		<1%
63	Internet	
etd.aau.edu.et		<1%
64	Publication	
Claudia Kandzia, Dirk Mueller. "Stability of large room airflow structures in a vent...		<1%
65	Internet	
spectrum.library.concordia.ca		<1%
66	Internet	
www.biorxiv.org		<1%

67 Publication
Barbara Griefahn, Christa Künemund, Ulrike Gehring. "The significance of air velo... <1%

68 Publication
Chao Qin, Xueren Li, Hai Guo, Xiaopu Lyu. "Evaluating and mitigating the individu... <1%

69 Publication
Markus, Simone Ariela Law. "Advancing Design Models for Estimating Groundwat... <1%

70 Publication
Seo, J., and Y. Choi. "Estimation of the air quality of a vehicle interior: The effect o... <1%

71 Internet
discovery.researcher.life <1%

72 Internet
www.athensjournals.gr <1%

73 Internet
www.ijmerr.com <1%

74 Publication
Eleonora Palka Bayard de Palka Bayard de Volo, Beatrice Pulvirenti, Aminhossein ... <1%

75 Publication
Mohammad Ali Joudi. "Radiation properties of coil-coated steel in building envelo... <1%

76 Publication
Pradip Majumdar. "Computational Fluid Dynamics and Heat Transfer", CRC Press,... <1%

77 Publication
Randa Mohamed Ahmed Mahmoud, Amr Sayed Hassan Abdallah. "Assessment of ... <1%

78 Publication
Sheng Zhang, Yalin Lu, Dun Niu, Zhang Lin. "Energy performance index of air dist... <1%

79 Publication
Su-Hoon Park, Kyung-Rae Lee, Se-Jin Yook, Hyun Bon Koo. "Enhancement and Ho... <1%

80 Publication
Tengfei (Tim) Zhang. "A simplified approach to describe complex diffusers in displ... <1%

81 Publication
Xiujie Li, Cheuk Ming Mak, Kuen Wai Ma, Hai Ming Wong. "Large eddy simulation ... <1%

82 Publication
Yalin Lu, Jiankai Dong, Hongyong Lu, Dun Niu, Sheng Zhang, Zhaosong Fang, Zha... <1%

83 Publication
Yukun Xu, Xiaobin Wei, Yunfei Xia, Yanlei Yu, Lingjie Zeng, Guangyu Cao, Jun Gao.... <1%

84 Publication
Zhang Lin, T.T. Chow, C.F. Tsang, K.F. Fong, L.S. Chan. "CFD study on effect of the ... <1%

85 Internet
journal.ksae.org <1%

86 Internet
mdpi-res.com <1%

87 Internet
pmc.ncbi.nlm.nih.gov <1%

88 Internet
public-pages-files-2025.frontiersin.org <1%

89 Internet
theses.hal.science <1%

90 Internet
www.frontiersin.org <1%

91 Publication
"Proceedings of the Fifth International Conference in Ocean Engineering (ICOE20... <1%

92 Publication
Ahmed A. Serageldin, Ali K. Abdelrahman, Shinichi Ookawara. "Parametric study ... <1%

93 Publication
Ahmed Awwad, Abouelmagd Abdelsamie, Mohamed H. Mohamed, Mohamed Fat... <1%

94 Publication
Andrius Jurelionis, Laura Gagytė, Tadas Prasauskas, Darius Čiužas, Edvinas Krugly... <1%

95 Publication
Giacomo Tognon, Angelo Zarrella. "Displacement ventilation: a systematic review... <1%

96 Publication
Haorui Wang, Junqi Wang, Zhuangbo Feng, Fariborz Haghighat, Shi-Jie Cao. "Intel... <1%

97 Publication
Ihab Hasan Hatif, Mohamed Kamar Haslinda, Nazri Kamsah, Keng Yinn Wong. "C... <1%

98 Publication
Jinghua Jiang, Ruifeng Wang, Yuxin Li, Ruijie Jia, Jing Li, Sheng Zhang, Zhang Lin. "... <1%

99 Publication
Mihailo Vasic, Vladimir D. Stevanovic, Branislav Zivkovic. "Uniformity of air flow fr... <1%

100 Publication
Mohamad Al Ali, Peter Platko. "Advances and Trends in Engineering Sciences and ... <1%

101 Publication
Mostafa Ramezani, Amir Mohammad Jadidi, Roohollah Rafee. "Pollutant and heat... <1%

102 Publication
Shuangshuang Liang, Bozheng Li, Xue Tian, Yong Cheng, Chunhui Liao, Jianxin Zh... <1%

103 Publication
Xuchao Wang, Sheng Zhang, Zhang Lin. "Graded Ventilation with Primary Supply ... <1%

104 Publication
Ying Sun, Theodore F. Smith. "Air flow characteristics of a room with square cone ... <1%

105 Publication
Zhongcheng Duan, Yilun Zi, Leilei Wang, Shichun Dong. "Research on the Optimiz... <1%

106 Internet
library.modot.mo.gov <1%

107 Internet
ntnuopen.ntnu.no <1%

108 Internet
pure.coventry.ac.uk <1%

109 Internet
savoirs.usherbrooke.ca <1%

110 Internet
ttu-ir.tdl.org <1%

111 Internet
upcommons.upc.edu <1%

112 Internet
usir.salford.ac.uk <1%

113 Internet
www.researchsquare.com <1%

114 Internet
www.scielo.org.za <1%

115 Internet
www.tandfonline.com <1%

116 Internet
www.teses.usp.br <1%

117 Publication
Abbas Khoshhal, Masoud Rahimi, Ammar Abdulaziz Alsairafi. "The CFD Modeling ... <1%

118 Publication
Adamu, Zulfikar, and Andrew Price. "The Design and Simulation of Natural Perso... <1%

119 Publication
Amanlou, Y.. "Applying CFD for designing a new fruit cabinet dryer", Journal of Fo... <1%

120 Publication
Ariva Sugandi Permana. "Urban Engineering", Routledge, 2025 <1%

121 Publication
Chao Huan, Fenghao Wang, Xiaozhou Wu, Zhang Lin, Zhenjun Ma, Zhihua Wang. "... <1%

122 Publication
Cheruku, Ba. "Modeling and finite element analysis of fluid structure interaction i... <1%

123 Publication
Fong, M.L.. "Environmental Protection by Elevated Indoor Temperature of Air Con... <1%

124 Publication
Gunilla BENGTSSON. "Lipoprotein Lipase: Some Effects of Activator Proteins", Eur... <1%

125 Publication
Hubbard, Neal. "Dual-Stage Thermally Actuated Surface-Micromachined Nanopos... <1%

126 Publication
Hwataik Han. "Chapter 3 Ventilation Effectiveness Measurements Using Tracer G... <1%

127 Publication
Hyeunguk Ahn, Donghyun Rim, L. James Lo. "Ventilation and energy performance... <1%

128 Publication
Ihab Jabbar Al-Rikabi, Jennifer Karam, Hayder Alsaad, Kamel Ghali, Nesreen Ghad... <1%

129 Publication
Kandil, Alaa-E. "Assessment of Displacement Ventilation for Schools in Alberta", P... <1%

130 Publication
Martin Heine Kristensen, Jakob Søland Jensen, Per Kvols Heiselberg. "Field study ... <1%

131 Publication
Mirzoyan, Artak D.. "Lateral Resistance of Piles at the Crest of Slopes in Sand.", Br... <1%

132 Publication
Muhammad Farhan Ejaz, Simo Kilpeläinen, Panu Mustakallio, Risto Kosonen. "The... <1%

133 Publication
Osama Sabah Almtuly, Mazlan Abdul Wahid, Hasanen M. Hussen, Mohd Ibthisha... <1%

134 Publication
Paul Fazio, Hua Ge, Jiwu Rao, Guylaine Desmarais. "Research in Building Physics a... <1%

135 Publication
Rajeev Kumar Singh, Amitava Paul, A. K. Ray. "Modelling of flow behaviour in cont... <1%

136 Publication
Renze Xu, Fan Wu, Lian Shen, Xiaowang Pan, Zhou Huang, Jianci Yu, Yuhui Huang.... <1%

137 Publication
Sang Hwan Park, Gong Hee Lee, Dong Kim, Kyoungsik Chang. "Assessment of the ... <1%

138 Publication
Sheng Zhang, Dun Niu, Teng Li, Zhang Lin, Fanghui Cheng, Yong Cheng. "Cooling ... <1%

139 Publication
Sheng Zhang, Yong Cheng, Jian Liu, Zhang Lin. "Subzone control optimization of a... <1%

140 Publication
Songbo Wu, Tian Li, Jiye Zhang. "Effect of combined side-wall air supply on ventila... <1%

141 Publication
Tadeusz Kuczyński, Anna Staszczuk, Marta Gortych. "Passive Design Strategies to ... <1%

142 Publication
Teng Li, Rui Wang, Zhe Zhang, Jiangang Lei, Wei Liu, Yong Cheng. "Airflow charac... <1%

143 Publication
Ulrike Passe, Francine Battaglia. "Designing Spaces for Natural Ventilation - An Ar... <1%

144 Publication
Xiangfei Kong, Chang Xi, Han Li, Zhang Lin. "A comparative experimental study o... <1%

145 Publication
Xiangfei Kong, Yufan Chang, Nana Li, Han Li, Wei Li. "Comparison study of therm... <1%

146 Internet
aaltodoc2.org.aalto.fi <1%

147 Internet
cdap.sliit.lk <1%

148 Internet
nozdr.ru <1%

149 Internet
openlib.tugraz.at <1%

150 Internet
pdfslide.net <1%

151 Internet

pure.tue.nl <1%

152 Internet

vbn.aau.dk <1%

153 Internet

www.nature.com <1%

iThenticate Page 14 of 122 - Integrity Overview Submission ID trn:oid:::3117:586998507